Interaction between UTES systems
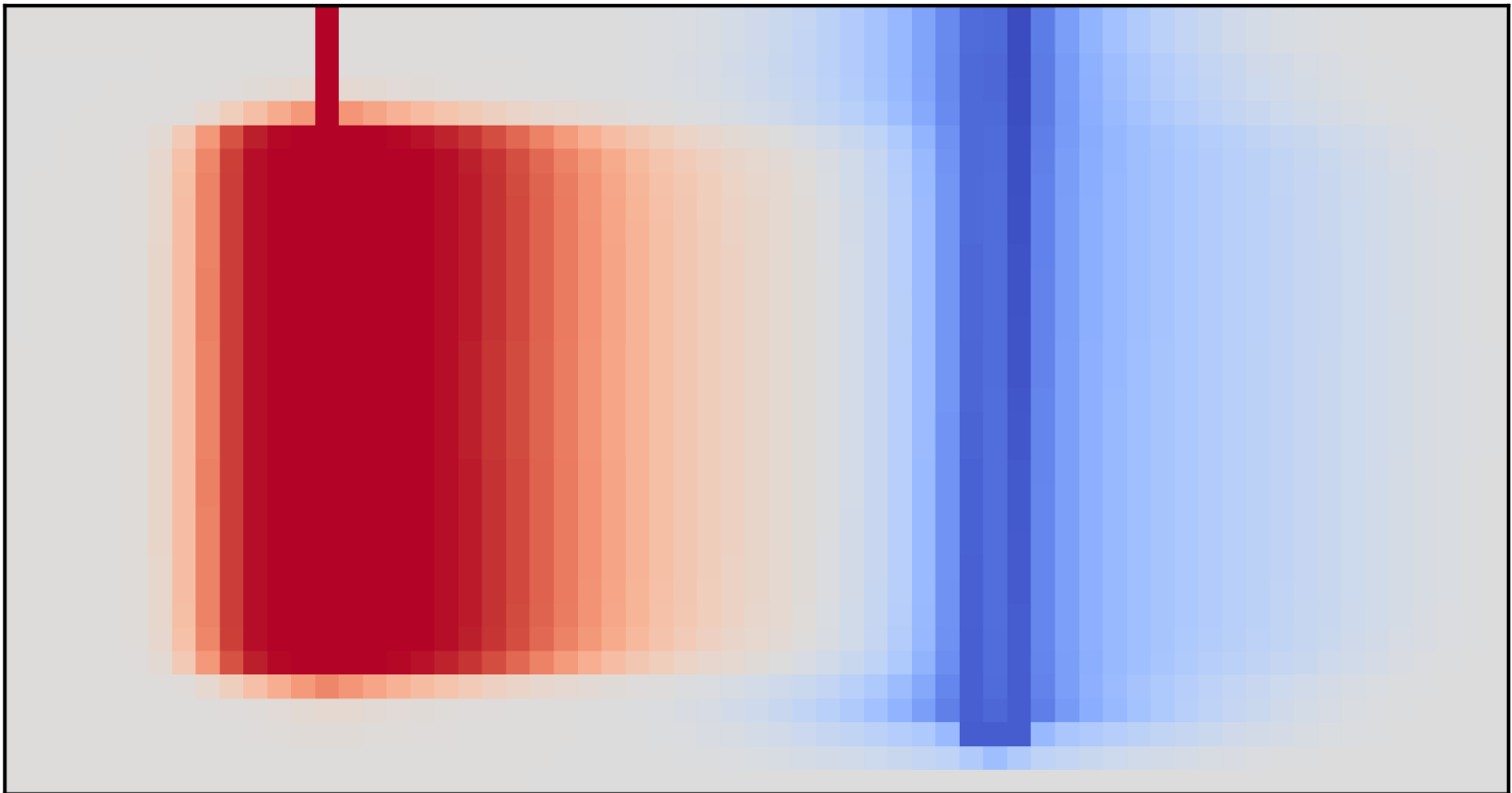
A simulation study to asses the effect of Aquifer Thermal Energy Storage systems on the efficiency of Borehole Heat Exchangers.

D. V. Koenders

TUDelft

Interaction between UTES systems

A simulation study to asses the effect of Aquifer Thermal Energy Storage systems on the efficiency of Borehole Heat Exchangers.

by

D. V. Koenders

to obtain the degree of Master of Science
at the Delft University of Technology,
to be defended publicly on Tuesday January 1, 2020 at 10:00 AM.

Student number:	4253612	
Thesis committee:	Dr. ir. J.M. Bloemendal,	TU Delft & KWR, supervisor
	Dr. N. Hartog,	Utrecht University & KWR, supervisor
	Prof. dr. ir. M. Bakker,	TU Delft
	Dr. P.J. Vardon,	TU Delft

An electronic version of this thesis is available at `http://repository.tudelft.nl/`.

TUDelft

Abstract

Underground thermal energy storage (UTES) is an efficient technique to fulfill the heating and cooling demand of buildings. UTES uses stable subsurface temperatures store and extract energy. This study covers two types of UTES systems: aquifer thermal energy systems (ATES), which store and extracts energy in aquifers by injecting or extracting warm or cold water, and borehole heat exchangers (BHE), which store thermal energy through conduction as warm or cold water is looped through a pipe installed in the subsurface. UTES systems in the Netherlands have seen a significant growth over the past years (Bloemendal, 2018) and are expected to contribute up to 20% of the heating and cooling demand of buildings by 2050 (Naber et al., 2016).

As more UTES systems are installed, the risk of unwanted interaction between different system increases. Studies have been conducted on the interaction between multiple ATES systems and on interaction between multiple BHE systems. However, ATES-BHE interaction is largely unknown. Few studies have been conducted. One found the interference of BHE systems on the efficiency of ATES systems to be minimal and interference of ATES systems on the efficiency of BHE systems to be significant (Drijver et al., 2013).

The objective of this study is to gather more insight in the interaction of ATES system on the efficiency of BHE systems. A numerical model is used to simulate an ATES well near a BHE system using SEAWAT (Langevin et al., 2008). The model is used to run different simulations, from which the efficiency of a BHE system is computed under different circumstances over a five year period. Simulations differed due to different parameters: ATES well temperature, number of aquifers in the subsurface, distance between both systems, and BHE system input.

Four conclusions are drawn from the results. First, groundwater and temperature interference from ATES systems affect the efficiency of a BHE system differently. Simulations show that the effect of groundwater flow induced by an ATES system always has a positive effect on the efficiency of a BHE system. The effect of temperature interference is dependent on the temperature of the ATES well. If the temperature of the ATES well increases the temperature gradient of the subsurface with respect to the BHE system input temperature, the BHE system operates at a greater efficiency, and vice versa. Groundwater was also found to interfere at larger distances between both systems compared to temperature.

Second, the degree of interference is related to the distance between the ATES and BHE system. For distances smaller than 0.5 times the thermal radius of the ATES system, interference from temperature was found to be dominant in the simulations. Thus, the net influence of an ATES well on the efficiency of a BHE system is dependent on well temperatures. However, as groundwater positively affects the efficiency of BHE systems, negative influences due to ATES well temperatures are smaller compared to positive influences. For distances larger than 0.5 times the thermal radius of the ATES system, groundwater interference was found to be the dominant factor. However, at these distances the net effect of ATES well interference was found to be insignificant. It can be concluded that for the setup used in simulations in this study that if interaction between an ATES system and BHE system is not desired, a distance of at least 0.5 times the thermal radius is advised. If significant interaction is desired, the distance between both systems should smaller than 0.5 times the thermal radius.

However, two points of concern have to be taken into account in relation to this second conclusion. First, the time step of 6 hours is relatively large. Simulations with smaller time steps showed a slightly lower degree of interference from the ATES system. This would allow UTES systems to be placed even closer together without significant interference. Due to computational and time restraints, simulations of multiple years have not been conducted with a smaller time step. Before applying the conclusions of this study to policy decisions, it is therefore advised to further explore simulations with smaller time steps over a longer period of time. Second, a discrepancy in the results of the simulations of balanced BHE systems was found. The cause of this discrepancy was an incorrect implementation of the variable density flow. Due to the nature of the cause, the efficiencies of the system in cooling phases are too small compared to reality. Conclusions have been based on the based on the outcomes of the system in heating phase. This does not make the results of this study useless. The results show system behaviour when ATES and BHE systems are placed close together. The exact degree of impact is uncertain due to the assumptions made during the research. However, the relative con-

clusions still hold true.

The third conclusion is that the depth placement of the ATES well screen has little to no effect on the amount of interference on the BHE system.

Fourth, it is important to realize that no energy is spontaneously generated or lost as BHE efficiencies increase or decrease respectively. Energy is simply exchanged between the ATES and BHE system through the subsurface. Whether that is disadvantageous depends on the energy demands of both systems. Most energy demands are imbalanced, meaning either cooling or heating demand is larger than the other. It is recommended to consider UTES system installations from a holistic point of view. Instead of trying to avoid interference with other systems, it is advised to consider combining systems when the combined energy demand of the systems is advantageous compared to their separate demands. Doing so is more complex and requires non-standardized policies for new installations. However, combining UTES systems when advantageous allows for imbalanced systems to be a part of a balanced overarching system and save energy.

Keywords: *Aquifer Thermal Energy Storage (ATES), Borehole Heat Exchanger (BHE), numerical model, interference, groundwater flow.*

Preface

This document marks the end of my time at TU Delft for the time being. It is the result my Master's Water Management and reflects a part of what I learned throughout the study. When I choose the topic for this thesis, I expected it force me out of my comfort zone as both part of the topic and type of research where new to me. Consequently, this project was not always easy and certain parts took longer than expected and often desired, which makes me appreciate the support I got throughout this project even more. There were upsides to this as well. I gained not only insight in the interaction between ATES and BHE systems, but also in my own work process, working at a company, the university and at the end even working from home.

Though this research was an individual project, many helped me along the way and I would like to express my appreciation to those.

First, I want to thank the members of my committee for their input and guidance. Mark Bakker for sparking my interest in groundwater and programming in the first place. And again for your input during my thesis process. Phil Vardon for not only providing input from a different viewpoint, but also providing ideas and possible solutions to that feedback. Niels Hartog for his guidance at KWR and providing valuable feedback throughout the process. And finally Martin Bloemendal, for guiding me through this project as my daily supervisor. Your input and interest in the subject matter helped me conduct this study as it stands before you.

In addition, Bas des Tombes deserves an expression of gratitude for his help with all the MODFLOW error messages I could not decipher on my own. I also want to thank my temporary colleagues at KWR for their input during my time there. Special thanks to Ina for all the carpool rides and conversations during the rides to and from Nieuwegein.

Furthermore, I wish to thank my friends at hokje 4.93 and 4.79 for their insight and support whilst working and even more for their companionship whilst not working. Jeroen, Leon, Stijn, Ludo, Bart, Sten, Ruben, Gijs, Bas, Gerben, Floris, Nicole, Ileen, Geerten, Maurice, Sophie, and Fransje, thank you for the coffee-breaks in the morning, the rounds table tennis in the afternoon and most of all the numerous games of cards we played during lunch. I have always felt at home at the fourth floor of the faculty, and believe the friends made during my Master's have been a big part of that. I also want to thank my (now ex-) housemates, Jorick and Vink. Especially during the months we all had to study from home I appreciated our joint breaks and home gym workouts.

Finally, I want to thank my parents, who made it possible for me to reach this point in my education. And I want to thank Roos, for all her support and patience throughout this study.

I hope you enjoy reading about the work I conducted.

D.V. Koenders
Heiloo, October 2020

Contents

Nomenclature

R	Retardation factor	$-$
R_{dist}	Distance ratio	$-$
V	Volume	m^3
v_k	Vertical hydraulic conductivity	md^-1
v_{gw}	Groundwater velocity	ms^{-1}

Sub- and superscripts

$()_{ambient}$ Ambient ATES well

$()_{aq}$ Aquifer

$()_{ATES}$ ATES well

$()_{cold}$ Cold ATES well

$()_{cool/cooling}$ Cooling function of BHE system

$()_{heat/heating}$ Heating function of BHE system

$()_h$ Hydraulic

$()_{in}$ In going

$()_{out}$ Outgoing

$()_{th}$ Thermal

$()_{warm}$ Warm ATES well

$()_{wellscreen}$ Well screen

$()_w$ Water

$()_{yearly}$ Yearly

1

Introduction

"Greenhouse gas emissions need to be reduced", "Fossil fuels need to be renounced as energy source", "Renewable energy sources need to be implemented", the Paris climate agreement triggered a transition in energy sources (Christoff, 2016). For the Netherlands, this results in a considerable reduction of greenhouse gas commissions (van Vuuren et al., 2017). Energy consumption however, has been relatively stable for the past 15 years (voor de Statistiek, 2019). Therefore, it is needed to find sustainable alternatives for long-used fossil fuels.

Worldwide, 40% of all energy is used for the heating and cooling demands of buildings (de Jonge et al., 2013), making it a significant contributor to total energy demands. In the Netherlands, 90% of the households are heated through the use of natural gas. Thus, current methods for household heating contribute significantly to the use of fossil fuels (Milieu, 2018). In order to advance the energy transition, methods to heat/cool houses in sustainable manner are needed.

Underground Thermal Energy Storage (UTES) can be used to heat and cool buildings in a sustainable manner. UTES makes use of the stable temperature of the subsurface to store and extract energy. This sustainable method of heating and cooling buildings reduces greenhouse gas emissions of household buildings with 60% for heating and up to 85% for cooling (Godschalk, 2017), making it a viable alternative to fossil fuels. In general, two types of UTES systems are used to heat and cool buildings in the Netherlands:

1. *Aquifer Thermal Energy Storage (ATES) systems:* ATES systems store heat in aquifers, natural layers of water-bearing materials in the subsurface. Figure 1.1 shows such a system as the second system on from the left. An ATES system consists of two wells, one cold and one warm. During warm periods, water from the cold well is used to cool the building. Doing so, the water heats up and is stored in the warm well. During the next cold period, the warm water is retrieved from the warm well and used to heat the building. The water cools down and is stored in the cold well. Then, a new warm period begins and water is retrieved from the cold well again.
   In an ATES system, water and thermal energy can freely move in the subsurface. This makes the system suitable to store large volumes of heat. ATES is therefore mostly used for bigger buildings, for example apartment or office buildings. The presence of an aquifer with sufficient capacity is needed to implement an ATES system.

2. *Borehole Heat Exchangers (BHE):* BHE systems circulate a medium through a (series of) pipe(s) in the subsurface, see Figure 1.1 on the far left. The water stays in the pipe and does not interact with the subsurface, but thermal energy can interact with the subsurface via conduction. Therefore, in cold periods, when the subsurface is relatively warm compared to the water in the pipe, thermal energy travels from the subsurface to the water in the pipe. Heating the water and cooling the subsurface. The warm water exiting the system is then used to heat the building. During warmer periods the opposite happens. Only thermal energy can move freely through the subsurface in this process. BHE systems have a smaller capacity compared to ATES systems and are therefore better-suited towards smaller buildings, for example households. BTES systems have less subsurface requirements compared to ATES systems as aquifers are not needed to store energy.
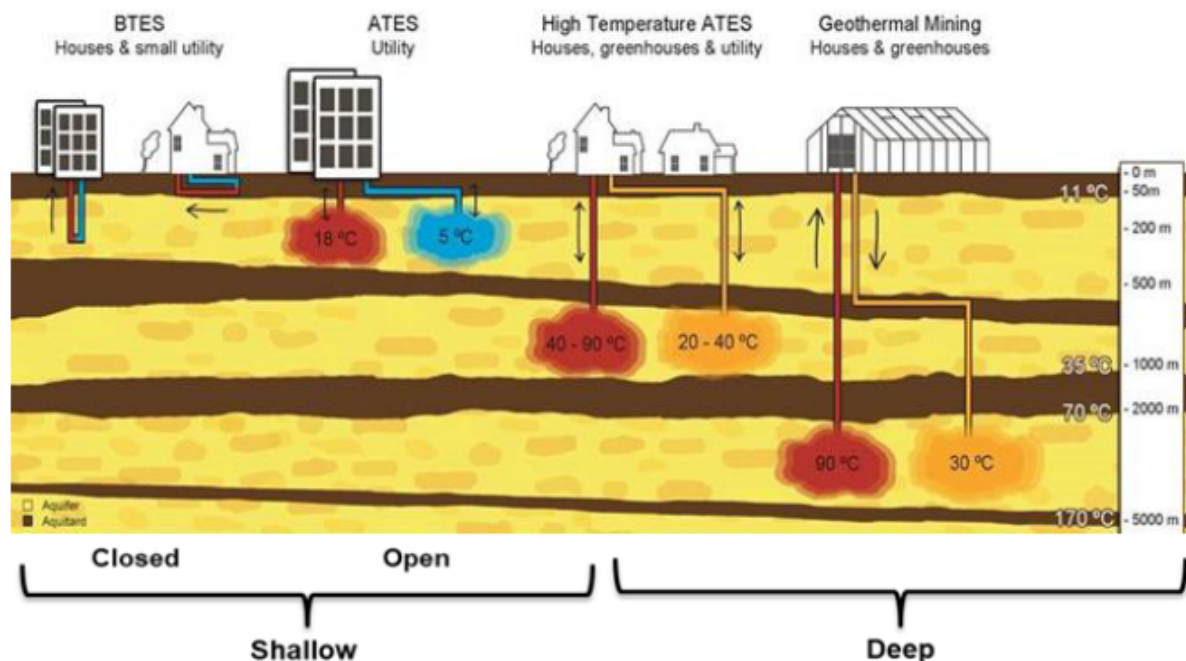
Figure 1.1: Various UTES systems. Deep systems (right) are not the subject of this research. Among shallow systems (left), ATES and BTES systems can be found. Bloemendal and Hartog (2018)

UTES systems in the Netherlands have seen a significant growth over the past years (Bloemendal, 2018). By 2050, UTES systems are expected to contribute up to 20% of the heating and cooling demand of buildings in the Netherlands. In order to fulfil such a demand, more UTES systems will be installed in the near future, over a hundred times as many as currently installed (Naber et al., 2016). As more UTES systems are installed, the pressure on use of the subsurface increases. Because buildings are located near each other in urban areas, different UTES systems are more likely to compete for space in the subsurface. This leads in turn to interaction between different systems. This is already happening in specific locations with high ATES potential, for example centre of Utrecht in the Netherlands (Bloemendal and Hartog, 2018). In order to warrant the efficiency of UTES systems in the future, the effect of interaction between different UTES systems needs to be taken account for. In particular the interaction between systems concerning ATES and BHE systems, as those are the most common types of systems used in the Netherlands.

Little research has been conducted on the effect of interaction between ATES and BHE systems so far. The interaction between two ATES wells of the same temperature has been studied and concludes that ATES efficiency improves if wells of the same temperature are placed closer together (Duijff, 2019). ATES systems mutually interact to a lesser degree than expected (Bloemendal and Hartog, 2018).

In other studies, interaction between ATES and BHE systems has been explored briefly. Interaction of BHE systems on ATES systems was found to be minimal. The influence of ATES systems on BHE systems however, was found to be more significant. The level of interaction depends on parameters like borehole placement, both along the depth of the subsurface as well as spatially, and considering the temperature of the ATES well (Drijver et al., 2013). More information however, is scarce. The modelling techniques used are not clear and specific conclusions are not drawn. How to deal with the interaction between ATES and BHE systems in practice is not clear.

Therefore, the interaction between ATES and BHE systems is needed. That is the subject of this study. To gain more insight in the mutual interaction between ATES and BHE systems when installed in close proximity and expand on current knowledge. The focus of the study is on the efficiency of BHE systems when placed in the thermal influenced area of an ATES system is present. By researching interaction between UTES systems, predictions can be made when these types of systems are planned to be installed close together and higher UTES efficiency can be achieved. Thus, more energy can be gained from this sustainable option for building heating and cooling. The study is defined along the following research question:

How is the efficiency of a Borehole Heat Exchanger affected by interference of an Aquifer Thermal Storage system?

To do so, it is needed to simulate thermal interactions between systems, therefore a simulation model is developed. This model is used to simulate various ATES and BHE setups and look into the efficiency of BHE system. With the data from the scenarios, insight in the mutual interaction between ATES and BHE systems is obtained.

This report continues with Chapter 2, which provides the necessary background information on ATES and BHE systems, as well as the key physical processes in the subsurface. Next, in Chapter 3, the numerical model is explained. Chapter 4 covers the results of the simulations. The discussion is presented in Chapter 5. Readers interested in the findings of this study are directed towards the conclusions in Chapter 6. Finally, the study ends with recommendations for the implementation of UTES systems and further research, which can be found in Chapter 7.

<div align="right">

2

</div>

Background

This chapter provides background information on ATES and BHE systems. The chapter starts with an introduction towards ATES system in Section 2.1, followed by an introduction towards BHE systems in Section 2.2. Next, a literature review on the current research on interaction between ATES and BHE systems is presented. This can be found in Section 2.3. Section 2.4 follows with a brief summary of the subsurface characteristics in the Netherlands.

2.1. A brief introduction to Aquifer Thermal Energy Storage

This section explains the processes occurring in an ATES system, along with the keywords associated with those processes. First, a general overview of the workings of an ATES system is given, followed by an explanation of how heat processes occur in ATES systems. Lastly, the characteristics and important definitions of an ATES system are described.

2.1.1. General working of an ATES system

A pipe is installed into a natural aquifer, enabling water to be pumped directly into the aquifer. The length of the pipe, and thus the depth of the system, depends on local geology, but shallow ATES systems can reach depths up to 400 meters in general (Bridger and Allen, 2005). The water is injected over a screened part of the pipe installed in the subsurface, This is called the well screen. The length of the well screen is dependent on the thickness of the aquifer. In general, water is injected in the aquifer along its entire depth. Exception being if the top of aquifer is located close to the surface, where energy loss to the surface can occur. ATES well screens are placed a distance from the surface in order to avoid thermal energy losses. An ATES system consists of two separate wells, one for warm 12°C-25°C and one for cold 5°C-12°C water. Wells are separated from each other to avoid thermal interaction and thus thermal energy losses. Separation can be done horizontally or vertically, see Figure 2.1. The striped part of the pipes in the figure represent the well screen of the ATES system. This is the part of the pipe where water is injected in the aquifer.

In colder periods, water is retrieved from the warm well and used to heat buildings. To do so, the water goes through a heat pump. In order to heat buildings, the water needs to be around 45°C-55°C. Water from the warm well reaches up to 25°C, a heat pump extracts heat from the groundwater to heat the building circuit to 45°C-55°C. Because thermal energy is extracted from the warm water, it cools down. The cold water is then stored in the cool well. During warm periods, the process is reversed. Cold water is retrieved from the cold well and used to cool the building. Afterwards, the water is stored in the warm well (Dickinson et al., 2009). If the heating demand is larger than the cooling demand, the system is not in equilibrium. More warm water is needed to fulfill the heating demand. This can be done by heating water through conventional methods. Alternative, more sustainable ways include using solar power to heat water in warm times and store it into the warm well.

Compared to BHE systems, ATES systems have more storage volume and require less investment. However, not all locations have a subsurface suitable for an ATES system, as sufficient aquifers have to be present. Also, ATES systems require more maintenance compared to BHE systems. Finally, ATES systems have more interaction with the subsurface due to both groundwater flow and thermal energy moving freely through the
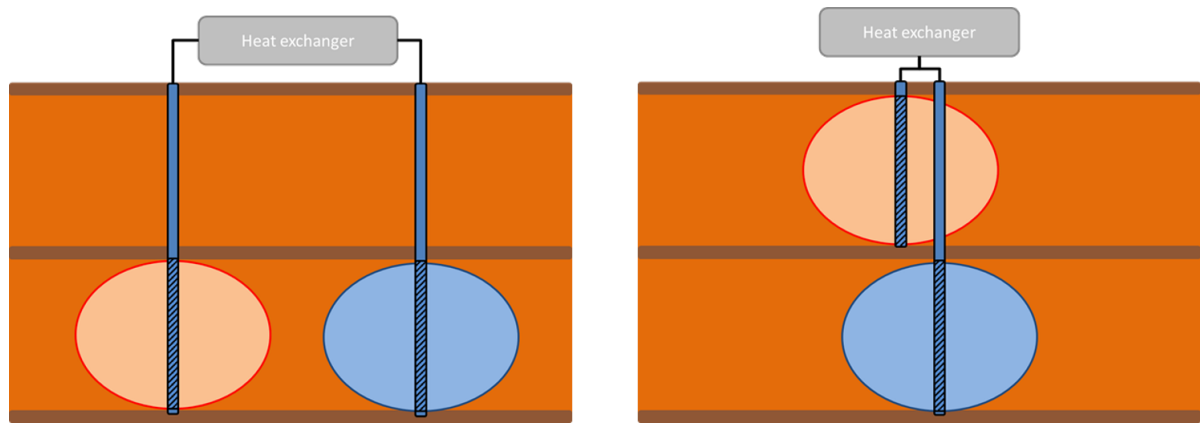
Figure 2.1: Horizontal (l) and vertical (r) separation of cold and warm wells.

aquifer (Drijver and Willemsen, 2001).

2.1.2. Heat transfer processes in an ATES system

Convective processes are often dominant in ATES systems. When water is pumped directly into the aquifer, the head around the borehole rises. Consequently, groundwater follows Darcy's law, see Equation 2.8, and travels away from the borehole. From areas with a high hydraulic head towards areas with a lower hydraulic head. When water is extracted from the aquifer, the opposite occurs. Along with this movement of groundwater, the thermal energy in the water travels as well, which is called convection. Convective processes near ATES systems also occur due to ambient groundwater flow. As the ambient groundwater flow travels past the borehole, the water body around the ATES system moves along with it, displacing any thermal energy in the water body.

Besides convective processes, conduction and dispersion also play an important role in ATES systems. On the edge of the thermal front, where a temperature difference between the water injected by the ATES system and the temperature of the water in subsurface occurs, conduction takes place. Thermal energy travels from high temperature groundwater to low temperature groundwater. Dispersion takes place when water travels through the ground with relatively high velocities. The dominant process is dependent on flow velocity. When the system starts injecting water at a constant rate, the thermal and hydraulic radius are small. Which means the area of the thermal front is small, causing high flow velocities at the edge of the thermal front. High velocities relate to higher amounts of dispersion. Thus, dispersion is dominant over conduction at this stage. As time passes and the thermal and hydraulic radius have increased as the water spreads through the subsurface, the thermal front becomes larger. This reduces groundwater velocity at the thermal front, reducing dispersion and increasing conduction losses. Conduction is now the dominant process.

Heat losses in ATES systems can be categorized in two categories. First, thermal energy is lost the boundaries of the stored volume due to dispersion and conduction. When small volumes of water are stored, dispersion is the dominant process. When larger volumes are stored, conduction becomes the dominant process.

Secondly, thermal energy is lost due to convective ambient groundwater flow as it displaces the water body. This is illustrated in Figure 2.2 for a warm water well. The ATES systems stores an amount of water underground. This bubble gets displaced by the ambient groundwater flow over time. When the extraction phase begins, the system extracts both the injected warm water and groundwater, with a lower temperature. Achieving a lower extraction temperature, resulting in a lower amount of thermal energy extracted.

2.1.3. ATES characteristics

This section introduces and explains several important characteristics of ATES systems.

Hydraulic radius

ATES systems store thermal energy in the subsurface, which contains mainly soil and water. As ATES systems are installed and used, the subsurface is disturbed and a new equilibrium has to be found. The water body
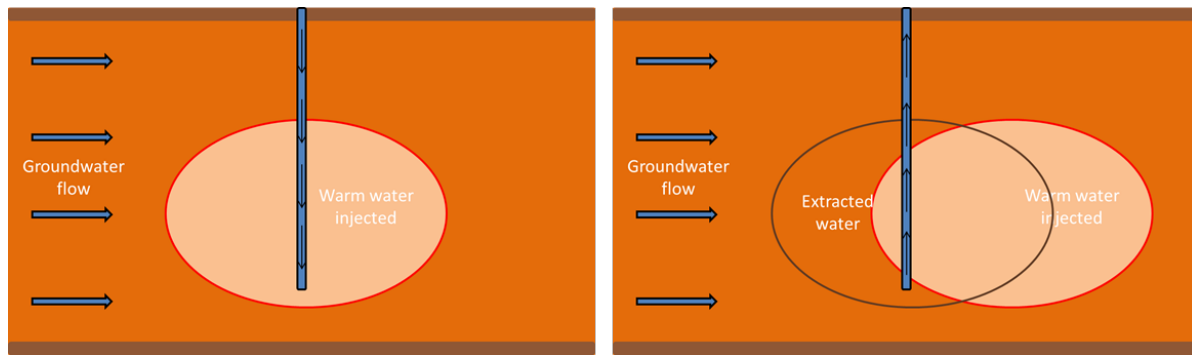
Figure 2.2: Heat loss due to ambient groundwater flow.

around an ATES system expands in the first years of usage. After five years, an equilibrium occurs. That is when ATES systems are most efficient.

This equilibrium is not a steady state. ATES systems injects and extracts water during the cycle. Doing so, groundwater and thermal energy are always moving. The groundwater travels in every horizontal direction after it has been injected in the aquifer. The well screens, where the water is injected, are multiple meters deep. Thus creating a cylinder of water around the well screen. The radius that creates a cylinder large enough the store the volume needed for the energy for the building is called the hydraulic radius, which is described as follows:

$$R_h = \sqrt{\frac{V_{in}}{n\pi L_{wellscreen}}} \quad (2.1)$$

where R_h is the hydraulic radius [L], V_{in} equals the injected water volume [L^3], n is the porosity of the porous medium [-] and L the length of the well screen [L].

Thermal radius

Within the hydraulic radius, a second, smaller radius can be found. The thermal radius, which is the radius of the area influenced by thermal energy based on the analytical solution for porous media (Bloemendal, 2018). Thermal energy travels slower compared to groundwater flow (Bloemendal and Hartog, 2018). Thus, the thermal radius is smaller compared to the hydraulic radius. The following equation describes the thermal radius of an ATES system:

$$R_{th} = \sqrt{\frac{V_i n c_w}{c_{aq}\pi L}} = \sqrt{\frac{n c_w}{c_{aq}}} R_h = \sqrt{\frac{1}{R}} R_h \approx 0.66 R_h \quad (2.2)$$

where R_{th} is the thermal radius [L], c_w the heat capacity of water [J M^{-1} K^{-1}], c_{aq} the heat capacity of the aquifer [J M^{-1} K^{-1}] and n the porosity of the aquifer [-]. The hydraulic and thermal radius are related, and the thermal radius can be approximated as the square root of one over the retardation factor R [-] times the hydraulic radius. Thermal retardation factor R is described as follows:

$$R = \frac{c_a q}{n c_w} \quad (2.3)$$

Due to the retardation factor, the thermal radius of an ATES is always smaller compared to the hydraulic radius. Figure 2.3 shows both radius's of an ATES system.

ATES efficiency

Efficiency is defined in this study as the ratio between the amount of thermal energy extracted from the system compared to the amount of thermal injected over an n-amount of cycles. The thermal recovery efficiency (η) only concerns the efficiency of the system in the subsurface. The following equation describes this relation.

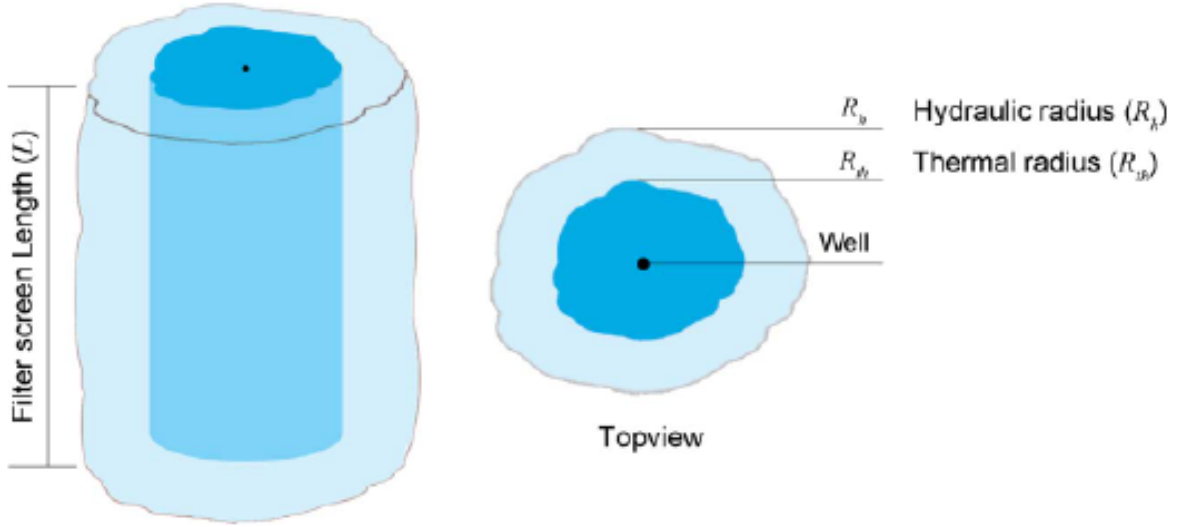$$\eta_{th} = \frac{E_{th,in}}{E_{th,out}} \quad (2.4)$$

Figure 2.3: Hydraulic and thermal radius of an ATES system (Bloemendal and Hartog, 2018).

where η_{th} is the thermal recovery efficiency [-], $E_{th,in}$ the amount of thermal energy injected in the aquifer and $E_{th,out}$ the amount of thermal energy recovered from the aquifer. The amount of thermal energy is described as follows

$$E = \Delta T Q \rho_w c_w \tag{2.5}$$

where ΔT the average temperature difference between the injected/extracted water and the average soil temperature [°C], Q the flow of water [L^3], ρ_w the density of water [ML^{-3}] and c_w the specific heat capacity of water [JM^{-1}K^{-1}]. For ATES systems, the true recovery efficiency can be defined by multiplying the extracted volume by its average temperature for each time step and dividing that over the injected volume times its average temperature for each time step:

$$\eta_{th,ATES} = \frac{\sum_{t_0}^{t_{end}} \Delta T_{out} Q_{out} \rho_w c_w}{\sum_{t_0}^{t_{end}} \Delta T_{in} Q_{in} \rho_w c_w} \tag{2.6}$$

$$\eta_{th,ATES} = \frac{\sum_{t_0}^{t_{end}} \Delta T_{out} Q_{out}}{\sum_{t_0}^{t_{end}} \Delta T_{in} Q_{in}} \tag{2.7}$$

A/V ratio and L/R_{th} ratio
The ratio of the area of the stored volume over the volume itself (A/V ratio) describes the relative contribution of boundary losses. A high A/V ratio means there is a relatively large amount of boundaries of the thermal zone. Since the boundaries are the location of conductive and dispersive processes, the majority of the heat losses, a high A/V ratio is a signal of an inefficient system. ATES systems with large storage volumes have a low A/V ratio, and thus high efficiency (Bloemendal and Hartog, 2018). The A/V ratio should be minimized for an efficient system.

Related to the A/V ratio is the L/R_{th} ratio, which describes the length of the well screen over the thermal radius. In general, systems with a high L/R_{th} ratio follow a cylinder, where injected water stays close to the well screen. The opposite, a low L/R_{th} ratio , has the shape of a pancake or disk. Extreme scenarios on both ends of the spectrum are not beneficial for the efficiency of the system, as for both a flat disk and an elongated cylinder the A/V ratio is high.

A minimal A/V ratio results in an optimal L/R_{th} ratio. According to Bloemendal and Hartog, the optimal L/R_{th} ratio is equal to 2.0 (Bloemendal and Hartog, 2018). This value was found by minimizing the surface area of the thermal radius. Doughty et al (1982) found the L/R_{th} ratio to be optimal between values of 1 and 4 (Doughty et al., 1982).
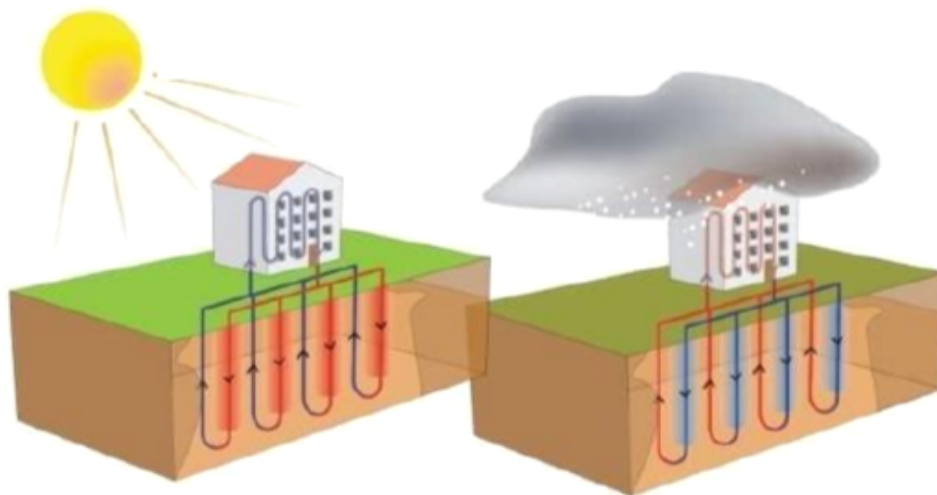
Figure 2.4: BHE system on a warm (left) and cool (right) day. (Waternet, 2020)

2.2. A brief introduction to Borehole Heat Exchanger

This section explains the processes occurring in an BHE system, along with the keywords associated with those processes. A similar structure as Section 2.1 is used. First, a general overview of the workings of an BHE system is given in Section 2.2.1, followed by the explanation of important processes concerning heat transfer in Section 2.2.2.

2.2.1. General working of a BHE system

BHE systems consist of a (series of) pipe(s) that loop(s) through the subsurface. The pipes are installed in boreholes. The pipe is often made of polyethylene. Space left in the borehole after pipe installment is filled with (thermal) grout. They can reach depths up to 200 meters and are considered shallow UTES systems. Water, or a glycerol-based thermal fluid, is pumped through the pipes. Figure shows this process as well. As the fluid travels through the pipe, it exchanges heat with the subsurface. During cool periods, the thermal fluid in the pipe is colder than the subsurface. Thus, thermal energy will travel from the subsurface to the pipe. Consequently, the fluid in the pipe heats up and the subsurface cools down. The relatively warmer fluid that is retrieved from the other end of the loop is then used to heat the building. To do so, a heat pump is required. The water from the end of the loop is about 3°C-4°C warmer compared to the fluid going in. In order to heat the building, a heat pump uses the energy from the subsurface BHE system to heat water up to 45°C-55°C. This water goes through a loop inside the building, heating it.

During warm periods the subsurface is colder compared to the fluid in the pipe and the opposite happens. Thermal energy travels from the pipe towards the subsurface, thus cooling the fluid in the pipe. The fluid is then used to cool the building. Sometimes, a heat pump is used in this case as well. Because thermal energy is added to the subsurface in this process, the subsurface surrounding the borehole(s) heats up during this period.

BHE systems have less environmental restrictions compared to ATES systems. However, BHE systems have a lower capacity too. Because of this, they are better suited for households, which have a lower energy demand (Lanahan and Tabares-Velasco, 2017).

2.2.2. Heat transfer processes in a BHE system

Conductive processes are dominant in BHE systems. The temperature difference between the fluid in the borehole(s) and the subsurface causes a heat flow between both, from high to low temperatures. The rate at which this thermal energy transfer occurs is dependent on the medium and the thermal energy gradient. Once thermal energy has been stored in the subsurface, it spreads due to more conductive processes.

Convective processes in BHE systems occur only due to ambient groundwater flow. One study found that groundwater flow has a positive effect on BHE systems that only heat or cool (Panteli et al., 2018). Groundwa-

ter flow displaces the thermal energy around the BHE system, allowing for a greater temperature difference between the BHE system and the subsurface.

For BHE systems that have both a heating and a cooling function, the impact of groundwater flow differs. The net impact of groundwater flow is dependent on the frequency with which the BHE system switches from heating to cooling. As the system changes from heating to cooling, the subsurface around the system is still relatively warm due to the heating phase. Thus, the cooling phase is more efficient for until the subsurface around the BHE system cools down again. During this period of time, groundwater flow has a negative effect on the BHE system as it displaces the profitable thermal energy around the pipe. However, after the subsurface reaches ambient temperatures, groundwater flow has a positive effect as it 'refreshes' the subsurface around the pipe, keeping thermal exchange rates constant. Thus, the net effect of groundwater flow on a BHE system is dependent on the frequency with which the system switches between heating and cooling. Frequent switches indicate a negative effect from groundwater flow, infrequent changes a positive effect. The exact result depends on the setup of the BHE system and subsurface characteristics. However, the effect of groundwater flow is found to be positive in general (Angelotti et al., 2014).

2.3. Governing processes

This section explains important processes that facilitate UTES technologies. First, in Section 2.3.1, the scope of the research is given. Next, different processes occurring in the subsurface in the fields of geohydrology (Section 2.3.2) and thermodynamics (Section 2.3.3) are explained. Finally, a review on the history of research on interaction between ATES and BHE systems is given in 2.3.4.

2.3.1. Scope

UTES systems operate above and below the surface. Above surface, a loop pipes warm/cold water through a building. Below surface, a separate loop pipes water through the subsurface. Both loops meet in a heat pump, which transfers the thermal energy and converts it to the required values for either above or subsurface loops. In this study, only the subsurface part of an UTES system is considered. Starting where the loop exists the heat pump and enters the subsurface and ending where the loop exits the subsurface and enters the heat pump again. Implications caused by this scope are discussed in Section 5.1.

2.3.2. Groundwater flow

Groundwater is water in the subsurface, held by a porous medium, for example sand. The subsurface exists of aquifers, layers of water-bearing material through which groundwater can flow with relative ease, and aquitards, layers of water-bearing material through which groundwater cannot flow with relative ease (for example clay). When an aquifer is surrounded by aquitards or otherwise enclosed by materials that do not allow water to flow through easily, it is called a confined aquifer. Aquifers can also be unconfined, but those fall outside the scope of this research as most UTES systems operate in confined aquifers.

The scientific field that studies groundwater is called geohydrology. The basis of groundwater flow rests in the formula that is called Darcy's law (Whitaker, 1986). It describes the flow of groundwater through a porous medium:

$$\vec{q} = -k\vec{\nabla}h \tag{2.8}$$

where $\vec{q}$ is now the specific discharge vector in the direction of flow [LT^{-1}], k the hydraulic conductivity [LT^{-1}] and $\vec{\nabla}$ the difference in hydraulic head [L]. Due to anisotropy, the hydraulic conductivity of a porous medium may differ in the three principal flow directions.

The hydraulic conductivity describes how easy a fluid travels through a porous medium. This is described as follows:

$$k = \frac{\kappa \rho g}{\mu} \tag{2.9}$$

where κ the intrinsic permeability of the porous medium [L^2], ρ the density of the fluid [ML^{-3}], g the acceleration of gravity [LT^{-2}] and μ the dynamic viscosity of the fluid [MLT^{-1}]. Given that aquifers in the simulations in this thesis are homogeneous, κ remains constant, just like the gravitational constant g. This means μ and ρ have the biggest impact on changes in the hydraulic conductivity in the simulations in this study.

2.3.3. Heat transport processes

In general, three heat transport processes can be distinguished: conduction, convection and dispersion. All three processes are described in this section. How these processes occur in ATES and BHE systems is described in Section 2.1.2 and Section 2.2.2 respectively. The terms heat and thermal energy are both used and have the same meaning in this context.

Conduction

Conduction occurs when areas with a high temperature are located next to areas with a lower temperature. In an UTES system, this occurs along the boundaries of the water bodies caused by the ATES system. Higher temperatures, and thus more thermal energy, causes the molecules to collide more than water and soil with lower temperatures. Because of this, heat travels from high temperature to lower temperatures. The temperature difference between the fluid in the borehole(s) and the subsurface causes a heat flow between both, from high to low temperatures. Conduction is described by Fourier's law (Bonetto et al., 2000):

$$q_x = -\lambda \frac{dT}{dx} \tag{2.10}$$

where q the local heat flux [WL^{-2}], λ the thermal conductivity of the porous medium [WL^{-1}K^{-1}] and ΔT the temperature gradient [K]. The flux is equal to the temperature difference times the thermal conductivity of the porous medium. Note that the equation for heat flux and discharge are very similar. Both are based on the concentration difference between both sides and the ease with which the concentration can travel through the porous medium.

Convection

Convective processes transfer heat due to the bulk movement of a fluid or gas, in this case groundwater. A big influence on convection is ambient groundwater flow. In the Netherlands, groundwater flows between 25-200 meters on a yearly basis (Pellenbarg, 1997). If ambient groundwater flow is present near a UTES system, thermal energy injected in the subsurface by the UTES system is transferred away from the system. In the case of ATES systems, injecting or subtracting water into/from the subsurface causes a groundwater flow from/towards the bore hole as well. Thus, heat is transferred in the same direction. Convection is described through the following equation:

$$\frac{\partial T}{\partial t} = -\nabla(vT) \tag{2.11}$$

where $\frac{\partial T}{\partial t}$ represents the concentration change over time [KLT^{-1}], ∇ represents the gradient vector in the x, y, and z direction [-], v is the groundwater velocity [LT^{-1}] and T is the temperature [K].

Dispersion

Dispersion is the local variation of pore flow velocity that results in mixing of water. This process is highly dependent on local geology and incredibly heterogeneous (Burdett and Judd, 1983). Dispersion is directly related to flow velocity: high flow velocities cause more energy loss due to dispersion. Dispersion, similar to conduction, occurs at the boundary of the water body of the ATES system. Dispersion is described as follows:

$$\frac{\partial T}{\partial t} = \nabla^2(DT) \tag{2.12}$$

where the dispersion coefficient D is described as:

$$D = \alpha \frac{q}{n} \tag{2.13}$$

where α is the dispersivity [m], q the specific discharge [m/d] and n the porosity [-]. Conduction and dispersion are both processes that induce heat loss at the boundary of the water body of the ATES system. The dominant process is related to the flow velocity of the fluid. High flow velocities cause dispersion to be dominant, lower flow velocities conduction (Bloemendal and Hartog, 2018). Other variables, such as the size of the cross-section and the shape of the thermal front also influence this relationship.

2.3.4. ATES-BHE interaction

Thermal interference by single BHE systems on an ATES system was found to be negligible (Drijver et al., 2013). This makes sense, as BHE system in general have a smaller capacity compared to ATES systems and their thermal radius is smaller as well. Thus, a single BHE system is simply too small to affect an average ATES system significantly. However, as far as interference was present, the temperature of the subsurface decreases up to 0.3°C For cooling purposes, this is beneficial. A lower subsurface temperature results in a higher temperature difference, thus decreasing the volume of water needed to fulfill cooling demands. For heating purposes, the opposite effect applies and more water needs to be used to fulfill heating demand. The effect of multiple BHE systems located in close proximity of an ATES system was not mentioned to be significant, clear data to back these conclusions are missing however.

Thermal interference by a warm ATES well on a BHE system was found to be significant (Drijver et al., 2013). During warm periods, the increased subsurface temperature makes cooling more difficult for the BHE system. But during cold periods, the same increased surface temperature allows easier heating. As heating demands in the Netherlands are greater compared to cooling demands, an increase in efficiency is likely. However, results varied between an 8% increase to a 7% decrease in efficiency, most scenarios experienced an increase in efficiency. These differences were not explained.

The effect of a cold ATES well on a BHE system was found to be insignificant. The thermal interference caused a decrease in the efficiency of the BHE system. However, the mitigating (thus positive) effect from the groundwater flow caused by the ATES system cancels out the negative effect. Efficiency varied between a 1% decrease and a 2% increase.

Finally, a larger ATES system was found to have an increased effect compared to a smaller ATES system. This makes sense as a larger ATES system has an increased capacity and will thus interfere more with a BHE system. The study suggests different options to mitigate these effects, among which adjusting the height and location of the wells and adjusting the temperature of the ATES well. It should be noted that the effect of the distance between the ATES and BHE system was not tested. This is an important parameter as it can greatly influence policy concerning UTES systems and optimal use of the subsurface.

Current Dutch laws and regulations concerning ATES and BHE interactions can be split up in two parts: installing a new closed system (BHE) near a current open system (ATES) and vice versa. When installing a new BHE system near a current ATES system, there may be no overlap in the depth of both along with placement in where the BHE system would be in the thermal influence zone of the BHE system, i.e. the thermal radius (SIKB, 2020). When installing a new ATES system near a current BHE system, similar criteria need to be complied with. There needs to be no overlap in the depths of both systems. Along with that, the BHE system should not be placed within the thermal and hydraulic radius of the ATES system. If overlap occurs, interference is currently assumed and systems should be placed further apart.

2.4. Geohydrology of the Dutch subsurface

This study is focused towards the interaction of ATES and BHE systems in the Dutch subsurface. In 2018, 85% of the ATES systems used worldwide, were located in the Netherlands (Fleuchaus et al., 2018). BHE systems do not have many subsurface requirements in order to function properly. ATES systems however, require aquifers of sufficient size in order to store the required amount of water. This is partly why most ATES systems in the world are installed in the Netherlands. Its subsurface consist of aquifers and aquitards, allowing for widespread use of ATES systems.

Geluk conducted a study about the geohydrological characteristics of the Dutch subsurface. Almost the entirety of the Netherlands rests above an aquifer between 50 meters in the east and 300 meters deep in the west of the country. Within the aquifer, aquitards are found (Geluk et al., 2007). Figure 2.5 shows an approximation of the aquifer/aquitard composition over a cross-section in the middle of the Netherlands. As seen in the picture, the west of the Netherlands has a three-layer aquifer. In the middle this becomes a two-layer system to ultimately end up in a single aquifer in the east. The aquifers consist of sand with a hydrological conductivity of 20-50 meters per day.

This study will assume two different cases to represent the Dutch subsurface. A single-aquifer system and a two-aquifer system. The single aquifer is 100 meters deep, consists of sand and is enclosed by an aquitard consisting of clay on both sides. This type of subsurface can be found in the middle and east of the Netherlands. In the east, the thickness of the aquifer would be smaller.
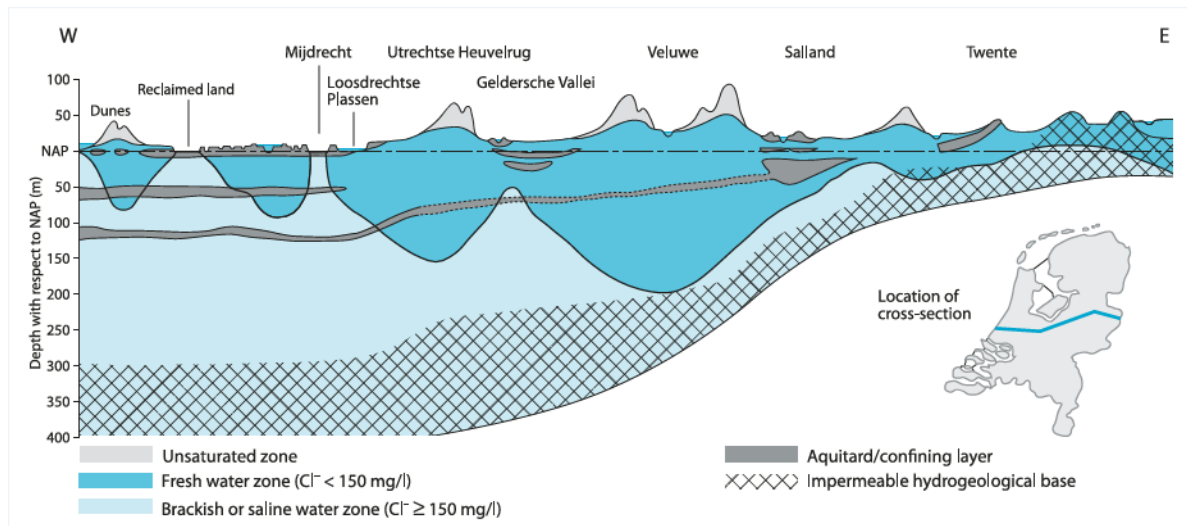
Figure 2.5: Cross-section of the Dutch subsurface (Geluk et al., 2007).

The two-aquifer system is similar, a third aquitard however is located in the middle of the original aquifer, splitting it into two smaller, equally large aquifers. This system is representative for the subsurface in the west of the Netherlands. The entire subsurface is assumed to be confined and saturated.

<div align="right">

3

</div>

Methods

In order to gain insight in the interaction between ATES and BHE systems in close proximity as described by the processes in the previous chapter, a numerical model was built to simulate these processes. This chapter describes the process of how the model came together. The chapter starts with Section 3.1 by describing the used simulation software. Next, in Section 3.2, the model setup is explained, followed by the scenarios in Section 3.3.

3.1. Simulation software

SEAWAT was used to simulate combined groundwater flow and thermal energy transport. SEAWAT uses MODFLOW and MT3D respectively to simulate those processes.

MODFLOW

MODFLOW is a computer program that solves groundwater flow through porous medium problems in three dimensions (Harbaugh et al., 2000). To do so it uses the finite-differences method. The model area is divided into cells, based on a grid in the horizontal plane and a specified number of layers. For each cell, the change in groundwater head in that cell is computed per time step. Water can be injected to or extracted from the system through the use of wells. Solutions are obtained through the following equations (Harbaugh et al., 2000):

$$\frac{\partial}{\partial x}(K_{xx}\frac{\partial h}{\partial x}) + \frac{\partial}{\partial y}(K_{yy}\frac{\partial h}{\partial y}) + \frac{\partial}{\partial z}(K_{zz}\frac{\partial h}{\partial z}) + W = S_S\frac{\partial h}{\partial t} \qquad (3.1)$$

where K_{xx}, K_{yy} and K_{yy} represent the hydraulic conductivity along their respective axis (x, y and z) [L/T], h is the hydraulic head [L], W the volumetric flux per unit volume representing sources or sinks [T^{-1}], S_S the specific storage of the medium [L^{-1}] and t time [T]. Input files for MODFLOW can be made with Python using the FloPy package as described by (Bakker et al., 2016). An additional advantage is that this allows for the many existing packages in Python to be used in the model setup.

MT3D

MT3D can be used in conjunction with MODFLOW in order to solve solute transport equations in the subsurface, the MT3D-USGS version is used in this study (Zheng et al., 2012). The following equation describes the general formula to solve the solute transport in a groundwater system used in MT3D software.

$$(1 + \frac{\rho_b K_d^k}{\theta})\frac{\partial(\Delta C^k)}{\partial t} = \nabla[\theta(D_m^k + \alpha\frac{q}{\theta})\nabla C^k] - \nabla(qC^k) - q_s'C_s^k \qquad (3.2)$$

where ρ_b is the bulk conductivity [ML^{-3}], K_d^k is the sorption coefficient [L^3M^{-1}], θ is the porosity [$-$], C^k is the solute concentration [ML^{-3}], t is the time [T], D_m^k is the molecular diffusion coefficient [L^2T^{-1}], q is the specific discharge [LT^{-1}] and α the dispersivity tensor [L].

The left side of the formula describes the rate of change of the concentration. The right describes several
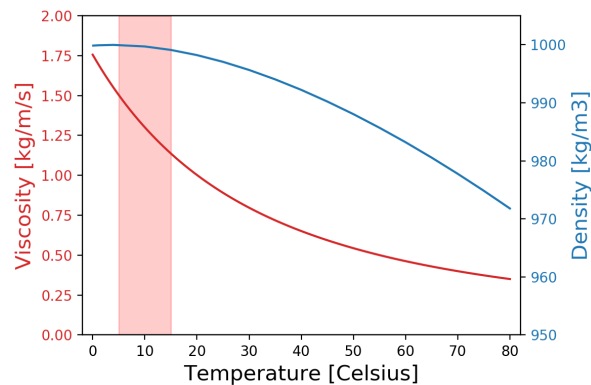
Figure 3.1: Density and dynamic viscosity of water relationship with temperature. The highlighted area is the expected temperature range of the model.

processes in the subsurface. From left to right the terms represent diffusion, dispersion, convection (or advection, which describes the same in the terminology used in this study) and the source term respectively.

The following equation describes heat transport and has been adjusted in order to show the similarity with Equation 3.2 (Thorne et al., 2006):

$$(1 + \frac{1-\theta}{\theta} \frac{\rho_s}{\rho} \frac{c_{P,solid}}{c_{P,fluid}}) \frac{\partial(\theta T)}{\partial t} = \nabla[\theta(\frac{k_{T,bulk}}{\theta \rho C_{P,fluid}} + \alpha \frac{q}{\theta})\nabla[T]] - \nabla[qT] - q_s' T_s \qquad (3.3)$$

where c_p is the specific heat capacity of the fluid or solid $[L^2 T^{-2-1}]$, T is the temperature [] and $k_{T,bulk}$ is the bulk thermal conductivity of the solid $[ML^3 T^{-2-1}]$. The left side of the equation describes the rate of change of temperature, effected by retardation. The right side describes different processes in the subsurface. The first term is conduction and dispersion, the second term convection and the last term is the source term.

The similarity between the mathematical approach behind solute transport and heat transport shows that the transport of thermal energy in the subsurface can be modeled using MT3D. This is also argued in the user manual of MT3D (Langevin et al., 2008).

There are three limitations when using MT3D for heat transport simulation (Langevin, 2009), all of which are adhered to when running simulations:

1. An isotropic representation of the thermal conductivity.

2. $D_{m,temp}$ is constant throughout the model run time.

3. Thermal conductivity should be influenced by temperature over large thermal ranges.

SEAWAT
SEAWAT is a program that couples MODFLOW and MT3D to include variable density and variable viscosity groundwater flow (Langevin et al., 2008). Both the density and dynamic viscosity of water are influenced by temperature. Figure 3.1 shows this relationship. The highlighted area shows the expected temperature range within the simulations.

The density of water varies between 1000 kg/m^3 for water of 5°C and 997 kg/m^3 for water of 25°C. Dynamic viscosity ranges between 1.55 kg/m/s for water of 5°C and 0.90 kg/m/s for water of 25°C, a change of over 40%. To estimate the influence of temperature-dependent density and viscosity, a series of test simulations is run. The model to test this consists of a single aquifer between two aquitards, with a BHE system in the middle. These tests are solely to determine the influence of different configurations regarding SEAWAT packages for further simulations. To solve for groundwater and temperature solutions, different methods are tested. First, the model is solved using SEAWAT with both the packages for variable density and variable viscosity. Next simulations are conducted using SEAWAT were only variable density or variable viscosity is accounted for, as well as a simulation using SEAWAT without any packages. Finally, a simulation is conducted where
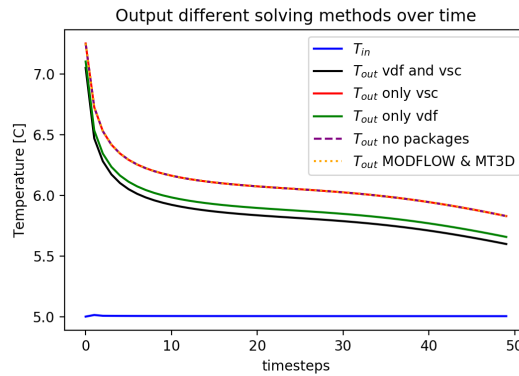
Figure 3.2: Results of a BHE model that compares the inclusion of variable density and variable viscosity flow.

MODFLOW and MT3D are used for groundwater and temperature solutions respectively. All simulations run for 50 time steps of 6 hours, only a BHE system is modeled. The temperature input of the BHE system ranges between 5°C and 15°C. The results can be found in Figure 3.2. The black line represents model output with both variable density and viscosity flow included. The green line represents model output with only variable density flow enabled. The remaining simulations, only variable viscosity flow, neither variable density nor variable viscosity flow and MODFLOW/MT3D solutions, are represented by the red, purple and orange lines respectively. Results show a difference in outcomes based on the packages enabled. SEAWAT without any packages (purple) and MODFLOW/MT3D (yellow) are expected to have the same outcome. However, SEAWAT with only variable viscosity flow has exactly the same outcome. This is unexpected as viscosity varies within the temperature ranges used in the simulation. Because of this, a different outcome is expected. Furthermore, a difference between the outcomes using only the variable density flow package and using both the variable density and variable viscosity flow simulation is observed. Thus, variable viscosity does only affect the outcome when variable density is also included.

A higher temperature results in lower density and viscosity. In turn, this affects the hydraulic conductivity of the water according to Equation ??, where κ is the intrinsic permeability [m^2], ρ the density [kg m^{-3}]. g the gravitational constant [m s^{-2}] and μ the viscosity [kg m^{-1} s^{-1}]. As density experiences a smaller value change compared to viscosity, the hydraulic conductivity increases as temperature increases. Other parameters that change due to variable density are molecular diffusion coefficient D_m and the sorption coefficient K_d, both of which increase as temperature increases. This in turn increases heat transport, see Equation 3.2. The results of Figure 3.2 show that both variable density and variable viscosity flow have a significant impact on the output of the model and need to be accounted for.

However, basic groundwater flow-solute transport models have a linear working. First, MODFLOW is used to compute the groundwater flow solution for all time steps. Next, MT3D is used to calculate the solute transport solution for all time steps. As a result only one value for density and viscosity can be used in the model.

By using SEAWAT, the groundwater flow and solute transport solutions are computed one time step at a time. After the solution has been calculated, the density and dynamic viscosity of each cell is determined for the next step based on the solute transport (or heat) solution of the current step. This way, variable density and viscosity can be accounted for in the modelling process. The relationship between the dynamic viscosity of water and temperature is approximated according to (Voss, 1984):

$$\mu_T(T) = 2.394 10^{-5} 10^{\frac{248.37}{T+133.15}} \tag{3.4}$$

Finally, it is noted that not only density and dynamic viscosity are temperature dependent. Water density influences the thermal diffusivity and thermal distribution factor, making both of those dependent on temperature. However, since simulations have a small variation over the expected temperature range, and the effect of the density variation on the thermal diffusivity and thermal distribution is even smaller, those changes are insignificant and are not included in the numerical model (Langevin et al., 2008).
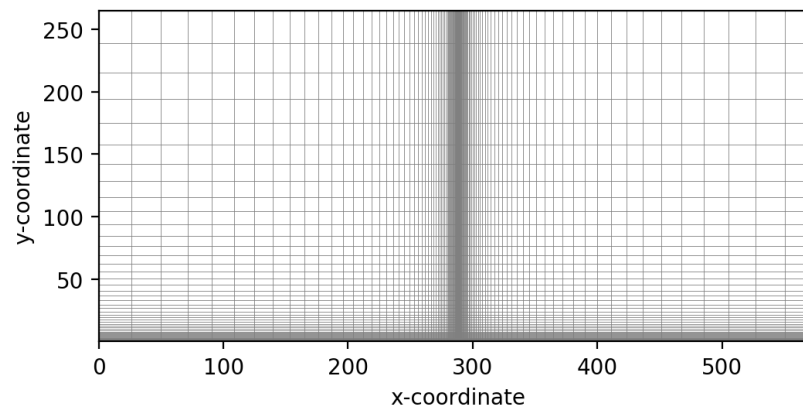
Figure 3.3: Simulation grid layout

3.2. Model Setup

This section describes the actual setup of the numerical model. The model is built up out of cells, which have properties. First, the layout of those cells, the spatial discretization, is explained. Next, the properties used in each cell are explained along with the actual materials used and their properties. The boundary conditions of the model are discussed. Then, the time step used in the model is explained. Finally, the configurations of the BHE and ATES systems are explained.

Spatial discretization

The model is discretized into cells. The size of these cells is described through the number and size of rows, columns and layers. Figure 3.3 shows the horizontal grid layout for the model, which shows the rows and columns. Only half of the total area is modelled due to the symmetric layout of the systems. This reduces model run time. The simulation grid focuses on the area surrounding the BHE system, located in the middle of the grid on the bottom row. Heat transfer via conduction is slow. In order to meet Peclet and Courant conditions, small time steps and spatial distances are needed. As the distance from the BHE system increases, cells gradually become larger. The ATES system is located on the left side of the BHE system, its exact location depends on the setup and is discussed in Section 3.3. Left of the ATES system, the model boundary is far enough away to ensure no boundary problems occur due to the ATES system.

Cell properties

The model area is divided into cells. MODFLOW computes the groundwater heads in each cell, MT3D calculates the temperature in each cell. In order to make the cells resemble the subsurface, each is given properties. The following properties are assigned to each cell:

- *Horizontal and vertical hydraulic conductivity:* the hydraulic conductivity describes the ease of a fluid traveling through a porous medium. The conductivity of a porous medium differs in the horizontal and vertical direction, which is called anisotropy. Based on literature, the vertical hydraulic conductivity is assumed to 10% of the horizontal hydraulic conductivity (Childs, 1957).

- *Porosity:* the amount of empty space of a material as a percentage. In fully saturated aquifers, which are assumed in this study, this empty space is filled with water. Thus, the porosity of a porous medium influences other variables, such as density and thermal conductivity.

- *Bulk density:* the specific weight of the material in a cell. Porosity is accounted for in this property. If, for example, a cell consists of sand and has a porosity of 30%, the bulk density is 70% packed sand and 30% water.

- *Bulk molecular diffusivity:* defines the speed of heat propagation by conduction during changes of temperature. A higher molecular diffusivity results in faster heat propagation. The thermal molecular diffusivity is calculated by dividing the bulk thermal conductivity of a material over the porosity of the material times the density and heat capacity of the fluid:

$$D_{m,temp} = \frac{n\kappa_w + (1-n)\kappa_s}{n\rho_w c_w} \tag{3.5}$$

where $D_{m,temp}$ is the bulk molecular diffusivity [], n is the porosity $[-]$, κ is the thermal conductivity of a material $[Wm^{-1}K^{-1}]$, ρ_w the density of water $[M^{L-3}]$ and c_w the specific heat capacity of water $[J^{L-3}K^{-1}]$.

- *Thermal distribution coefficient:* represents the thermal equilibrium between the fluid and the solid and is calculated as:

$$K_d = \frac{c_s}{\rho_w c_w} \tag{3.6}$$

where K_d the thermal distribution coefficient [], c_s the specific heat capacity of the solid $[J^{L-3}K^{-1}]$, ρ_w the density of water $[M^{L-3}]$ and c_w the specific heat capacity of water $[J^{L-3}K^{-1}]$.

Material properties
Different materials can be distinguished when modeling UTES systems: soil properties, pipe and grout properties and heat carrier fluid properties (HCF) need to be specified.

Soil properties
Aquifers are assumed to consist of packed sand and are enclosed by aquitards of packed clay. Both soil types are assumed to be completely saturated with water (Sudicky, 1986). In practice, materials in both aquifers and aquitards are heterogeneous and variate spatially. For the numerical model however, it is assumed that aquifers consists solely of packed sand, with no further variations. The aquitards on the top and bottom of the aquifer consist of packed clay. The properties of both soil types can be found in Table 3.1. Due to anisotropy, the vertical hydraulic conductivity is one tenth of its horizontal component.

Heat carrier fluid properties
The HCF is the fluid that circulates through the pipe of the BHE system. Three different types of HCF's are described in Table 3.1. These HCF's differ in freezing point: water freezes at 0°C, 25%-monoethylenglycole at -14°C and 29%-ethanol at -18.5°C. The expected temperature range of the BHE system is 5°C to 15°C. Because none of the HCF's are expected to freeze within these ranges, the HCF with the highest freezing point is used in the numerical model: water. Water does not have a hydraulic conductivity. However, this property is used to guide the water along the pipe. This is explained in the Paragraph about BHE configuration later in this Section.

Grout and pipe properties
In practice, a circular borehole is drilled. In this borehole a U-shaped pipe is place, see Figure 3.7. The remainder of the borehole is filled with a filler material: grout. These materials occupy little space, especially in relation to the entire area influenced by the BHE system. In the numeric model, cells with sizes as small as one centimeter would have to be put in. These small cells cause computational havoc. Thus, grout and pipe cells are combined into one cell, which is called a grout cell. These cells simulate both the pipe material and the filler material. Thus, its properties are a combination of the two. An average system contains 7% pipe material and 93% grout (Hellström and Sanner, 2000), the 'bulk grout' cells follow the same distribution.

Three different types of grout are distinguished: standard bentonite/cement grout, thermally enhanced grout and water (Hellström and Sanner, 2000). Different types of thermally enhanced grout can be distinguished as well. They consist of standard grout with the addition of a thermal enhancer in the form of limestone, silica, sand, graphite and other aggregates. Each of which has different advantages and disadvantages. In this study, thermally enhanced grout is used and defined as concrete with the addition of limestone (Hellström and Sanner, 2000). Its properties can be found in Table 3.1 along with the pipe material in BHE systems, which is often polyethylene (Hellström and Sanner, 2000), and the resulting properties of the 'bulk grout' cells, which follow a distribution of 7% pipe material and 93% grout material. Since the pipes are waterproof, the grout cell have a porosity of 0.

Boundary and initial conditions
Without modification, all cells in the model are active. Meaning water and temperature can move freely in

Table 3.1: Material properties used in numerical model.

Material	$h_k[mday^{-1}]$	$v_k[mday^{-1}]$	$n[-]$	$\rho[kgm^{-3}]$	$k[Wm^{-1}K^{-1}]$	$c[Jkg^{-1}K^{-1}]$
Sand	25	2.5	0.32	2120	1.8	800
Clay	0.00864	0.000864	0.40	1746	1.8	1381
Water	0.0001-500	0.0001-500	1.00	1000	0.58	4192
'bulk grout' cell	0.01	0.01	0	2016	1.52	1860

and out of the cell. Constant head and temperature cells are placed along the outer boundary of the model, as well as the top and bottom layer. Water and temperature enter and exit the model through the ATES and BHE system. The grid boundary is located far enough from both systems that no interaction with the boundary is expected based on the simulation time.

Furthermore, inactive cells are located along the turn of the BHE pipe. This ensures water follows the shape of the BHE pipe. The BHE system setup is discussed further in this section. Initial ground temperature is 10°C. The aquifer is fully saturated.

Temporal discretization
An important variable in the simulations is the time step. The modelling time step affects accuracy and run time. Smaller time steps provide increased accuracy, sometimes to an unnecessary degree, and increase total run time. Too large a time step however, may cause the model to react slowly to changes and can cause, in relation with a relatively small spatial discretization, numerical issues. In order to find a suitable time step, different model characteristics have to be analyzes. First, the solver used in the model needs to be addressed. Next, model behavior under different time steps is tested using a simple model. Finally, a time step is chosen and the results of the chosen time step need to be addressed.

For groundwater solutions the Courant number describes the number of cells water is allowed to move through in one time step. Because of the high flow velocity in the BHE pipe and small diameter of the pipe, a limitation in the model is given that the Courant number does not exceed 1. Groundwater solutions are obtained using the preconditioned conjugate gradient (PCG) method. This method solves explicitly. Both the head change and difference between inflow and outflow need to be very small before convergence is found.

MT3D allows for different solving methods. A first categorization can be made between Langrangian, Eulerian-Langrangian and Eulerian methods. Eulerian methods solve for transport using a fixed grid, are mass conservative and handle dispersion and reaction problems effectively. However, for advection dominated problems with many field conditions, numerical dispersion and oscillation can arise in Eulerian methods (Zheng et al., 1999). An Eulerian method is chosen in this study.

To see whether the simulations are advection dominated or diffusion dominated, the Péclet number can be checked. The Péclet number is the ratio of the advective transport rate over the diffusive transport rate. Or, in heat transfer:

$$Pe = \frac{c_w \rho_w uL}{\kappa} \tag{3.7}$$

where c_w is the heat capacity of water [J M^{-1} K^{-1}], ρ_w is the density of water [L^3/M], u is the local flow velocity [L/T], L is the characteristic length [L], which is commonly taken as the cell width, and κ is the bulk thermal conductivity. For Péclet numbers higher than 1, advection plays a larger role compared to diffusion (or conduction). Advection dominated situations occur for Peclet ratios larger than 2 (Zheng et al., 1999).

In the model, flow velocities differ depending on the distance from the ATES well screen. The total injected volume is fixed for all simulations, thus the flow velocity can be computed for each distance from the well screen. Figure shows the flow velocity of the water injected by the ATES system based on the distance from the well screen in the left graph. The cell width, or characteristic length, also differs across the model. This means that the advection ratio is dependent on the cell size and the distance from the ATES system. The diffusion ratio is fixed for all cells as the bulk thermal conductivity is the same in the entire aquifer.

On the right side, Figure 3.4 shows whether advection or diffusion dominates based on the distance from the ATES well screen and the cell size. The brown area indicates a diffusion dominated cell, with a Péclet number smaller then 1. The green area represents cells with a Péclet number larger then 2, where advection
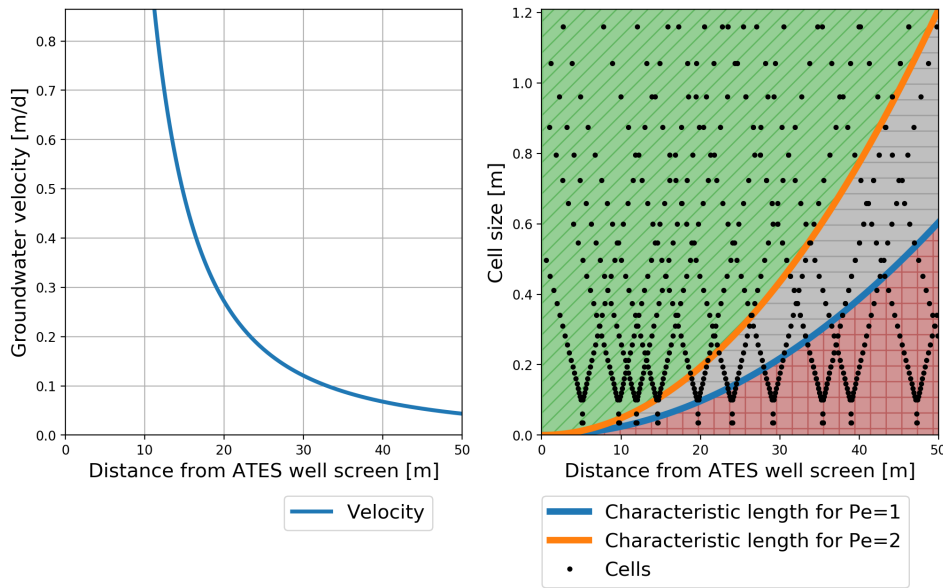
Figure 3.4: Flow velocity of groundwater induced by the ATES system over distance from the system (left). Right figure describes the Péclet number based on cell size and distance from the ATES well screen. The black dots are cell size and distance combinations found in simulations.
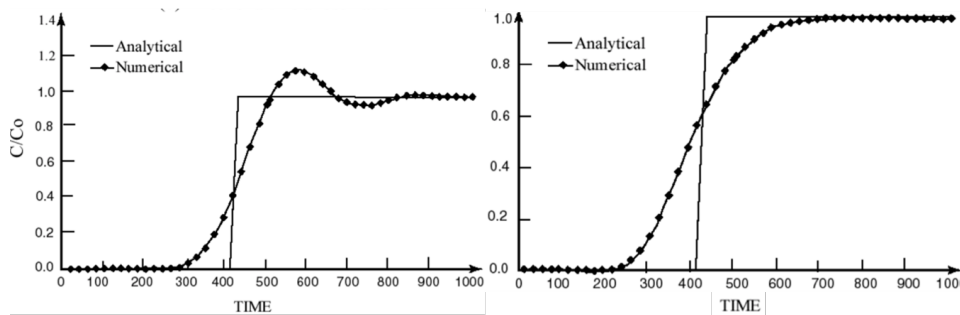

Figure 3.5: How artificial oscillation (left) and numerical dispersion (right) can influence model output (Zheng et al., 1999)

dominates. For cells with Péclet numbers between 1 and 2, neither advection nor diffusion can be considered the dominant force. This is represented by the grey area. The black dots are cell widths in relation to the distance from the ATES system for different distances between the ATES and BHE system. The smaller cell sizes occur around the BHE system, diffusion is the dominant process here. As cells move away from the BHE system, they increase in width. There, advection plays a dominant role. It can be concluded that both advection and diffusion play an important role in the model. Based on this, the Eulerian method is chosen to solve for solute transport solutions, while accounting for problems that may arise due to its characteristics: numerical instability and oscillations.

Within the Eulerian methods exists the generalized conjugate gradient (GCG) method. The dispersion, reaction and sink/source and advection terms are solved implicitly using the standard finite difference method. Both spontaneous oscillation and numerical dispersion are cause for concern when interpreting the outcome of the model in advection dominated models. Figure 3.5 shows how artificial oscillation (left) and numerical dispersion (right) can influence results. Artificial oscillation can be distinguished by concentration values moving around the analytical solution in a sinusoidal fashion. Numerical dispersion can be seen when the concentration front changes gradually where it should change sharply.

In order to choose a time step, different time steps are investigated through the use of a simple model. The model consists of solely a BHE system in the subsurface. Time runs for 30 days. For the first 15 days the BHE input temperature is 5°C, for the last 15 days the input temperature of the system is 15°C. The temperatures
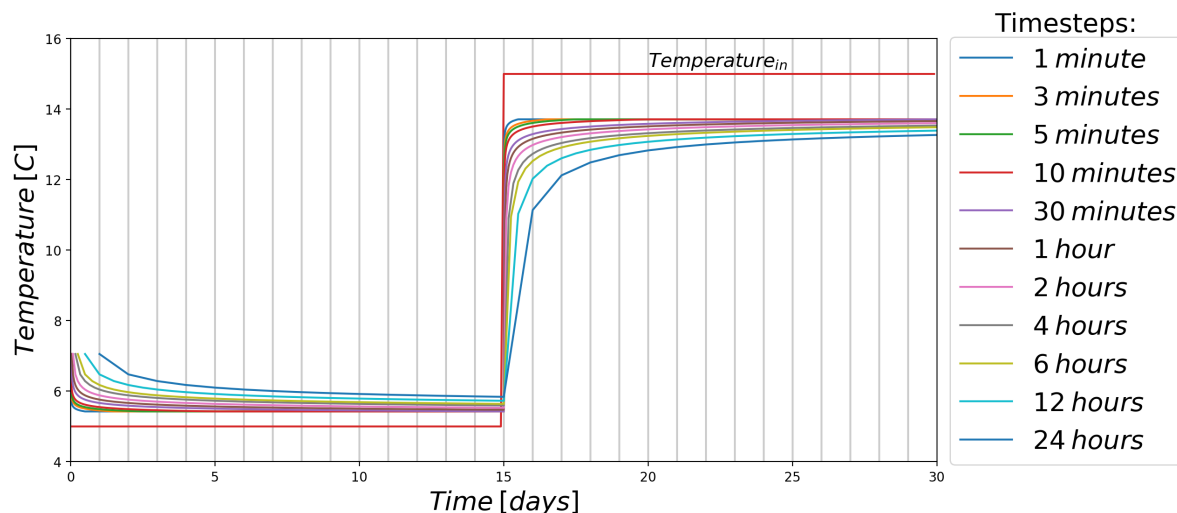
Figure 3.6: Model response over time for different time steps. The red line represents the input temperature. The other colors represent the output temperature for different time steps.

correspond with the input temperatures of a BHE system in heating and cooling phase respectively as used in further simulations. A time step of 1 minute, 3 minutes, 5 minutes, 10 minutes, 30 minutes, 1 hour, 2 hours, 4 hours, 6 hours, 12 hours and 24 hours have been simulated. The output temperatures of the system over time are shown in Figure 3.6.

As expected, smaller time steps respond quicker to an input temperature change compared to larger time steps. It can also be seen that after 15 days, the temperature output of the BHE system differs for different time steps, the difference increases as less time has passed after a temperature change. The output temperature after 15 days for time steps up to 30 minutes was the same, all these simulations reached an equilibrium within 15 days. For the time steps larger than 30 minutes, an equilibrium was not found within 15 days, but took a longer period of time. However, all time steps eventually reached the same equilibrium Furthermore, it can be seen that the model output does not suffer from spontaneous oscillations. The results in Figure 3.6 also do not show patterns associated with numerical dispersion. Temperature differences between input and output are between 2°C and 3°C . These results are in line with BHE systems in practice (Nguyen et al., 2017). Ideally, a small time step, for example 1 second, is used for further simulations. This would give the most accurate results and reduce the chance of numerical errors. However, running a multiple year simulation with a time step of 1 second would require large amounts of computer memory and large amounts of time. A simulation time of 5 years minimum is desired. After 5 years, ATES efficiencies reach up to 90% of final efficiencies. The run time of a simulation of 5 years with a 1 second time step is estimated to take at least several weeks. Running series of these simulations is not feasible within the research time. Therefore, a larger time step of 6 hours is chosen for the scenario simulations, while accounting for the for the slower adjustment period that is consequential. A detailed analysis of this consequence is discussed in Section 5.2.

BHE configuration
The implementation of BHE systems in a finite-difference groundwater model has been studied before (Panteli et al., 2018). The same approach to implement a BHE system has been taken in this model. By assigning cell properties in a particular order, a pipe can be replicated. Figure 3.7 shows the setup of this method, from a top and side view. Blue cells represent water, grey cells the pipe and filling material, black cells represent inactive cells. By adjusting the horizontal and vertical hydraulic conductivity, water can be guided in a U-shape. The water cell at the beginning of the system is given an inflow and a temperature, acting as a well. At the end of the pipe, the water can leave the system.

The hydraulic conductivity property of the cells allows for the water to be guided through the cell. Normally, water does not have a horizontal and vertical hydraulic conductivity as that property describes the ease with which a fluid (e.g. water) travels through a medium with pore space. In this case however, the hydraulic conductivity can be used to lead water through the pipe. In the vertical pipe segments, the water has a high vertical hydraulic conductivity. The horizontal hydraulic conductivity is then 0 m/d. This ensures water
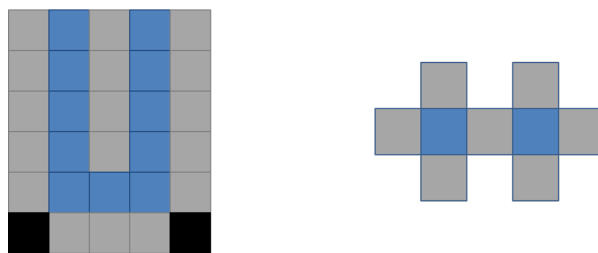
Figure 3.7: Schematized side (left) and top (right) view of a BHE system in the numerical model. Blue cells represent water, grey cells represent grout and pipe material.
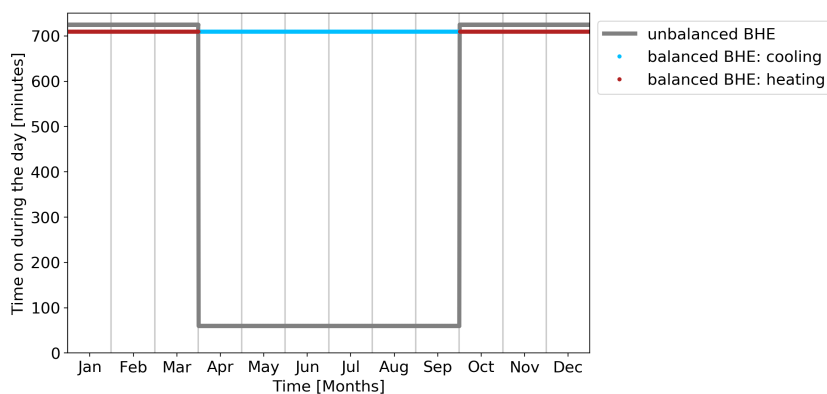

Figure 3.8: pumping schemes for a BHE system with only a heating function and an BHE system with both a heating and cooling function.

travels down/up the vertical part of the pipe. Along the horizontal segment, the horizontal hydraulic conductivity is high and its vertical component is 0 m/d, which leads the water along the pipe. In the corners, both the horizontal and vertical hydraulic conductivity is high, allowing the water to travel along the corner. The water has to follow the path, thus creating a BHE system. Inactive cells (black cells in Figure 3.7) are placed alongside the turn in the system. This ensures no leakage occurs.

BHE systems are active or idle during the day based on energy needs (BodemenergieNL). The fluid flowing through the pipe moves with a speed of 1 m/s when the system is active. Based on the required amount of energy during a day, the system runs for a certain amount of time. For the remainder of the time, the system is turned off. This pattern of heating, cooling or idle has been replicated in the numerical model. If the system heats, water with a starting temperature of 5 °C circulates through the system. In cooling mode, the water starts with a temperature of 15 °C. In idle periods, the system does not circulate water.

Two types of BHE systems have been modelled. The first type has only a heating function, these are most commonly found in the Netherlands (Bakema et al., 2016). Following a simplified pumping scheme in the form of a block function, two different periods in a year have been identified. A cold period, ranging from October until March. During this time, the system heats during half the day and is turned off during the other half. The warm period starts in May and ends in September. During this period, household heating is not needed and the system only provides energy for warm water. The system is active in heating mode for one hour and turned off for the remainder of the day. Figure 3.8 shows the pumping scheme for the BHE system that only has a heating function.

The second BHE type has a heating and cooling function. Its pumping scheme can be found in Figure 3.8. During the cold period, the pattern is the same as the first type. During the warm season however, the system heats for half the day and is idle for the remainder. In practice, a BHE system is often also used to produce hot tap water in the warm season. For simulations in this thesis, the tap water function is omitted and a balanced BHE system is used in order to have a clear insight in the effect of ATES interference on heating and cooling functions of the BHE system.

ATES configuration
ATES systems are resembled as a line of wells in the numerical model. Wells can inject or extract water into or from the subsurface. A temperature can be assigned to the well using the SSM-package of MT3D (Zheng
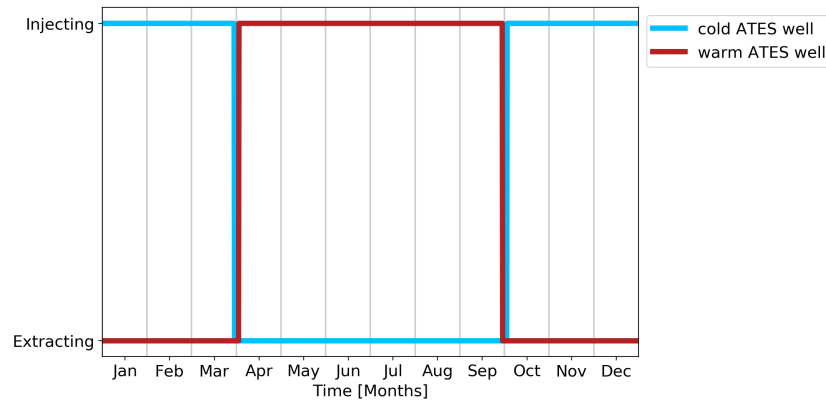
Figure 3.9: pumping schemes for a cool and warm ATES well.

et al., 2012). By creating a line of wells across different layer, with the same row and column, a well screen can be simulated. Thus replicating an ATES system. In reality, a pipe connects the well screen with the surface. This is not simulated in the numerical model as it does not significantly effect the model outcomes. Instead, it only adds to the complication of the model and run time.

Furthermore, ATES systems consist of a cold and a warm well. In the model, only one of the wells is simulated. The wells of the ATES system are separated by at least three times their thermal radius (Sommer et al., 2014). This is done to prevent their thermal zones from interacting with each other. Therefore, a BHE system can only be influenced by one of the ATES wells, which is replicated in the numerical model.

The ATES system in the simulations has a fixed thermal radius of 50 meters in all simulations. Based on the length of the well screen, the total injected volume is chosen. More specifics are given in Section 3.4, where the scenario setup is discussed. The corresponding volume is then injected into the aquifer following a simplified pumping scheme as seen in Figure 3.9. Warm wells inject water during the April-September, and extract water in October-March. Cold wells have an opposite pattern, extracting during April-September and injecting throughout October-March.

3.3. Scenarios
In order to get insight in the effect of ATES systems on BHE systems, scenarios are run. The models are compared to a simulation where the BHE system operates without any interference. Note that there are two of these base cases: one where the BHE system only has a heating function and one where the system has both a heating and a cooling function. Based on the literature review, the following parameters are tweaked:

- *The setup of the subsurface.* A difference between a single aquifer and two-aquifer subsurface is made. In the two-aquifer subsurface, the ATES system is placed in the top or bottom aquifer, the BHE system is placed along the entire modelled subsurface. The different subsurface setups can be found in Figure 3.10. The well screen lengths for the single and double aquifer subsurface systems are 87 and 39 meters respectively. The injected volume and well screen length of the ATES system in a single aquifer subsurface are relatively large compared to the average system in the Netherlands, the smaller system in the double aquifer subsurface is comparable to an average system in the Netherlands (Bloemendal and Hartog, 2018).

- *Distance between both systems.* The time a BHE system is exposed to the influences of an ATES system is dependent on the distance between both systems. This distance is expressed through the distance ratio, which is introduced as the ratio of the distance between the ATES and BHE system over the thermal radius of the ATES system. The volume of the ATES system is chosen in such a way that the thermal radius of the system is always 50 meters. The distance between both systems is varied in order to achieve different distance ratios. For both BHE system input types, a distance ratio of 0.25, 0.50, 0.75 and 1.00 is used initially. For the case where the BHE system only has a heating function, distance ratios of 0.10, 0.20, 0.30, 0.40, 0.60, 0.70, 0.80 and 0.90 are simulated as well.

- *The temperature of the ATES system.* In reality, the ATES well is either warm or cool, which translates to
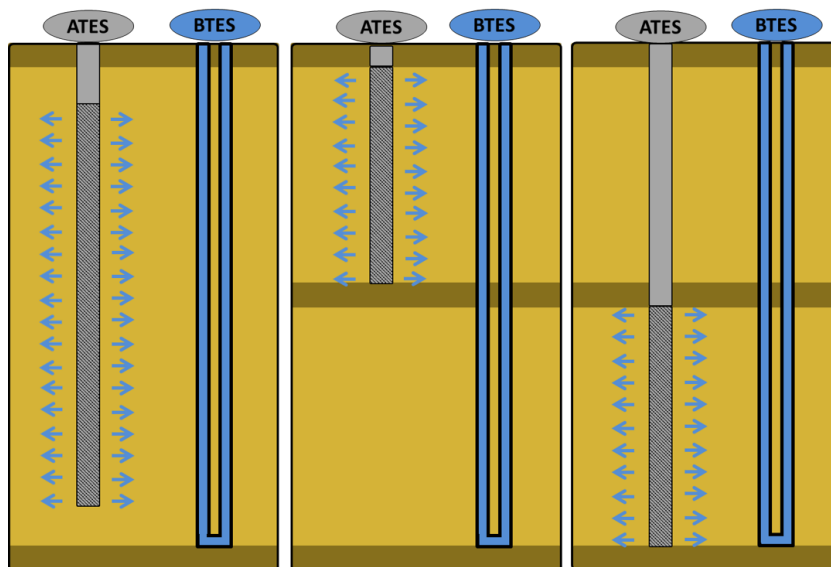
Figure 3.10: Subsurface setups used in simulation. Single aquifer (left figure) and double aquifer with the ATES system in either the top (middle figure) or bottom (right figure).

a temperature of 15°C or 5°C respectively. A well temperature of 10°C is also used in the scenarios in order to examine the effect of groundwater flow caused by an ATES system on the efficiency of a BHE system. The subsurface has a temperature of 10°C as well. Thus, in simulations where the ATES well is 10°C, only interference from groundwater induced by the ATES system occurs.

- *Functions of the BHE system.* Two types of BHE systems are simulated: BHE systems with only a heating function and BHE system with both a heating and a cooling function. The system with a heating function only has an unbalanced energy load. The system with two functions is balanced.

3.4. Assessment Framework

In order to compare the output of different simulations, criteria are required. This is called the assessment framework. Two criteria are used to evaluate simulation results: the average energy per time step from the BHE system and the trend of the average energy per time step over five years.

Average energy per time step

In order to compare the efficiency between BHE systems in different setups, the average energy per heating and or cooling time step is computed for each year. If a system is active for five years, a series of five numbers describe its performance in practice. The BHE system has either only a heating function or both a heating and cooling function. In the case of a system that has only a heating function, the average energy gained per time step is the sum of the energy gained in each time step over the number of heating or cooling time steps, where the gained energy is the temperature difference between the input and output of the system in a time step times the volume of water going through the system in the same time step times the density of water and the specific heat capacity of water, see Equation 3.8.

In order to compare different systems, the results of each simulation are divided by the results of a simulation where the BHE system does not experience interference from an ATES system but all other variables are equal. The output of a simulation with a BHE system without interference is described in more detail in Appendix A.

$$\overline{E}_{heat,year} = \frac{\sum_{t_{heat,yearstart}}^{t_{heat,yearend}} \Delta T Q \rho_w c_w}{n_{timesteps,heat}} \tag{3.8}$$

If the system has both a heating and a cooling function, a second variable describes the averages energy per time step per year for the cooling mode:

$$\overline{E}_{cool,year} = \frac{\sum_{t_{cool,yearstart}}^{t_{cool,yearend}} \Delta T Q \rho_w c_w}{n_{timesteps,cool}} \tag{3.9}$$

where, in both equations, E is the average energy per heating/cooling time step in a year [J T^{-1}], ΔT is the temperature difference between the entrance and exit of the BHE system is [°C]. Q is the amount of water flowing through the pipe during a time step [M^3 T^{-1}]. ρ_w is the density of water [M L^{-3}], c_w the specific heat capacity of water [J kg^{-1} K^{-1}] and $n_{timesteps}$ the number of time steps the system heats or cools during a year[−]. Depending on the size of the time step, the unit can be converted to Watts as Watt equals J/s. Thus, if the time step is for example 6 hours, dividing the outcome of the equations above through 6 * 3600 = 21600 seconds give the average amounts of Watts per time step.

Energy trend
Both the ATES and the BHE system start at the beginning of the model time. However, UTES systems do not reach peak efficiency until after multiple years (BodemenergieNL). Because of this, results for the first or second year might not be representative for the majority of the UTES systems lifespan. Thus, a trend in the results needs to be established in order to identify which results can be labeled as representative. If the results are stable (i.e. not changing significantly), the system is assumed to be in equilibrium and the results are assumed to be representative for the majority of the systems lifespan. A result is considered stable if it differs no more than 5% from the result of the previous year. This inherently means that the first year of results is not stable and therefore not representative for the system.

4

Results

This chapter focuses on the results produced from the scenarios introduced in the previous chapter. First, the results of the simulations of a BHE with only a heating function are discussed, starting with the single aquifer subsurface scenarios 4.1. Next, the scenarios of the double aquifer subsurface are described in Section 4.2. Second, the results of the BHE system with both a heating and a cooling function are discussed. Starting with the single aquifer subsurface scenario results in Section 4.3. and continuing with the results of the double aquifer subsurface in Section 4.4. Finally, the relation between the distance ratio and degree of interference is established in Section 4.6.

4.1. Unbalanced BHE system in a single aquifer subsurface

This section covers the results of the scenarios concerning a BHE system with only a heating function in a single aquifer. Paragraph 4.1.1 concerns the results of an ATES well with an ambient water temperature, which determines the impact of groundwater flow caused by an ATES system on the efficiency of a BHE system. The effect of a colder and warmer temperatures due to an ATES system are covered in Paragraphs 4.1.2 and 4.1.3 respectively. Finally, in Paragraph 4.1.4, further testing is conducted.

4.1.1. Ambient ATES well in a single aquifer subsurface

The ambient ATES well serves to examine the effect of groundwater flow on the efficiency of a BHE system. However, an ambient ATES well does not exist in practice and therefore does not have a natural pumping scheme. To account for this, simulations have been performed for both an ambient well that has the pumping scheme of a warm well as one that follows the pumping scheme of a cold well. The results can be found in Figure 4.1. The outcomes are near-identical for distance ratios of 0.50, 0.75 and 1.00. For a distance ratio of 0.25, a difference occurs. However, this difference is considered small. The ambient ATES well simulations serve to identify the impact of groundwater flow induced by an ATES system. Therefore, it is not necessary to simulate both ambient ATES wells that follow the pumping scheme of a warm ATES well as well as an ambient well that follows the pumping scheme of a cold ATES well. In further simulations, ambient wells will follow the pumping scheme of a warm well.

Looking further into the results, a smaller distance ratio has a larger effect compared to a larger distance ratio. This is to be expected as the BHE system is exposed to the influence of the ATES system longer as the distance ratio decreases. The effect of ATES induced groundwater flow has a positive effect on the efficiency of the BHE system with only a heating function. Earlier studies found that the influence of groundwater flow on a BHE system can be positive or negative dependent on the frequency the BHE system switched from heating to cooling (Panteli et al., 2018). In a system that switches frequently, the residual heat or cold from the previous mode allows for greater temperature differences in the current mode and thus a more efficient systems. For a BHE system that only has a heating function, the effect from groundwater flow is positive, albeit to a small degree for distance ratios greater than 0.5.
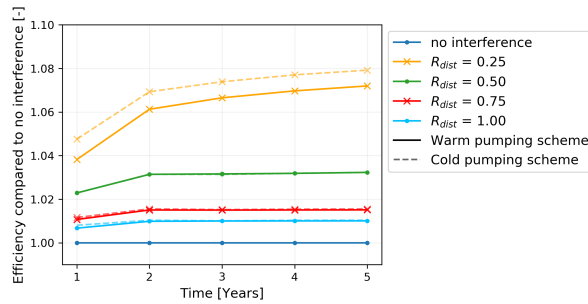
Figure 4.1: Efficiency of a BHE system in the presence of an ambient ATES well injecting in summer and extracting in winter (solid line) compared to a BHE system with no ATES system present for different distances over multiple years (dashed line).
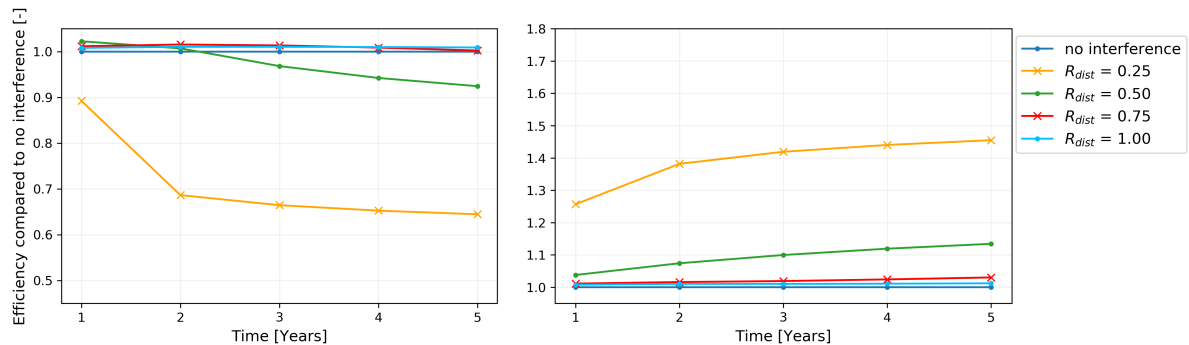

Figure 4.2: Efficiency of a BHE system in the presence of a cold (left) and warm (right) ATES well compared to a BHE system with no ATES system present for different distances over multiple years.

4.1.2. Cold ATES well in a single aquifer subsurface

Figure 4.2 shows the results of a cold ATES well near a BHE system. Two clear effects are noticeable. First, a decrease in the efficiency of the BHE system is clearly noticeable when the ATES well is nearby the BHE system. For a distance ratio of 0.25, the efficiency drops by one third compared to no interference after five years of exposure. A system twice as far away, at a distance ratio of 0.50, still experiences a reduction in efficiency. Though the effect appears later and is less pronounced. At a distance ratio of 0.75, only a very small reduction in efficiency appears as 5 years have passed. For the first 4 years, the efficiency is even increased compared to no interference. For a distance ratio of 1.00, the efficiency remains increased for the entire time the model was run. This is the second effect. Groundwater flow induced by the ATES well has a positive effect on the efficiency of the BHE system. For the cases of a distance ratio of 0.50 and 0.75, the net effect of the negative influence of a cold well and the positive influence of groundwater flow is positive as very little cold water reaches the BHE pipe.

4.1.3. Warm ATES well in a single aquifer subsurface

BHE efficiency increases when the system is placed near a warm ATES well, see Figure 4.2. This is logical as the ATES system raises the temperature around the BHE, increasing the temperature difference between the fluid in the pipe and the subsurface and allowing for a greater energy transfer. The positive effect is more pronounced when the distance between both systems is small, resulting in a smaller distance ratio. Similarly to the cold well results, the effect is most pronounced for a distance ratio of 0.25 and still noticeable to a smaller degree when the distance ratio increases to 0.50. At a distance ratio of 0.75, a very small increase occurs in the fifth year. And at a distance ratio of 1.00, only a positive effect due to groundwater flow induced by the ATES system can be found.

4.1.4. Further testing

In both the case of a hot and cold ATES system, the interference of the ATES well on the efficiency of the BHE system seemed to become insignificant between a distance ratio of 0.50 and 0.75. In order to further pinpoint at which distance the system becomes insignificant, the model for all ATES temperatures was run
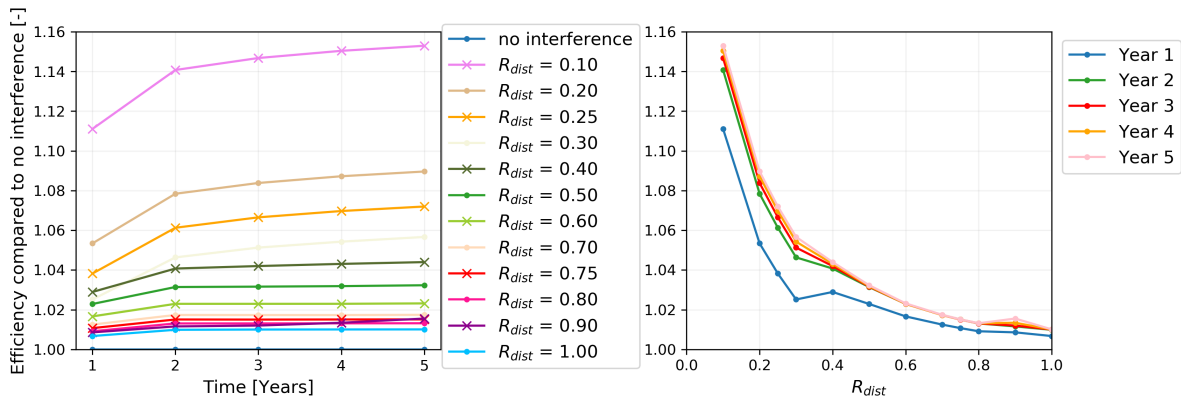
Figure 4.3: Efficiency of a BTES system in the presence of an ambient ATES well at different distance ratios. Left figure shows the evolution of the interference over multiple years for different distance ratios. Right figure shows the effect of interference at different distance ratios for multiple years.
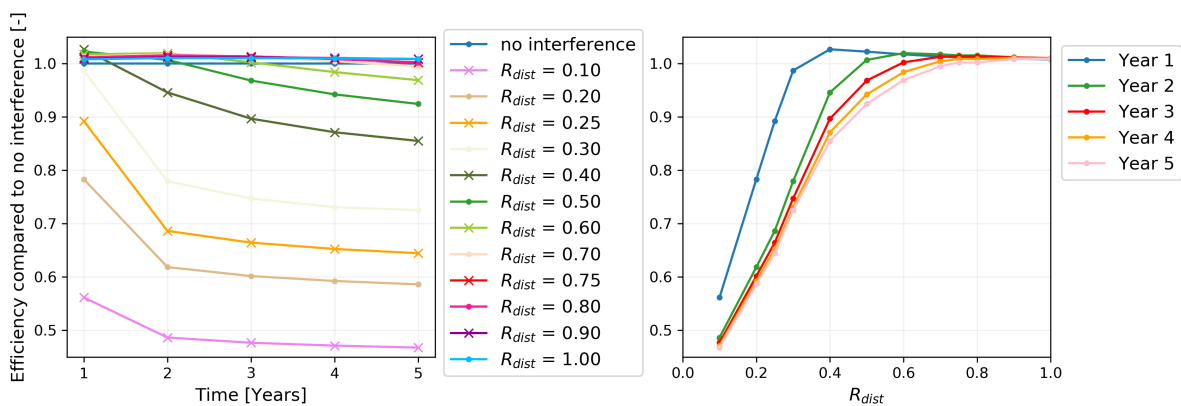

Figure 4.4: Efficiency of a BTES system in the presence of an cold ATES well at different distance ratios. Left figure shows the evolution of the interference over multiple years for different distance ratios. Right figure shows the effect of interference at different distance ratios for multiple years.

with a wider array of ratios: 0.10, 0.20, 0.30, 0.40, 0.50, 0.60, 0.70, 0.80 and 0.90. The results can be found in Figures 4.3, 4.4 and 4.5. The left figure shows a more extensive version of the graphs presented multiple times in Section 4.1, the right graph shows the efficiency of the system as the distance ratio increases, for multiple years. From top to bottom the results for an ambient, a cold and a warm ATES well are presented respectively.

The extra results confirm the trend found in Section 4.1. Around a distance ratio of 0.60, the influence from the ATES system is so small that it can be called non-influential. Even after five years, a distance ratio of 0.60 causes only a 1% increase and 3% decrease in the case of a warm and cold ATES well respectively.

4.2. Unbalanced BHE system in a double aquifer subsurface

This section explains the results of a heating only BHE system in an double aquifer subsurface. Ambient wells are covered first, in Section 4.2.1. Followed by cold and warm ATES wells in Sections 4.2.2 and 4.2.3 respectively. Results are presented in duos. The left graph in the figure shows the results with the ATES well located in the top aquifer, the left graph of the ATES well in the bottom figure.

4.2.1. Ambient ATES well in a double aquifer subsurface

The presence of an ambient ATES well in the top or bottom aquifer shows a similar effect compared to the presence of an ambient well along the entire BHE system, as can be seen in Figure 4.6. BHE efficiency is enhanced due to groundwater flow induced by the ATES well for all distance ratios. Smaller distance ratios have an increased effect. This is again due to the longer exposure to ATES well at smaller distance ratios. A difference in results between a well in the top aquifer and a well in the bottom aquifer can be observed. This
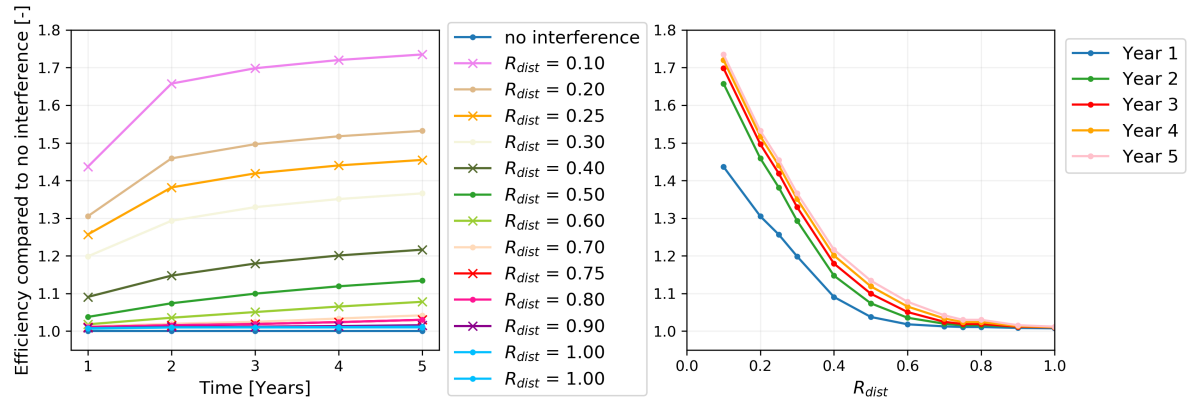
Figure 4.5: Efficiency of a BTES system in the presence of an warm ATES well at different distance ratios. Left figure shows the evolution of the interference over multiple years for different distance ratios. Right figure shows the effect of interference at different distance ratios for multiple years.
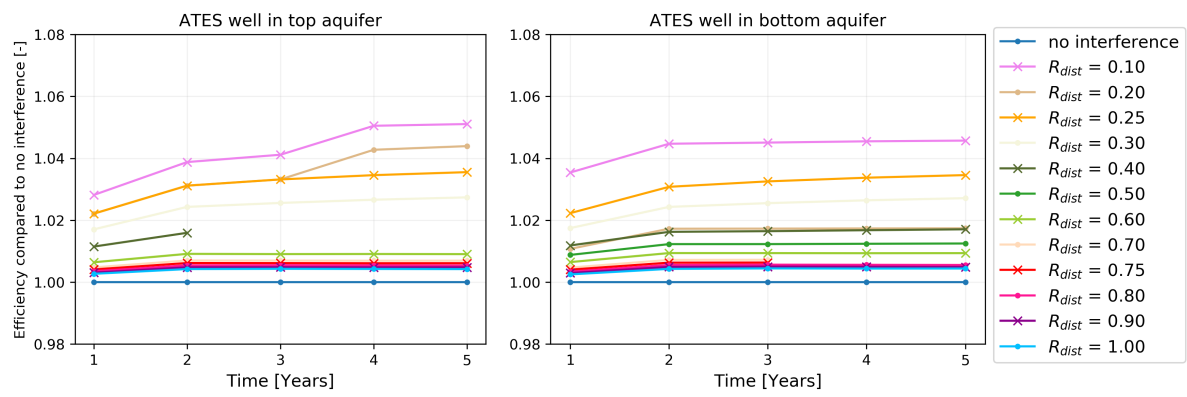

Figure 4.6: Efficiency of a BHE system in the presence of an ambient ATES well in the top aquifer (right) and bottom aquifer (left) of a two aquifer subsurface compared to a BHE system with no ATES system present for different distances over multiple years.

is partly due to a difference in well screen length for both cases. The top aquifer is 39 meters, the bottom aquifer 36 meters. However, when adjusted, there is still a discrepancy between both results.

This can be explained by the path the water in the BHE system follows. If the ATES system is placed in the top aquifer, it influences the fluid in the BHE system in the beginning and at the end of the pipe. As opposed to when the ATES system is placed in the bottom aquifer, where it influences the fluid in the BHE system in the middle of the pipe. Figure 4.7 shows a BHE pipe from beginning to end. The green areas are under the influence of an ATES system when it is placed in the top aquifer, the red areas are under the influence from ATES systems in the bottom aquifer. For top aquifer ATES systems, interaction occurs until the fluid exits the BHE pipe. For bottom aquifer ATES systems, interaction stops before the fluid exits the pipe. This causes the difference in results. Top aquifer ATES systems have a very slightly higher influence on BHE systems in this ambient scenario.

4.2.2. Cold ATES well in a double aquifer subsurface

The effect of the presence of a cold ATES well in the top or bottom aquifer is similar, as can be seen in Figure 4.8. Both graphs show the same trend: a cold ATES well has a negative effect on the efficiency of the BHE system. Furthermore, a smaller R_{dist} has an larger effect on the interference, as does time. Similar effects were observed for a cold ATES well in a single aquifer. The degree of interference is smaller compared to

Figure 4.7: BHE pipe under the influence of ATES well in the top aquifer (green) or bottom aquifer (red).
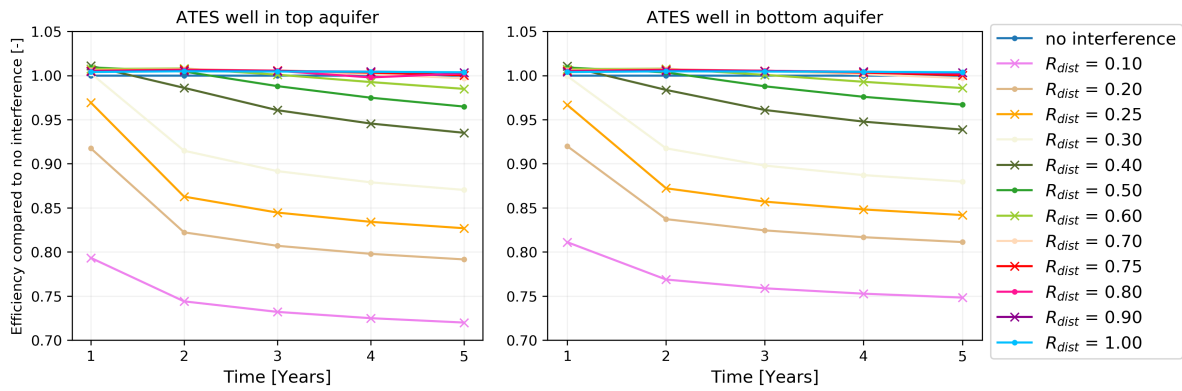
Figure 4.8: Efficiency of a BHE system in the presence of a cold ATES well in the top aquifer (right) and bottom aquifer (left) of a two aquifer subsurface compared to a BHE system with no ATES system present for different distances over multiple years.
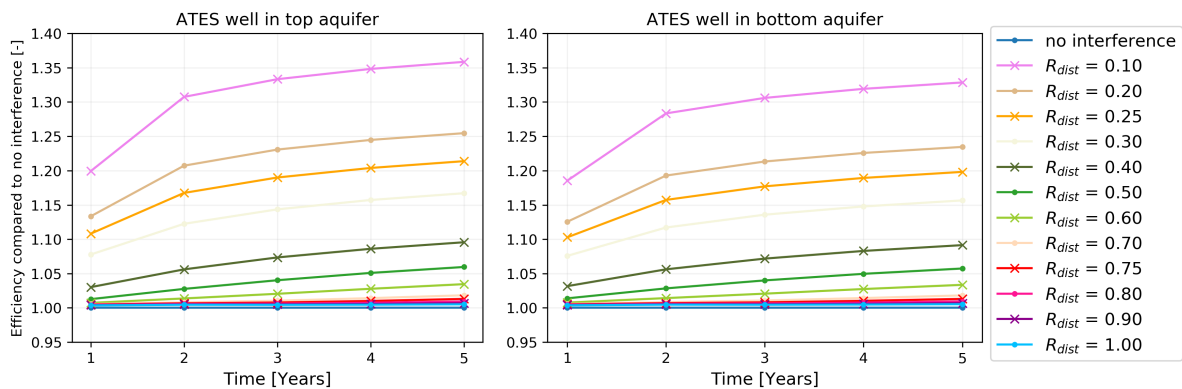

Figure 4.9: Efficiency of a BHE system in the presence of a warm ATES well in the top aquifer (right) and bottom aquifer (left) of a two aquifer subsurface compared to a BHE system with no ATES system present for different distances over multiple years.

the single aquifer. Where an ATES system over the whole length of a single aquifer reduced the efficiency of the BHE system to 47% compared to the case of no interference, an ATES well in a double aquifer (and thus less then half the length of the modeled subsurface) reduces the efficiency of a BHE system to 72% of its original efficiency when the ATES well is located in the top aquifer and 75% of its original value when the well is located in the bottom aquifer. The difference between top and bottom aquifer can again only partly be explained by a slight difference in well screen length. Adjusted, placement of the ATES well in the top aquifer seems to have a slightly increased effect compared to an ATES well in the bottom aquifer again. This can be explained due to the same mechanic as in 4.2.1. Top aquifer cold ATES system have a slight increased interaction with BHE systems as well.

4.2.3. Warm ATES well in a double aquifer subsurface

Interference from a warm ATES well again has a positive effect on the efficiency of a BHE system. The results are presented in Figure 4.9. Lower distance radius and a more exposed years increase the effect. Similar to previous results, the positive effect from a warm ATES well is larger compared to the negative influence from a cold ATES well. This is due to the positive effect from groundwater flow induced by the ATES system in both cases. Again, an increased effect in the top aquifer can be observed compared to the bottom aquifer.

4.3. Balanced BHE system in a single aquifer subsurface

This section covers the results of BHE systems with both a heating and a cooling function. Efficiency is calculated for both the heating and the cooling mode and compared to the results of a model where no interference took place. The section starts by covering the results from the ambient ATES well in Section 4.3.1, followed by the results from the cold and warm ATES well in Sections 4.3.2 and 4.3.3 respectively
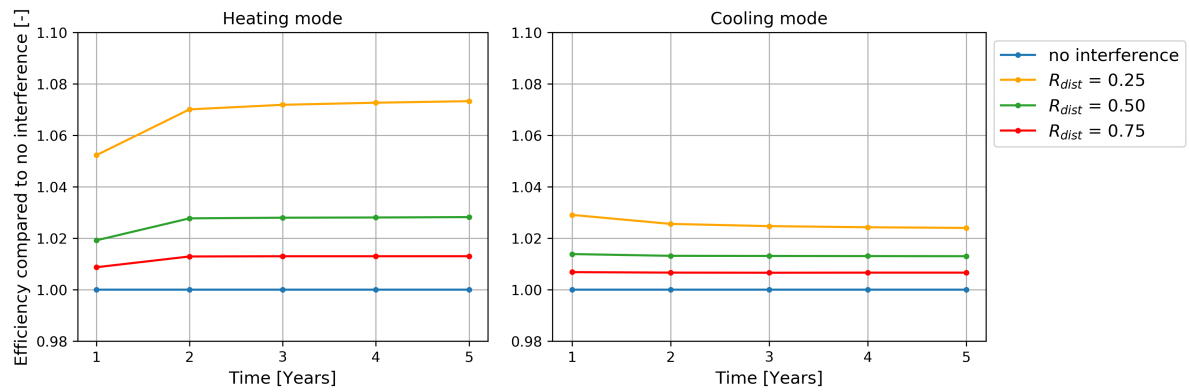
Figure 4.10: Efficiency of a BHE system with both a heating and a cooling function in the presence of an ambient ATES compared to a BHE system with no ATES system present for different distances over multiple years.
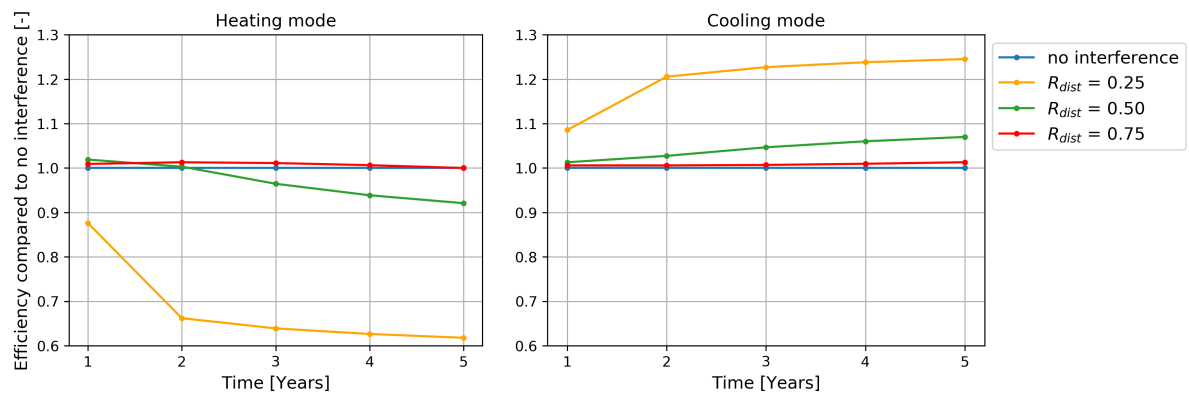

Figure 4.11: Efficiency of a BHE system with both a heating and a cooling function in the presence of a cold ATES compared to a BHE system with no ATES system present for different distances over multiple years.

4.3.1. Ambient ATES well

The results for the efficiency of a balanced BHE system in the presence of an ambient ATES system compared to a balanced BHE system without any influences can be found in Figure 4.10. Groundwater flow induced by the ATES system increases the efficiency in all scenarios. Heating efficiencies are similar to those of a BHE system with only a heating function. Cooling function efficiencies however, experience a smaller increase than expected. As the system is balanced, a similar effect on heating and cooling efficiencies was expected. Yet, in cooling mode the system experiences a smaller in increase in efficiency compared to heating mode. A partial explanation for this discrepancy is given in Section 4.5

Another trend similar to BHE systems that only have a heating function is that the effect in the efficiency of the BHE system due to interference from the ATES system becomes insignificant after a distance ratio of 0.50. Finally, from the second year of interference onward, the effect of groundwater flow stabilizes.

4.3.2. Cold ATES well

A cold ATES well has a negative effect on the hating mode and positive effect on the heating mode of the ATES system, see Figure 4.11. The negative effect on the heating mode is larger compared to the positive effect on the cooling mode. As the system is balanced, the net effect on the BHE system is negative. Smaller distance ratios once again have an increased effect. Similar to earlier results, the effect from interference becomes insignificant when the distance ratio is greater than 0.5. Also similar to the results from the ambient well and balanced BHE systems in a single aquifer scenario, the BHE system experiences less interaction when in cooling mode. This is discussed in Section 4.5

Different from the results from the ambient well, the effect from the cold well does not stabilize after the first year of interference. Instead, the effect progresses and does not stabilize completely until after the 5 years modelled.
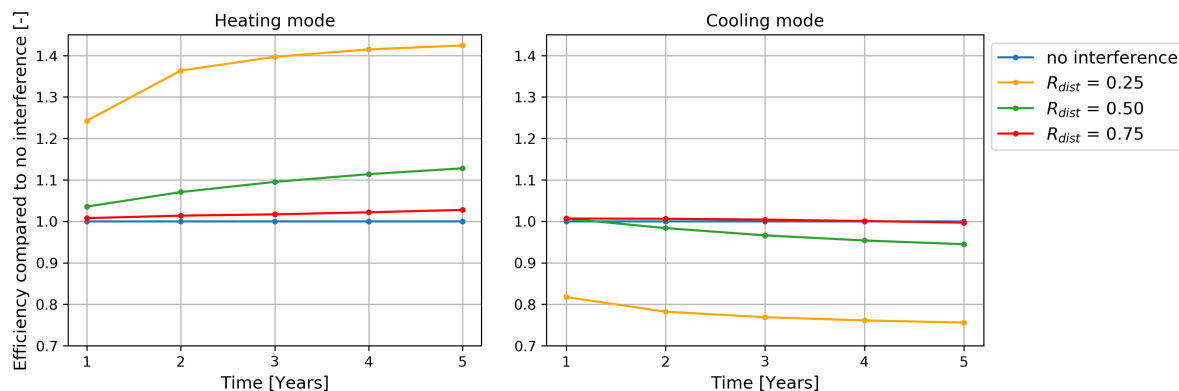
Figure 4.12: Efficiency of a BHE system with both a heating and a cooling function in the presence of a warm ATES compared to a BHE system with no ATES system present for different distances over multiple years.

4.3.3. Warm ATES well

The warm ATES well has the opposite effect of its cold counterpart, see Figure 4.12. Heating is increased in the BHE system and cooling efficiency is decreased. Similarities to the cold well can be found. First, the heating mode of the warm well experiences a larger effect on the efficiency due to the interference from the ATES well compared to the cooling mode, making the net effect positive. This is an interesting result as the net effect of the cold ATES well was negative. Section 4.5 goes deeper into this result. Second, the effect due to interference does again not stabilize after the first year. It can be concluded that temperature changes stabilize over a longer time period compared to groundwater flow changes. Finally, the distance ratio again plays an important role in the matter of effect due to interference from the cold ATES well. Distance ratios exceeding 0.5 seem to have a marginal effect on the efficiency of the BHE system.

4.4. Balanced BHE system in a double aquifer subsurface

This section covers the results of BHE systems with both a heating and a cooling function in a double aquifer subsurface, comparable to the subsurface in Section 4.2. Efficiency is calculated for both the heating and the cooling mode and compared to the results of a scenario where no interference took place.

4.4.1. Ambient ATES well in a double aquifer subsurface

The result of interference of an ambient ATES well in the top or bottom aquifer of a two aquifer subsurface on the efficiency of a BHE system with both a heating and cooling function that spans across both aquifers can be hypothesized by combining the effects in Sections 4.2.1 and 4.3.1, where both the results of the double aquifer with a BHE system that only has a heating function and the results of an ambient well interfering with a BHE system with two functions over half its length can be found respectively. Following these results, an ambient well in the top or bottom aquifer would influence both functions of the BHE system positively. Heating more compared to cooling and the top aquifer slightly more compared to the bottom aquifer due to the slight difference in aquifer length.

The results from the scenario's can be found in Figure 4.15, which match the hypothesized results. Again, a smaller R_{dist} has a larger effect. The influence of groundwater induced by the ATES well seems stable after the second year of influence. Furthermore, cooling experiences a smaller positive influence compared to heating and the bottom aquifer has a slightly smaller impact, similarly to the simulations in a single aquifer. It should also be noted that there is a higher influence for large distance ratios compared to the single function BHE system. For a distance ratio of 1.00, the heating and cooling BHE system shows a stable positive influence of 1.05 times the original efficiency . For a BHE system with only a heating function, the experienced increase in efficiency at the same distance ratio is 1.01 times the original efficiency. Smaller distance ratios (0.25 and 0.50) have a similar increased efficiency compared to those of the BHE system with only a heating function. This is due to the fact that the groundwater flow induced by the ATES system allows the BHE system to more effectively use the previously stored energy from the last cycle. Without groundwater flow, the BHE system only benefits from cold/warm water directly next to the BHE pipe, after that groundwater has become warmer/colder, further benefits go more slowly as they depend on conduction. With groundwater, more cold/warm groundwater around the pipe is cycled and used, thus increasing efficiency. Figure 4.13
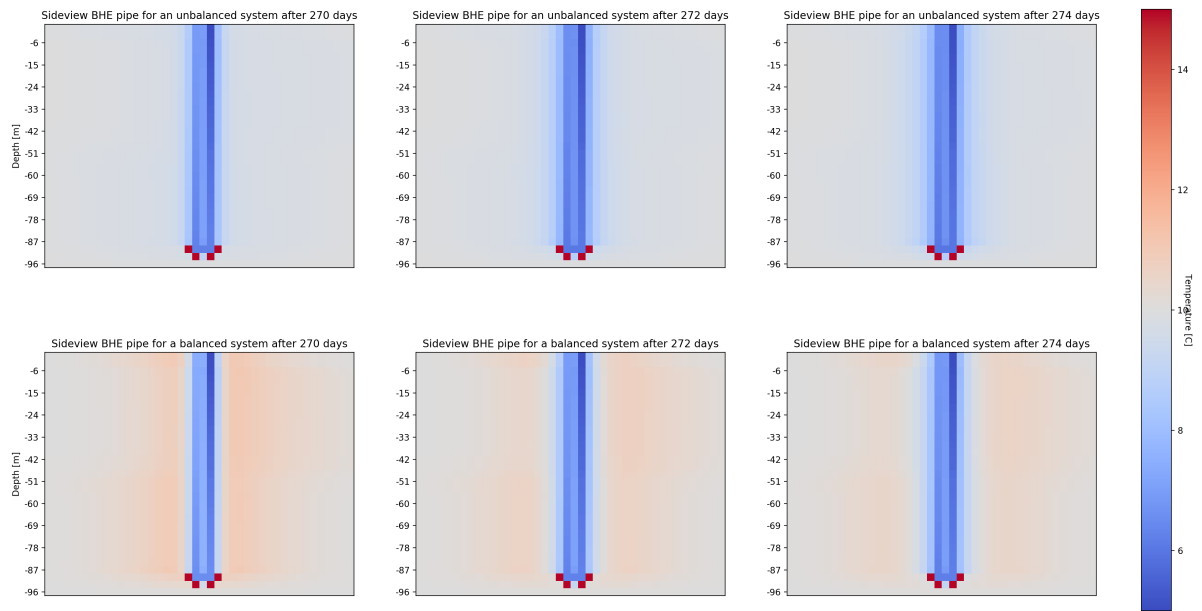
Figure 4.13: Subsurface temperatures surrounding a BHE system right after a cooling phase for unbalanced (top) and balanced (bottom) simulations at different time steps.
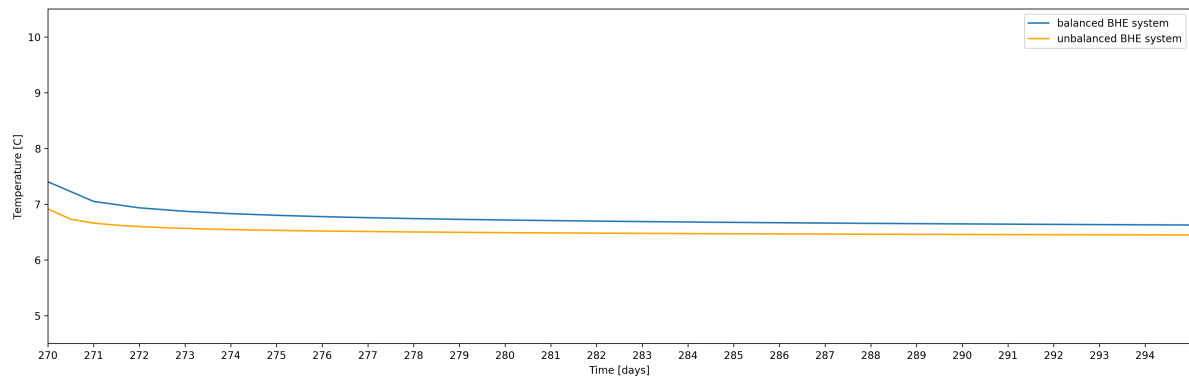

Figure 4.14: Output temperatures of a balanced and unbalanced BHE system just after a cooling phase. The red and blue areas indicate heating and cooling periods respectively, with the red and blue lines the input temperatures of the BHE system. The numbers represent the average temperature difference between in- and output during a heating or cooling phase

shows this process. The top figures show the area surrounding the BHE pipe in an unbalanced simulation over different time steps. The bottom figures show the same for an balanced simulation. It can be seen that the subsurface surrounding the BHE pipe in the balanced simulation is warmer compared to the unbalanced simulation due to the previous cooling cycle. Due to this, the BHE system operates at a greater efficiency for the first period of time. Figure 4.14 shows the output temperatures for the BHE system in both cases from the start of the heating cycle until the end of the first year of simulations. Output temperatures for the balanced system are higher compared to the unbalanced system, resulting in a more efficient system.

Finally, there seems to be no difference between influence from an ATES system placed in the bottom aquifer compared to placement in the top aquifer. This opposed to the results for a BHE system with only a heating function, where the top aquifer has a slightly larger influence. This can be attributed to the duration of the heating and cooling phases of the BHE system. For a BHE system with only a heating function, thermal energy is extracted from the subsurface continuously. For a BHE system with both a heating and cooling system, thermal energy is added and extracted alternately. Thus, where efficiency in an unbalanced BHE system is mainly sourced from groundwater interaction, efficiency in a balanced BHE system is sourced from the previously stored cold/warmth.
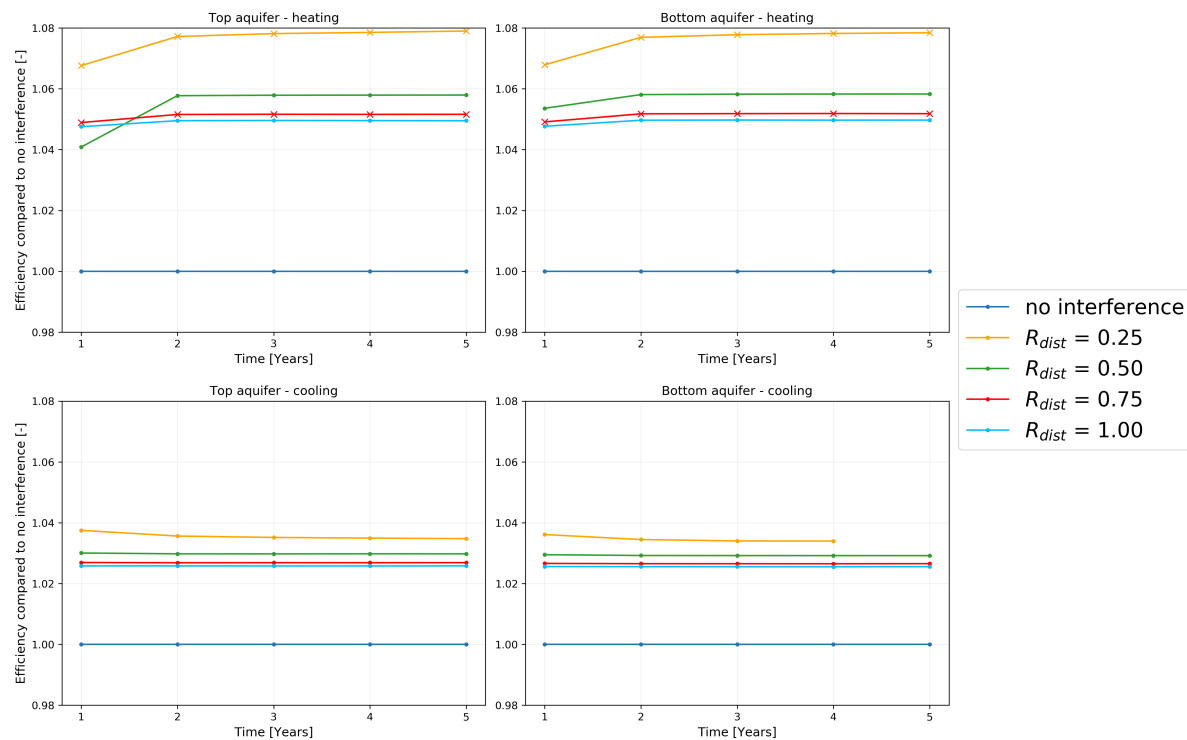
Figure 4.15: Efficiency of a BHE system with both a heating (top) and a cooling (bottom) function in the presence of an ambient ATES well in the top (left side) or bottom aquifer (right side) compared to a BHE system with no interference for different distances over multiple years.

4.4.2. Cold ATES well in a double aquifer subsurface

Results can be found in Figure 4.16. Data for the simulation of an ATES system in the bottom aquifer with a distance ratio of 0.25 is absent. However, the results between the bottom and top aquifer are nearly identical for all other simulations. As expected, heating efficiency decreases for small distance ratios while cooling efficiencies increase. Given the ATES well is cold, this is logical. The cold groundwater from the ATES well causes a larger temperature gradient when the BHE system cools and a smaller gradient when the system heats.

Furthermore, scenarios with a distance ratio of 0.50 and larger seem to experience a a positive influence from the cold well, even in heating mode, due to groundwater flow from the ATES system. This effect was not observed in the single aquifer case (Section 4.1.2) and is due to the increased influence of groundwater in double aquifer scenarios compared to the single aquifer scenarios. The amount of positive interference is the same as for the ambient scenario. At a distance ratio of 1.00, there is no longer interference from the temperature component of the ATES well. There is still however, interference from groundwater flow, as the hydraulic radius reaches further compared to the thermal radius. Thus, at a distance ratio of 1.00, only groundwater interference induced by the ATES system is present. At a distance ratio of 0.75, interference from temperature is minimal (6% of the time) and interference can mainly be attributed to groundwater flow induced by the ATES system.

4.4.3. Warm ATES well in a double aquifer subsurface

The warm ATES well shows opposite results compared to the cold well again, see Figure 4.17: an increase in heating efficiency alongside a decrease in cooling efficiencies. The threshold for significant interference in the first five years lies around 0.50 for heating and 0.75 for cooling. Larger distance ratios experience no longer interference due to the temperature of the ATES system, be it positive or negative, only the positive interference from groundwater flow which was found in the case of a cold ATES system as well.

Figure 4.16: Efficiency of a BHE system with both a heating (top) and a cooling (bottom) function in the presence of a cold ATES well in the top (left side) or bottom aquifer (right side) compared to a BHE system with no interference for different distances over multiple years.
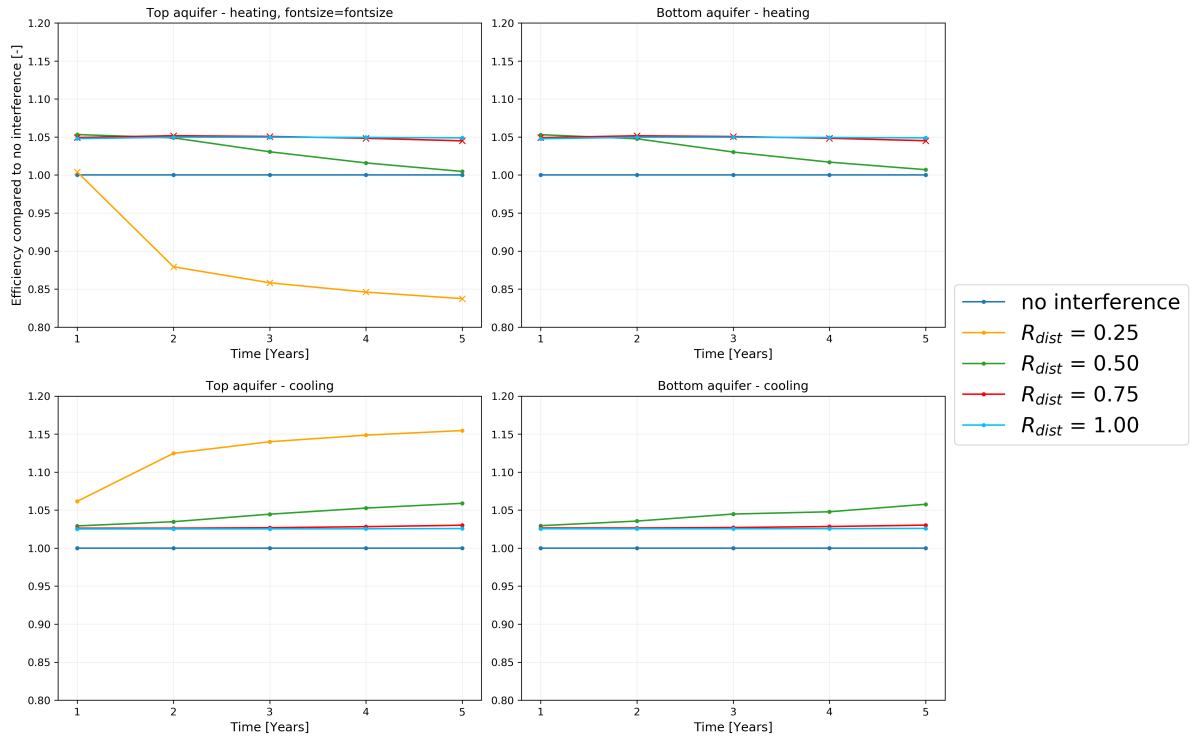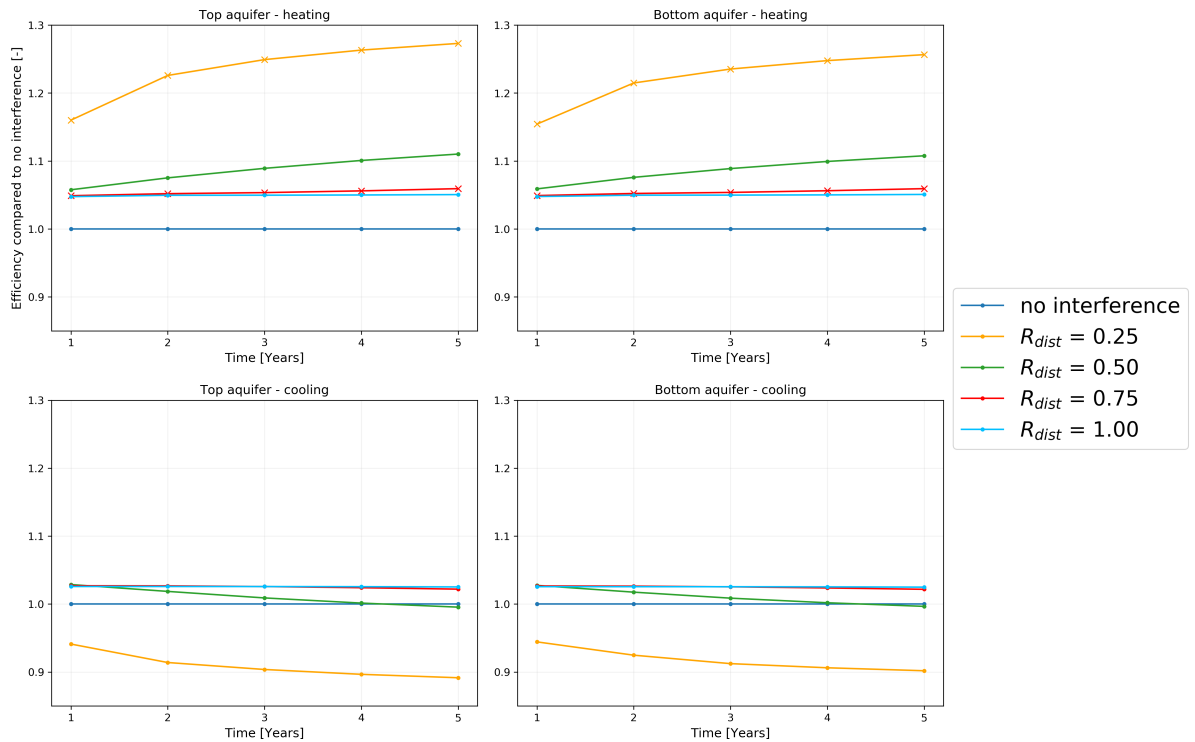

Figure 4.17: Efficiency of a BHE system with both a heating (top) and a cooling (bottom) function in the presence of a warm ATES well in the top (left side) or bottom aquifer (right side) compared to a BHE system with no interference for different distances over multiple years.
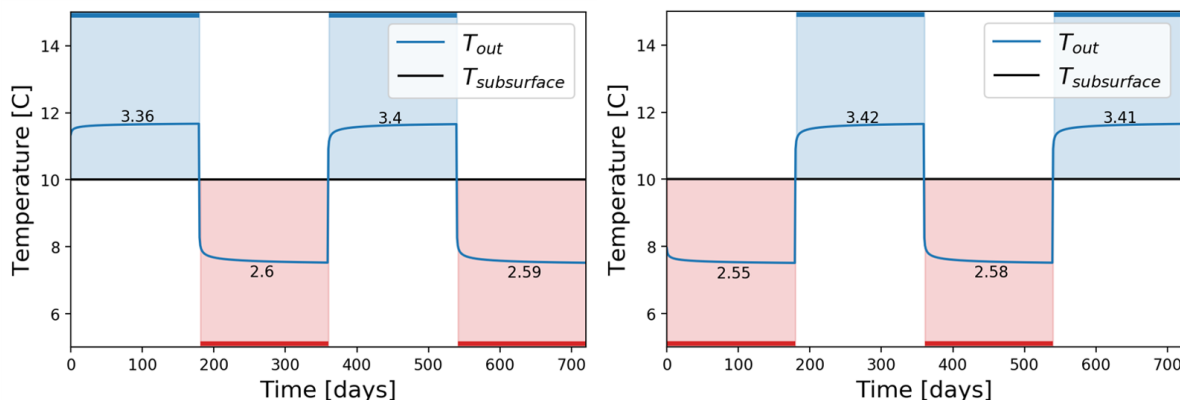
Figure 4.18: Output temperatures of a balanced BHE system simulated over two years without interference starting in summer (left) and winter (right).

4.5. Discrepancy in results of balanced BHE systems

In Sections 4.3 and 4.4 it was observed that when a BHE system is in cooling mode, it experiences less interference from ATES systems than when in heating mode. This is unexpected, as the BHE system is balanced and heating and cooling demands are equal. Both heating and cooling occur for the same amount of time and with a same temperature difference compared to the subsurface. Thus, in ambient scenarios a similar effect of ATES-induced groundwater flow on heating and cooling efficiencies is expected. Instead, cooling efficiencies are still increased, but to a lesser extend. In simulations with a cold, ambient or warm ATES well present, the impact of the ATES system is also smaller when the BHE system performs a cooling function. This section further explores possible causes for this discrepancy.

Before looking into the relative differences between simulations without and with interference, it is interesting to look at a simulation without interference. Figure 4.18 shows the output temperatures of a BHE system in a subsurface with single aquifer in two scenarios. The setup is of the BHE system is identical to those in all other scenarios: during heating phases the systems circulates water with a starting temperature of 5°C, during cooling phases the starting temperature of the water is 15°C. The right figure shows the output from a scenario where the BHE system is balanced and starts with a heating phase of six months, followed by a cooling phase of six months. In the left figure, the systems remains balanced but starts with a cooling phase. This setup is simulated for two years. The numbers in show the average temperature difference between input and output temperatures during a heating or cooling phase.

Results show that during cooling phases higher temperature differences are achieved compared to heating phases. As input characteristics are the same for both heating and cooling, this is unexpected. The cause of the discrepancy was found in the settings of the variable density flow package of SEAWAT, which resulted in incorrectly calculated densities of warmer water (thus during cooling phases). In turn, this caused warmer water to travel slower through the subsurface (not the pipe as flow quantities and thus velocity is specified separately) and cooling phase outcomes to result in an incorrect smaller temperature difference.

The behaviour of temperature throughout the subsurface has been further analyzed through temperature plots over time and contour plots to ensure not further abnormal behaviour occurs. Subsurface temperatures over time at differences distances from the BHE system showed normal behaviour for both the simulation starting with a heating phase, as well as the simulation starting with a cooling phase. Figure 4.19 shows the temperature in the subsurface over time at different distances from the BHE system. The left graph shows a simulation starting with a cooling period, the right starting with heating period. The results of both simulations show normal behaviour of the temperature over time. Closer to the BHE system, temperatures are higher compared to larger distances from the BHE system. Also, temperature changes occur quicker at smaller distances from the BHE system.Contour plots of the temperature in the subsurface in different layers at different time steps were analyzed as well. The results can be found in Appendix A, along with a more detailed analysis. Again no irregular processes are observed in the contour plots.

The discrepancy in the temperature difference between the heating and cooling phase of the BHE system explains the difference in impact of the ATES systems. The interference of the ATES system in a simulation is
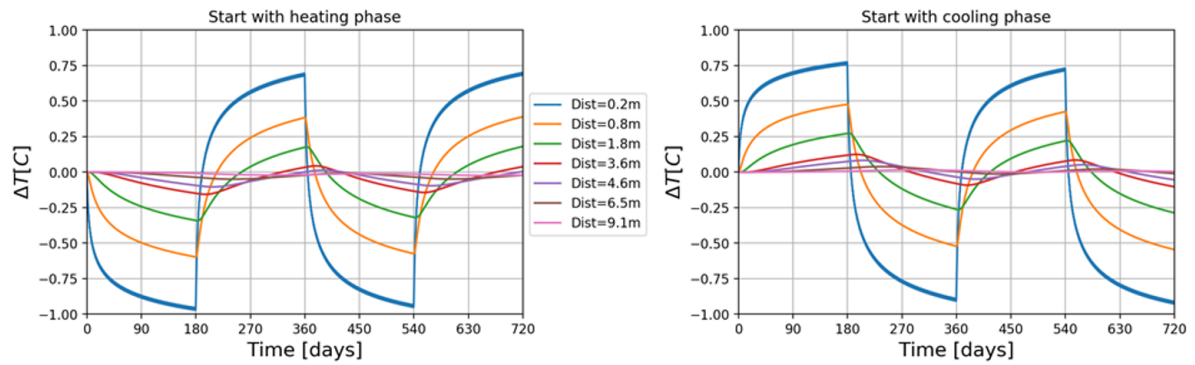
Figure 4.19: Subsurface temperatures halfway through the aquifer at different distances from a BHE system simulated over two years without interference starting in summer (left) and winter (right).
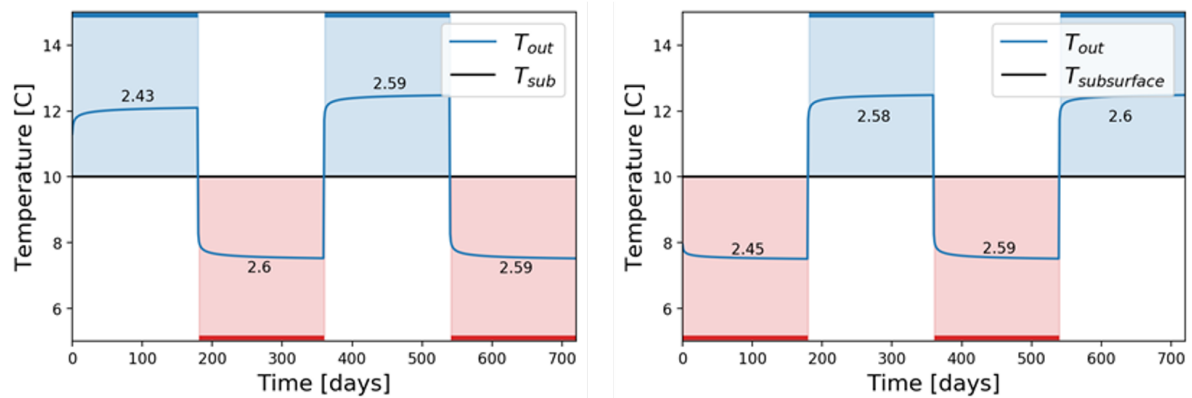

Figure 4.20: Output temperatures of a balanced BHE system simulated over two years without interference starting in summer (left) and winter (right) without the discrepancy.

the same for the BHE system in both heating and cooling mode. As the cooling mode has a larger temperature difference between input and output temperatures, the impact of the ATES system is smaller compared to the impact on the temperature difference during heating mode. The discrepancy in the impact of an ATES system on the efficiencies of a BHE system in heating or cooling mode can be attributed to the discrepancy in temperature difference between input and output temperatures of the BHE system in both modes.

Finally, it is important to be aware of the implications the discrepancies unfolded in the last paragraphs may have on the interpretations of the results when drawing conclusions. The previous paragraphs gave the insight that the absolute impact of ATES systems on BHE efficiencies is highly dependent on the temperature setup of the systems. In this study, input temperatures of both systems had the same temperature difference with respect to the subsurface: 5°C. Based on the cause of the discrepancy, the results of the heating phases are correct. For an unbalanced BHE system, this changes nothing from the results at the beginning of this chapter as the unbalanced BHE system only has a heating function. For a balanced BHE system, this means the efficiencies of the heating phases display the correct results, whereas the results of the cooling phases are too small compared to reality. This is shown in Figure 4.20.

4.6. Relation between distance ratio and interference

The results of Sections 4.1 through 4.4 show a clear relation between the distance ratio and degree of interference from an ATES system on the efficiency of a BHE system. Their relation however, is not linear, but follows the shape of an function related to the inverse of the distance ratio. Interference from ATES systems seem to trail off for distance ratios of 0.66 and larger. Figures 4.3, 4.4 and 4.5 show this relation clearly. Figure 4.21d shows the two different inverse functions. Notice the similarity in shape to the results of the simulations.

Based on the similarities between both functions, it can be assumed that the degree of interference can be predicted by a formula in the shape of Equation 4.1. Where I is the amount of influence from an ATES system
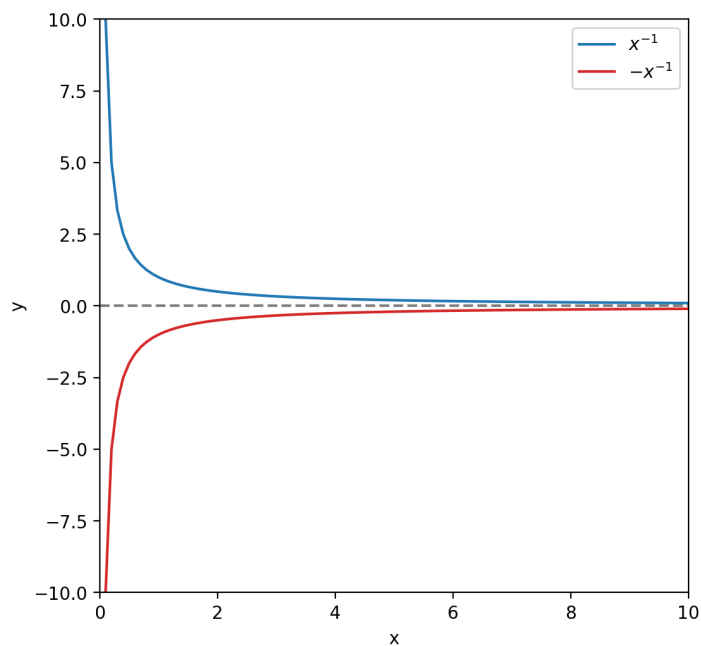
Figure 4.21: Two inverse functions, notice the similarities to Figures 4.3, 4.4 and 4.5.

[-], ΔT is the temperature difference between the subsurface and the fluid when it enters the BHE system [°C] and R_{dist} is the distance ratio [-].

$$I = \Delta T R_{dist}^{-1} \tag{4.1}$$

Exposure time

Figure 4.22 shows the relation between the size of the thermal radius in relation to the amount of water injected or extracted by the ATES system, assuming steady injection rates and equal injection and extraction volumes. As the water injected by the ATES system spreads in a circle, it takes only a quarter of the total volume of water to be injected for the thermal radius to reach half of the total thermal radius. Next, the thermal radius reaches its halfway point again after three quarters of the total injected volume is extracted again. Thus, if a BHE system is located at a distance ratio of 0.50, it experiences thermal exposure to the ATES system for three-quarters of the total cycle of the ATES system. The relation between the thermal radius and exposure time is given in Figure 4.23. A similar equation can be established for the hydraulic radius, this assumes the hydraulic radius is 1.5 times the thermal radius, as explained in Equation 2.2. Both equations are visualized in the left graph in Figure 4.23. BHE systems are exposed to groundwater influence from an ATES system for a longer period of time compared to influence to temperature changes from an ATES system. Furthermore, the shape of the exposure time equations does not correlate with the degree of influence with respect to the distance ratio. Thus, the amount of interference is not directly related to only the exposure time.
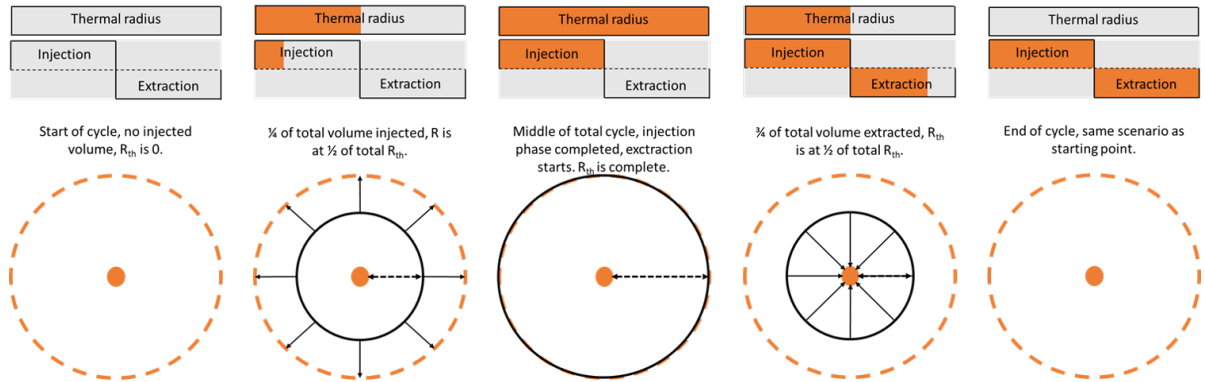
Figure 4.22: Relation between the size of the thermal radius in relation to the part of the injection and extraction cycle.
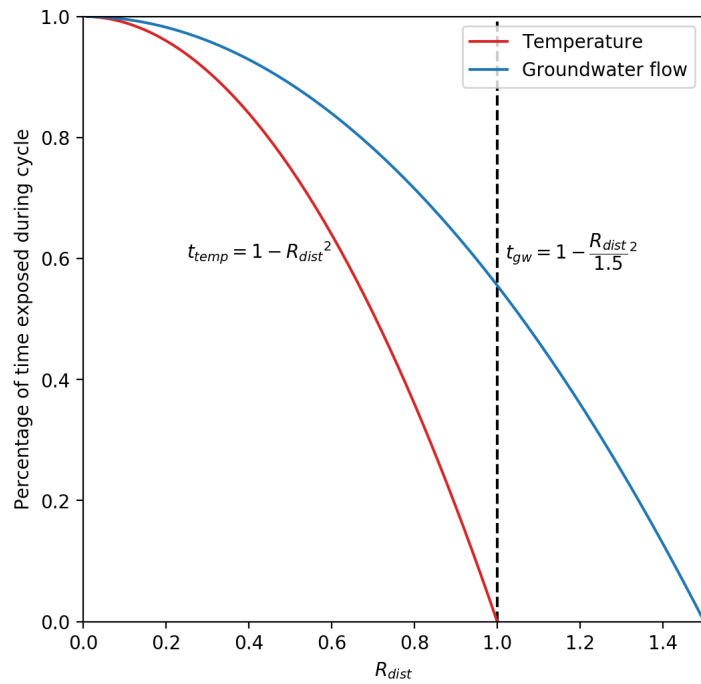

Figure 4.23: Relation between the distance ratio and the percentage of the cycle a BHE system is exposed to the groundwater and temperature components of ATES influence.

Predicting the degree of interference

The exposure time relations show that a BHE system is exposed to groundwater flow and temperature influences from an ATES system for different amounts of time. This was also acknowledged in the results from the simulations. Taking into account the different amounts of influence of groundwater flow and temperature induced by ATES systems, a formula that predicts the amount of interference from an ATES system on the efficiency of a BHE system can be formed. A basic form of such a formula is given in Equation 4.2. The formula exists of two parts, the first predicting the interference from groundwater, the second interference from temperature. Variables a through g can be estimated by curve-fitting the equation to the data points from simulations. The process would be to determine the influence of groundwater flow only first, through results of simulations with an ambient ATES well and only the first half of the equation. Next, add the second part of the equations and fit the resulting formula to results of simulations with warm and cold ATES wells.

For this study, the absolute ΔT is 5°C for both warm and cold ATES well simulations. Therefore, a predictive formula would not hold much value and a curve fit is not conducted. Furthermore, to check if the predictive formula holds any general value, more simulations with a wider range of variables should be tested. Distance ratios for ATES wells with a larger/smaller total injected/extracted volume, different well screen and BHE pipe overlap ratios, different ATES well temperatures amongst the possible variables. However, the process described in this section is a start to a general predictive formula for the interference of an ATES system on a BHE system.

$$I = a + (b\Delta T)(c v_{gw}^{-d}) + (e\Delta T)(f v_{gw}^{-g}) \tag{4.2}$$

<div style="text-align: right; font-size: 4em;">5</div>

Discussion

Before applying the found results to practice, different aspects of the study have to be considered. This chapter will focus on these considerations. First, in Section 5.1, the limitations in the used methodology are discussed. Next, the setup of the model is discussed in Section 5.2, followed by the results of this study compared to other studies in Section 5.3. Finally, Section 5.4 discusses the practical limitations concerning the results of this study.

5.1. Limitations in used methodology

UTES Scope

The scope of the UTES systems of the study was explained in Section 2.3.1. Only the subsurface part was taken into account for this study. Any results concerning in- or decreased BHE efficiency thus only concern the cold/heat extraction from the subsurface. However, this does not translate directly to an equal increased efficiency change for the complete system. An increased efficiency results in a higher temperature gradient for the heat pump to work with. First, cooling and heating periods need to be distinguished. In cooling periods, the heat pump only activates if the temperature retrieved from the subsurface part of the system is insufficient to cool the building. With a more efficient BHE system, and thus lower output temperatures during cooling periods, the heat exchanger has to be used less frequently. In heating periods, the heat pump is always used to heat the output of the subsurface part of the system up to required temperatures. This conversion is not perfect, heat gets lost. Thus, the complete system experiences a smaller increase in efficiency compared to the subsurface part during heating periods (Duijff, 2019).

ATES efficiency

The increase or decrease in BHE efficiency is not free energy. This energy comes from or goes to the ATES well nearby. Thus, what the BHE system gains in energy, is lost in the ATES system, and vice versa. The influence of a single BHE system on the efficiency of an ATES system can be up to 0.4%, depending on the distance between the systems (Drijver et al., 2013). This is mostly due to the difference in size of both systems. An average ATES system has a yearly energy demand roughly six times as large as an average BHE system (Drijver et al., 2013).

This seems disadvantageous at all times. However, UTES systems in practice are often imbalanced. Meaning either heating or cooling demand is higher compared to the other. To counter this, UTES systems have to gain energy from other sources or discharge leftover thermal energy. An alternative solution for this imbalance is to combine systems with different imbalances. By placing BHE systems in the thermal zones of ATES systems, the thermal energy balance of the entire system can be tweaked. This concept is explained more thoroughly under the header practical considerations further in the discussion.

Time step

As discussed in the analysis of the temporal discretization and seen in Figure 3.6, larger time steps result in slower respond times. The 6 hour time step has a significantly slower curve towards an equilibrium compared to the 1 minute time step. This influences the final outcome of the simulations. In order to estimate how the final results are influenced by the larger time step, simulations were conducted with a smaller time step to
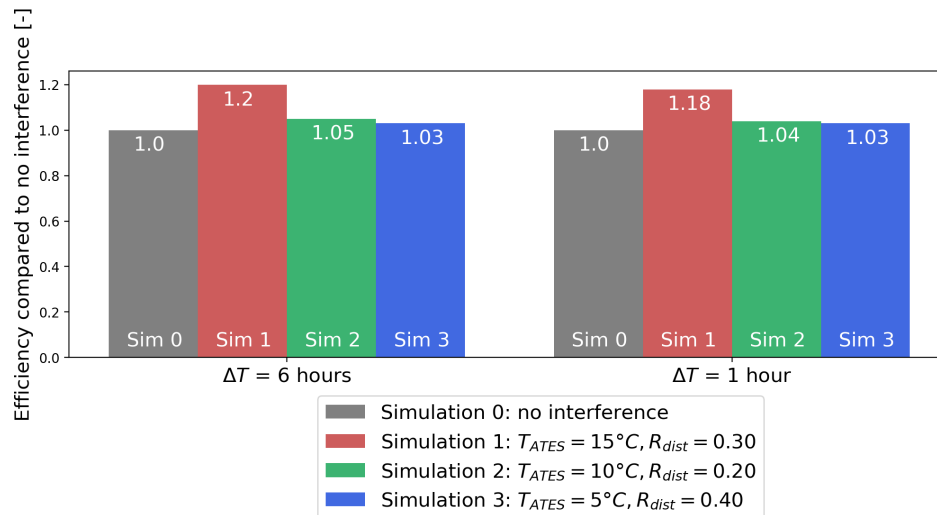
Figure 5.1: Efficiencies of a BHE system in four different scenarios. Right bars represent the outcome for a 6 hour time step, left bars the outcomes of a 1 hour time step.

see how the model outcomes behave. Ideally, 1-minute time step simulations would be conducted. However, simulating 1 year with a time step of 1 minute would result in over half a million time steps. The computational capabilities and research time for this study are simply too small to do so. Instead, simulations with a time step of 1 hour were run for an in-model time of 1 year. The following scenarios were simulated:

- Single aquifer subsurface, no interference.

- Single aquifer subsurface, ATES well temperature of 15°C at a distance ratio of 0.30.

- Single aquifer subsurface, ATES well temperature of 10°C at a distance ratio of 0.20.

- Single aquifer subsurface, ATES well temperature of 5°C at a distance ratio of 0.40.

Figure 5.1 shows the outcome of these simulations. Since only one year was simulated, the results are represented by a bar graph. The left series of bars represent the simulations with a 6 hour time step, the right series of bars those with a 1 hour time step. The results show the same trend in the relative outcomes of simulations with both time steps. The results of the 1 hour time step show a slightly lower degree of interference compared to the 6 hour time step. This should be kept in mind when interpreting the results.

As a smaller time step is expected to result in slightly lower interference from the ATES system, the results would be dampened slightly as well. ATES systems have a slightly smaller impact on BHE system efficiencies and over smaller distances. Thus, the distance between both systems needed in order to prevent negative interaction would be slightly smaller as well. ATES and BHE systems would be able to be placed closer together.

5.2. Model setup limitations

Homogeneous aquifers

Aquifers used in the scenarios were homogeneous, perfect rectangles of sand, aquitards homogeneous, perfect rectangles of clay. In practice, this is not the case. Aquifers and aquitards are heterogeneous, and thermal properties are equally heterogeneous throughout both, possibly leading to preferential flow paths for both groundwater and thermal energy. Heterogeneous aquifers lead to a decrease in system efficiency (Sommer et al., 2013). However, as results were presented on a relative base compared to the case of no influence, no significant relative change based on this principle is expected. The absolute values for BHE efficiencies might decrease, but their ratio stays approximately the same.

Preferential flow paths however, could lead to different results. As groundwater and thermal energy disperse unevenly around the ATES well, the BHE system experiences unexpected interference. Studies show that preferential flow paths lead to faster travel of groundwater along these paths (Bianchi et al., 2011). This could be both an in- or decrease in interference, based on the specific heterogeneity of the aquifer. More research concerning this specific topic could lead to further insights.

A single ATES system
Simulations in this study that investigated the effect of temperature interference only had ATES wells with a temperature difference of 5°C with respect to the subsurface. It is also interesting to study the effects of other temperature differences. Simulations with a balanced BHE system pointed out that confirmed that the impact of ATES interference is highly dependent on the temperature differences between the ATES well temperature and the subsurface, as well as the difference between the BHE input temperature and the subsurface. The temperatures used in this study are representative for current UTES systems in the Netherlands. However, in the future energy demands may change, and with that the characteristic temperatures of UTES systems. Due to climate change, the subsurface temperature may change as well. Insight in the relationship of ATES and BHE systems with different temperature gradients can provide a great topic for further insight in general ATES-BHE interaction.

As for the impact of a single temperature gradient setup on the interpretations of the results, it is important to realise that absolute values based on the results only apply to the temperature gradients used in this study. In order to substantiate absolute conclusions that can be applied to ATES-BHE interaction in general, more temperature gradients have to be simulated. Relative conclusions are more likely to hold true for other temperature gradients as well. Though it remains important to realise that those conclusions too are supported on simulations with only a single temperature gradient.

Ambient groundwater flow
Groundwater flow was present in the models, yet only groundwater flow induced by ATES systems. These flows had a very specific, balanced, pattern. In practice, ambient groundwater flow can also be present and affects both the thermal and hydraulic zone of the ATES well and the thermal distribution around the BHE system.

The impact of groundwater flow on the interference between ATES and BHE system depends on the temperature of the ATES well with regards to the BHE system temperature and the direction of ambient groundwater flow. Ambient groundwater flow that travels from the ATES well towards the BHE system is expected to increase interference. The ambient groundwater flow displaces the thermal and hydraulic radius of the ATES well towards the BHE system, thus increasing interference (Angelotti et al., 2014). If groundwater flow flows from the BHE system towards the ATES system, the opposite occurs and the interference from the ATES well is expected to decrease.

Other Influences
As stated previously, simulated areas are of perfect shape and free of other interference (e.g. ambient groundwater flow). In practice, the subsurface is not a blank canvas where UTES systems can be installed as wished. Instead, the subsurface is used for numerous other services. For example drinking and wastewater transport, energy transport and other cables and pipes. When installing UTES systems, these systems need to be accounted for. Their influence on the installed product is expected to be minimal as all systems are horizontal, whereas UTES systems are vertical. Their overlap, and thus matter of influence, is therefore small.

Simplified pumping schemes
UTES system pumping schemes used in this study were simplified block functions, see Figures 3.8 and 3.9. In practice, heating and cooling phases can still be identified, but ATES and BHE system input is more complex and less uniform as it follows daily energy demands. The expectation for more realistic input patterns is that interference from groundwater flow induced by ATES systems will have a stronger effect on efficiencies. In the numerical model, input temperatures were 5°C, 10°C and 15°C, with the model jumping frequently between those inputs. This causes the system to profit from the energy injected or extracted in the previous step. In practice, input temperatures change more gradually. This causes the system to benefit less from previously stored or extracted energy. However, when an ATES well is nearby, groundwater flow induced by the ATES system keeps the temperature around the BHE system stable, first at subsurface temperatures, then at the temperature of the ATES well, increasing efficiency as seen in Sections 4.1.1 and 4.3.1. This effect is expected to be stronger for more realistic input data. The effect of the temperature of the groundwater well is expected to be similar. When combined, this results in a smaller negative effect of interference and increased positive effect of interference. However, further research with more complex and realistic pumping schemes is advised to confirm this hypothesis.

Short simulation period
Simulations in this study concerned only the first five years of ATES and BHE system. In practice, UTES systems have lifespans up to 25 years. After installation, a warm up period can be seen where UTES system have not yet reached their peak efficiency. To account for this, only 'stable' results have been used for the empiric relations in Chapter 4. Results that differed more than 5% or 0.01 percent point from the result of the previous year are considered to be part of the warm up period and were not taken into account for further conclusions.

Furthermore, simulations assumed that both systems started their life cycle at the same time. In practice, this will not always be the case. Often, one UTES system is already installed and operates at peak efficiency. These scenarios were not simulated, but can be approximated. If a BHE system is to be installed near an ATES system at peak efficiency, the ATES system will have a bigger impact on the BHE efficiency during its warm up period. Vice versa, if an ATES system is to be installed near a BHE system at peak efficiency, the ATES system will have a relatively smaller effect on the BHE efficiency during its warm up period.

5.3. Results of other studies
The impact of ATES systems on the efficiency of BHE systems has not been studies extensively yet. However, studies concerning the effect of groundwater flow on the efficiency of a BHE systems have been conducted. One study researched the impact of groundwater flow on multiple BHE systems through a finite element model that describes groundwater flow and heat transport similar to the software used in this study (Dehkordi and Schincariol, 2014). Another studied the impact of groundwater flow on a BHE system through a numerical MODFLOW model (Panteli et al., 2018). Both studies show results similar to those found in this study. Detailed comparisons can be found in Section A.1.

5.4. Practical considerations
Distance ratio in practice
The average thermal radius of an ATES in the Netherlands is 60 metres (Bloemendal and Hartog, 2018). When applied to the distance ratios used in the simulations, the smaller distance ratios correlate to a distance of 6, 12 or 15 meters in practice. In many cases, these distances are simply to small occur in practice. The average size of a housing parcel in the Netherlands is 131.7 m^2 (en wonen). The smaller distance ratios simulated will therefore not occur if systems are placed in the middle of a parcel. Simulations shows that distance ratios of at least 0.66 had small to no impact on the efficiency of BHE systems. This would relate to a distance of 40 metres in practice. In concentrated urban areas, placing UTES systems 40 metres apart can prove to be a challenge and should be managed carefully if negative interaction is to be avoided.

Combining energy demands
The energy demands of the ATES and BHE systems in this study have always been considered separately. However, considering a holistic view for energy demands from systems that interact with each other offers an interesting viewpoint. As mentioned previously, UTES system often operate under an imbalanced energy demand, which requires systems to discharge or generate the surplus of cold/heat. Another method, is to purposefully create interaction in the subsurface between UTES systems with opposite energy demands. Doing so, the energy demand of the systems can be combined in order to reduce imbalances. Due to the fact that ATES systems have a larger energy demand than BHE systems, multiple BHE systems can be located within the thermal radius of the ATES system in order to combine their demands.
It should be noted that this sounds ideal, but is difficult to realize in practice. If systems are near one another, their climatic conditions are the same, which forms a part of the energy demand. Thus, if an imbalance is present in the energy demand of a system due to climatic conditions, it is probable that nearby systems experience a similar imbalance. However, energy demands are not only based on climatic conditions, but also depend on building usage. For example, office buildings have a larger cooling demand compared to household buildings, which have an energy demand more geared towards heating. Office buildings also have a larger energy demand compared to household buildings and often use ATES systems as UTES energy source. Combining energy demands by placing UTES systems deliberately within the thermal range of other systems can reduce the net imbalance of the complete system.

Practical relevance
The results of the simulations can be relevant for all UTES owners. Simulations show that systems placed within the thermal radius of the ATES system do not always interfere. This is important for new UTES system

owners as they are currently bound by legislation that prevents them from installing new UTES systems when they interfere with current systems. For existing UTES owners with an imbalanced system, the possibility to combine UTES systems and consider their energy balance from a holistic point of view is interesting as well. The introduction of new UTES systems can reduce imbalances of current systems.

Due to the size difference of ATES and BHE systems, a BHE system can save relatively more energy compared to an ATES system. In order for an ATES system to experience a significant imbalance reduction, multiple BHE systems need to be located within its thermal radius. Further research concerning this setup is advised.

Mitigation methods

In the case that interference is not desired, but the proximity of the UTES systems is cause for concern relating interference, mitigation methods might be considered an option. For example insulating the half of the BHE system that lies in the same aquifer as the ATES system. Exploratory simulations show that BHE efficiencies do increase slightly when the affected half of the pipes are insulated. However, whether such a method is cost-effective depends on the local setup of the BHE system, installing techniques, used materials and energy demand.

Studies have also investigated the orientation of the BHE pipes with respect to the ambient groundwater flow and found that it made no difference in BHE efficiencies (Panteli et al., 2018). In addition, orienting the BHE pipes as desired is difficult in practice due to installing techniques.

6

Conclusion

The goal of this research is to gain insight in the effect of interference from an ATES system on the efficiency of a BHE system when placed in close proximity. To do so, a numerical model that simulated an ATES and a BHE system in the subsurface was developed using MODFLOW and MT3D. Next, this model was used to run different simulations. The outcomes of the simulations were then processed to compare different scenarios. Multiple conclusions concerning the effect of interference from an ATES system on the efficiency of a BHE system can be drawn based on these outcomes.

Firstly, groundwater and temperature interference from ATES systems affect the efficiency of a BHE system differently. Simulations show that the effect of groundwater flow induced by an ATES system has a positive effect on the efficiency of a BHE system. In all ambient ATES well scenarios, where only groundwater flow induced by the ATES system affected the BHE system, BHE efficiencies increased. This effect is dependent on the rate of change in temperature input of the BHE system. With frequent temperature changes, the positive groundwater influence is expected to decrease.

The effect of temperature interference is dependent on the temperature of the ATES well. If the temperature of the ATES well increases the temperature gradient of the subsurface with respect to the BHE system input temperature, the BHE system operates at a greater efficiency, and vice versa. Groundwater was also found to interfere at larger distances between both systems compared to temperature, which is logical as the hydraulic radius of the ATES system is larger compared to the thermal radius.

Secondly, the degree of interference is related to the distance between the ATES and BHE system. For distances up to 0.5 times the thermal radius of the ATES system, the temperature influence was found to be dominant for the simulated temperature gradients. Thus, the net influence of an ATES well is dependent on whether the ATES well temperature aids or hinders the BHE system with cooling or heating. However, as groundwater positively influenced the BHE system, negative effects due to ATES well temperatures are smaller compared to positive effects. For distances greater than 0.5 times the thermal radius of the ATES system, groundwater interference becomes dominant with the simulated temperature gradient. However, at these distance ratios the net effect of ATES well interference was found to be small and can be considered insignificant. Also, the effect of groundwater interference is dependent on the BHE input characteristics, which were explored only briefly in this study. Based on the outcomes of the simulations conducted in this study, it can be concluded that if interaction between an ATES system and BHE system set up as simulated in this study is not desired, a distance of at least 0.5 times the thermal radius is advised. If significant interaction is desired, the distance between both systems should be no larger than 0.5 times the thermal radius.

However, two points of concern have to be taken into account when applying this second conclusion. First, the time step of 6 hours is relatively large. Simulations with smaller time steps showed a slightly lower degree of interference from the ATES system. This would allow UTES systems to be placed closer together without significant interference. Due to computational and time restraints, simulations of multiple years have not been conducted. Before applying the conclusions of this study to policy decisions, it is therefore advised to further explore simulations with smaller time steps over a longer period of time. Second, a discrepancy in the results of the simulations of balanced BHE systems was found. The cause of this discrepancy was an incorrect implementation of the variable density flow. Due to the nature of the cause, the efficiencies

of the system in cooling phases are too small compared to reality. Conclusions have been based on the based on the outcomes of the system in heating phase. This does not make the results of this study useless. The results show system behaviour when ATES and BHE systems are placed close together. The exact degree of impact is uncertain due to the assumptions made during the research. However, the relative conclusions still hold true.

The third conclusion is that the influence of the depth location of the ATES system was tested by running simulations with two aquifers. The ATES system was placed in only the top or bottom aquifer, the BHE system in both aquifers. From the results can be concluded that the depth placement of the ATES well screen has little to no effect on the amount of interference on the BHE system.

Finally, it is important to realize that no energy is spontaneously generated or lost as BHE efficiencies increase or decrease respectively. Any increase or decrease in BHE efficiency due to temperature change induced by the ATES system is balanced by the energy the ATES system loses or gains. Whether that is disadvantageous depends on the energy balance of both systems. Strategic placement of BHE systems in the thermal radius of ATES wells can aid in balancing the energy of all systems by combining them.

7

Recommendations

This chapter introduces and explains recommendations based on research conducted in this study. The recommendations are divided into practical recommendations and recommendations for further research. First, in Section 7.1, practical recommendations are given. These apply to the installation and management of ATES and BHE systems in areas where subsurface space is under pressure. Next, in Section 7.2, recommendations for further research are given.

7.1. Practical recommendations

Based on the conclusions of this study, it is recommended that current regulations concerning the distance between ATES and BHE systems are subject to change. Currently, Dutch laws and regulations prefer the BHE system to be installed outside of the thermal and hydraulic radius of the ATES system. This would relate to a distance ratio of 1.50 (the hydraulic radius of the ATES system in terms of thermal radius). This study showed the degree of interference is dependent on the velocity of the groundwater induced by the ATES system and the temperature difference between both systems. The degree of interference is related to the inverse of the distance ratio. For ATES and BHE installations that resemble the setup of this study, interference between systems was found to be minimal for distances greater than 0.5 times the thermal radius of the ATES system. This distance is dependent on the temperature setups of both systems. However, it does show that the distance between UTES systems can be smaller than currently allowed. This allows for more UTES systems to be installed in total, which in turn can make UTES more viable as a more sustainable energy source.

Furthermore, it is recommended to consider UTES installation from a holistic point of view. Instead of trying to avoid interference with other systems, it is advised to consider other UTES systems near the to be installed system and combine systems when advantageous. Doing so is more complex and requires a non-uniform solution for new installations. However, combining UTES systems when advantageous allows for imbalanced systems to be a part of a balanced overarching system and save energy.

This advice is most useful for existing systems, as distance requirements can be smaller compared to current legislation. Furthermore, mainly BHE systems are impacted by this research as the impact on ATES systems is expected to be small. However, when multiple BHE systems are located within the thermal radius of an ATES system, significant interference may occur.

7.2. Recommendations for further research

The conclusions and limitations of this study are ground for further research. For example, more scenarios could be ran to explore the impact of other variables. Including, but not limited to, the effect of ambient groundwater flow on the efficiency of both systems, the effect of multiple BHE systems in the thermal radius of an ATES system or the effect of multiple ATES systems on a single BHE system, a different balance between heating and cooling in the BHE system and more realistic input data for both the ATES and BHE system. The impact of increased efficiencies on the heat pump of the BHE system is also an interesting topic for further research.

The influence of different temperature gradients is a good parameter to consider in further studies as well. In this research, both the cold and warm ATES well had a 5°C temperature gradient with respect to the ambient subsurface temperature. The degree of interference in both cases was also the same. However, whether

temperature follows a linear relationship or has a different shape has not been explored in this study and remains and interesting topic for further research.

Another topic for further research is the effect of groundwater flow induced by the ATES system. This study concluded that groundwater flow increases the efficiency of the BHE system, even when the distance between both systems equals the thermal radius. Further research could explore whether groundwater flow is advantageous for BHE efficiencies when the BHE system is located out of range of the thermal radius but still within the hydraulic radius of the ATES system and how often BHE input temperatures need to switch in order for the effect to be negative.

In the results, a discrepancy between the results of the cold and warm phase of the BHE system was found. When cooling, the system experienced less interference from the ATES system. This was unexpected as heating and cooling were balanced. The discrepancy originates from the fact that in simulations, during cooling phases, a higher/lower temperature difference between the in- and output temperatures of the BHE system occurs. This results in the discrepancy between the impact of an ATES well on the heating and cooling phase of the BHE system. An explanation for the discrepancy in the simulations has been found in the settings of the variable density flow settings, however due to computational and time limitations, no new simulations could be carried out. Further research on this topic is advised.

The results for a BHE system with both a heating and cooling function showed different outcomes. The effect of groundwater interference was different for heating and cooling, while both functions were active for the same amount of time. Furthermore, a cold ATES well had a larger negative effect on the heating function compared to the positive effect on the cooling function, resulting in a net negative function. Meanwhile, the warm ATES well had a larger positive effect on the heating function compared to the negative effect on the cooling function, resulting in a net positive function. As the BHE system was balanced, these results are unexpected and ground for further research.

In this study, MODFLOW 2000 was used to create a model and run simulations. A more recent version exists: MODFLOW 6. However, that version did not yet allow for temperature simulations at the time of this research. In future research, if MODFLOW 6 supports temperature simulations through solute transport, MODFLOW 6 is recommended to simulate UTES systems. MODFLOW 6 allows for grid cells to be divided up into smaller cells, which makes simulating BHE systems requiring small grid cells, more efficient. In turn, this increases model stability and decrease model run time.

Bibliography

A. Angelotti, L. Alberti, I. La Licata, and M. Antelmi. Energy performance and thermal impact of a borehole heat exchanger in a sandy aquifer: Influence of the groundwater velocity. *Energy Conversion and Management*, 77:700–708, 2014.

G. Bakema, F. Schoof, et al. Geothermal energy use, country update for the netherlands. In *European Geothermal Congress*, 2016.

M. Bakker, V. Post, C.D. Langevin, J.D. Hughes, J.T. White, J.J. Starn, and M.N. Fienen. Scripting modflow model development using python and flopy. *Groundwater*, 54(5):733–739, 2016.

M. Bianchi, C. Zheng, C. Wilson, G.R. Tick, G. Liu, and S.M. Gorelick. Spatial connectivity in a highly heterogeneous aquifer: From cores to preferential flow paths. *Water Resources Research*, 47(5), 2011.

J.M. Bloemendal. The hidden side of cities: Methods for governance, planning and design for optimal use of subsurface space with ates. 2018.

J.M. Bloemendal and N. Hartog. Analysis of the impact of storage conditions on the thermal recovery efficiency of low-temperature ates systems. *Geothermics*, 71:306–319, 2018.

BodemenergieNL. Leergang bodemenergie - ontwerp en realisatie ondergrondse gesloten systemen.

F. Bonetto, J.L. Lebowitz, and L. Rey-Bellet. Fourier's law: a challenge to theorists. In *Mathematical physics 2000*, pages 128–150. World Scientific, 2000.

D.W. Bridger and D.M. Allen. Designing aquifer thermal energy storage systems. *ASHRAE Journal*, 47(9):S32, 2005.

K. Burdett and K.L. Judd. Equilibrium price dispersion. *Econometrica: Journal of the Econometric Society*, pages 955–969, 1983.

E.C. Childs. The anisotropic hydraulic conductivity of soil. *Journal of Soil Science*, 8(1):42–47, 1957.

P. Christoff. The promissory note: Cop 21 and the paris climate agreement. *Environmental Politics*, 25(5): 765–787, 2016.

H. de Jonge, M. Koenders, and B. de Zwart. Bodemenergiesystemen kunnen dichter bij elkaar. 2013.

S.E. Dehkordi and R.A. Schincariol. Effect of thermal-hydrogeological and borehole heat exchanger properties on performance and impact of vertical closed-loop geothermal heat pump systems. *Hydrogeology Journal*, 22(1):189–203, 2014.

S.E. Dehkordi, R.A. Schincariol, and B. Olofsson. Impact of groundwater flow and energy load on multiple borehole heat exchangers. *Groundwater*, 53(4):558–571, 2015.

J.S. Dickinson, N. Buik, M.C. Matthews, and A. Snijders. Aquifer thermal energy storage: theoretical and operational analysis. *Geotechnique*, 59(3):249–260, 2009.

C. Doughty, G. Hellström, C.F. Tsang, and J. Claesson. A dimensionless parameter approach to the thermal behavior of an aquifer thermal energy storage system. *Water Resources Research*, 18(3):571–587, 1982.

B. Drijver and A. Willemsen. Groundwater as a heat source for geothermal heat pumps. *International summer school on direct application of geothermal energy, International Geothermal Association, Bad Urach, Germany, September*, pages 17–20, 2001.

B. Drijver, R. Wennekes, and S. de Boer. Interferentie tussen open en gesloten energiesystemen. 2013.

R. Duijff. Interaction between multiple ates systems: Analysis of thermal and geohydrologic performance. 2019.

Bouwen en wonen. Nederlanders wonen op steeds krapper perceel. URL https://www.bouwenwonen.net/artikel/Nederlanders-wonen-op-steeds-krapper-perceel/44706.

P. Fleuchaus, B. Godschalk, I. Stober, and P. Blum. Worldwide application of aquifer thermal energy storage–a review. *Renewable and Sustainable Energy Reviews*, 94:861–876, 2018.

M.C. Geluk, W.A. Paar, P.A. Fokker, T. Wong, D.A.J. Batjes, and J De Jager. Geology of the netherlands. In *Royal Netherlands Academy of Arts and Sciences*, pages 27–42, 2007.

B. Godschalk. How aquifer thermal energy storage (ates) is catching on in japan. 2017. URL https://www.iftechnology.nl/aquifer-thermal-energy-storage-wko-in-dutch-is-catching-on-in-japan.

A.W. Harbaugh, E.R. Banta, M.C. Hill, and M.G. McDonald. Modflow-2000, the u. s. geological survey modular ground-water model-user guide to modularization concepts and the ground-water flow process. *Open-file Report. U. S. Geological Survey*, (92):134, 2000.

G. Hellström and B. Sanner. Earth energy designer. *User's Manual, version*, 2, 2000.

L.F. Konikow and J.D. Bredehoeft. Groundwater models cannot be validated. *Advances in water resources*, 15 (1):75–83, 1992.

K. Korhonen, N. Leppaharju, P. Hakala, and T. Arola. Simulated temperature evolution of large btes-case study from finland. 2018.

M. Lanahan and P.C. Tabares-Velasco. Seasonal thermal-energy storage: A critical review on btes systems, modeling, and system design for higher system efficiency. *Energies*, 10(6):743, 2017.

C.D. Langevin, D.T. Thorne Jr, A.M. Dausman, M.C. Sukop, and W. Guo. Seawat version 4: a computer program for simulation of multi-species solute and heat transport. Technical report, Geological Survey (US), 2008.

Christian D Langevin. Seawat: A computer program for simulation of variable-density groundwater flow and multi-species solute and heat transport. Technical report, US Geological Survey, 2009.

Natuur Milieu. Gasmonitor 2018,. 2018.

N. Naber, B. Schepers, M. Schuurbiers, and F. Rooijers. Een klimaatneutrale warmtevoorziening voor de gebouwde omgeving. 2016.

A Nguyen, P Pasquier, and D Marcotte. Borehole thermal energy storage systems under the influence of groundwater flow and time-varying surface temperature. *Geothermics*, 66:110–118, 2017.

N. Panteli, J.M. Bloemendal, B. des Tombe, M. Bakker, and H. Witte. Assessment of the effect of groundwater flow on the performance of borehole thermal energy storage systems. In *EGU General Assembly Conference Abstracts*, volume 20, page 9772, 2018.

N.B. Pellenbarg. Groundwater amangement in the netherlands: background and legislation. In *ILRI workshop groundwater management*, pages 137–149, 1997.

SIKB. Handhavingsuitvoeringsmethode bodemenergiesystemen voor gemeentelijke taken (hum be, deel 2). *SIKB*, 2020.

W. Sommer, J. Valstar, P. van Gaans, T. Grotenhuis, and H. Rijnaarts. The impact of aquifer heterogeneity on the performance of aquifer thermal energy storage. *Water Resources Research*, 49(12):8128–8138, 2013.

W.T. Sommer, P.J. Doornenbal, B.C. Drijver, P.F.M. Van Gaans, I. Leusbrock, J.T.C. Grotenhuis, and H.H.M. Rijnaarts. Thermal performance and heat transport in aquifer thermal energy storage. *Hydrogeology Journal*, 22(1):263–279, 2014.

E.A. Sudicky. A natural gradient experiment on solute transport in a sand aquifer: Spatial variability of hydraulic conductivity and its role in the dispersion process. *Water Resources Research*, 22(13):2069–2082, 1986.

D. Thorne, C.D. Langevin, and M.C. Sukop. Addition of simultaneous heat and solute transport and variable fluid viscosity to seawat. *Computers & geosciences*, 32(10):1758–1768, 2006.

D.P. van Vuuren, P.A. Boot, J. Ros, A.F. Hof, and M.G.J. den Elzen. *The implications of the Paris climate Agreement for the Dutch climate policy objectives.* PBL Netherlands Environmental Assessment Agency, 2017.

Centraal Bureau voor de Statistiek. Energieverbruik gedaald in 2018. 2019. URL `https://www.cbs.nl/nl-nl/nieuws/2019/16/energieverbruik-gedaald-in-2018`.

C.I. Voss. A finite-element simulation model for saturated-unsaturated, fluid-density-dependent groundwater flow with energy transport or chemically-reactive single-species solute transport. *Water Resources Investigation Report*, 84:4369, 1984.

Waternet. Hoe je zout water uit wko-systemen het beste kunt lozen. 2020.

S. Whitaker. Flow in porous media i: A theoretical derivation of darcy's law. *Transport in porous media*, 1(1): 3–25, 1986.

C. Zheng, M.C. Hill, G. Cao, and R. Ma. Mt3dms: Model use, calibration, and validation. *Transactions of the ASABE*, 55(4):1549–1559, 2012.

Chunmiao Zheng, P Patrick Wang, et al. Mt3dms: a modular three-dimensional multispecies transport model for simulation of advection, dispersion, and chemical reactions of contaminants in groundwater systems; documentation and user's guide. 1999.
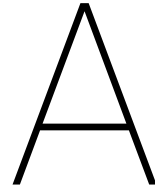
Model evaluation

In general, scientific research requires models to be validated and verified in order to put weight to their outcomes and conclusions. However, this is not possible for groundwater models according to Konikow and Bredehoeft, who state that "groundwater models are embodiments of scientific hypotheses" (Konikow and Bredehoeft, 1992). Their conclusion is that models can only be tested and invalidated. This appendix does so by evaluating the numerical model described in Chapter 3. Evaluation occurs in three steps in this appendix. First, output temperatures for both BHE and ATES systems are evaluated in Sections A.1 and A.2 respectively. Finally, in Section A.3, the presence of all geothermal processes expected to be present in the model is verified.

Most results from in this appendix are based on a simulation with a single aquifer. The exception being a simulation where the efficiency of an ATES system without interference is simulated. The BHE system has only a heating function and is located at a R_{dist} of 0.50 of a cold ATES well. A full test concerning possible invalidation of the model would require all possible simulations to be evaluated. Due to time and computational power restrictions, this is not done. Instead, the first three years of a single simulation are analyzed. Other simulations vary in ATES well temperature, BHE input patterns, R_{dist} and number of aquifers. ATES well temperature is not expected to lead to different insights as a cold ATES well results in the largest temperature gradients in the model. Concerning the BHE input patterns, only a cooling functions is added in certain simulations. This causes no larger temperature gradients compared to the used simulation. The simulated distance ratio is in the middle of the R_{dist} range. The smallest distance ratio has the most interference. However, the degree of interference is not significantly different from the used simulation. Finally, the number of aquifers is also not expected to cause significant differences in model behavior. A double aquifer results in less interference between both systems, and thus less possibly problematic scenarios.

A.1. BHE system results

Figure A.1 shows the in- and outgoing temperatures of the BTES system for cool and warm periods. The left graph shows the BHE system during cool periods. Heating ($5°C$ input) and inactive time steps ($10°C$ input) follow each other. The graph is from the beginning of a cool phase, which can be noticed as the system is still moving towards an equilibrium.

The right graph shows the BHE system temperatures during warm periods. In these periods, the system has one heating time step followed by 23 inactive time steps. Just over one cycle can be seen in the graph. The system experiences a quick dip due to the heating time step and then recovers back towards the equilibrium over the following inactive time steps. During this phase, heating is more efficient. A larger difference between the in- and outgoing temperatures can be observed during the heating time step. This makes sense as less energy is extracted from the subsurface during warm periods. Thus, when the system is heating it allows for a larger temperature gradient and a more efficient system.

These results are compared to other studies concerning BHE systems. Panteli conducted a case study of a BHE system in the Netherlands using a similar numerical model (Panteli et al., 2018). The results can be found in Figure A.2. The data is more realistic, and thus does not follow the block function of this study. However, similar patterns can be observed. Both models have a temperature difference of around $1.5°C$ and
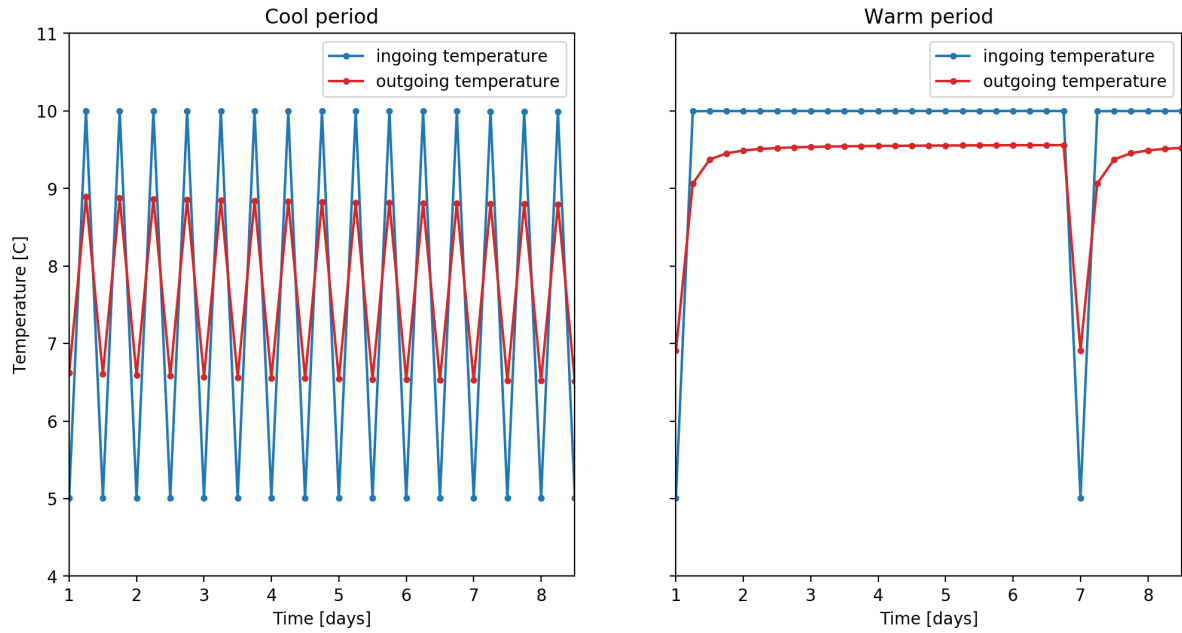
Figure A.1: Simulation input and output for the BHE system during cool (left) and warm (right) periods.

Table A.1: Yearly energy results for a BHE system without interference.

	Year 1	Year 2	Year 3	Year 4	Year 5
$E_{yearly}[MWh]$	145.55	140.71	139.84	139.33	138.97
W/m	0.0240	0.0232	0.0231	0.0230	0.0229

respond quickly to a change in input temperature.

A study from Finland utilizes a model based on other finite-elements software to simulate a case study (Korhonen et al., 2018). Simulations did not use block function input, but realistic data. The results can be found in Figure A.3. Similar patterns concerning response time and temperature differences between input and output can be observed.Finally, A study researched the impact of groundwater flow on multiple BHE systems through a finite element model that describes groundwater flow and heat transport similar to the software used in this study (Dehkordi et al., 2015). The results can be found in Figure A.4 and show similarities to the results of the BHE system in simulations of this study.

Based on similarities between expected behavior and actual behavior and similar trends with other studies in the same field, the BHE output of the model is considered to be behaving appropriately.

For simulations without any interference, the yearly energy generated by the BHE system can be found in Table A.1, along with the watt per meter for the system.

A.2. ATES system results

Figure A.5 shows the average well screen temperature for a simulation where only a cold ATES well is present. Cold ATES well inject during cold periods, September through March, and extract during warm periods, April through October. The recurring pattern in the graph shows said behavior. ATES efficiency can be calculated as the fraction of injected energy over extracted energy for each year. For a simulation without any interference, ATES efficiency was 0.47, 0.76, 0.81, 0.83 and 0.84 for the first five years respectively. These values are in line with other studies (Bloemendal and Hartog, 2018).

A.3. Geothermal processes

Three main geothermal processes where identified in Chapter 2: conduction, convection and dispersion. Figure A.6 shows a side view of the temperature around the BHE installation at four different moments in time. The BHE pipe is located in the middle and has cold water injected which circulates and warms up slightly.
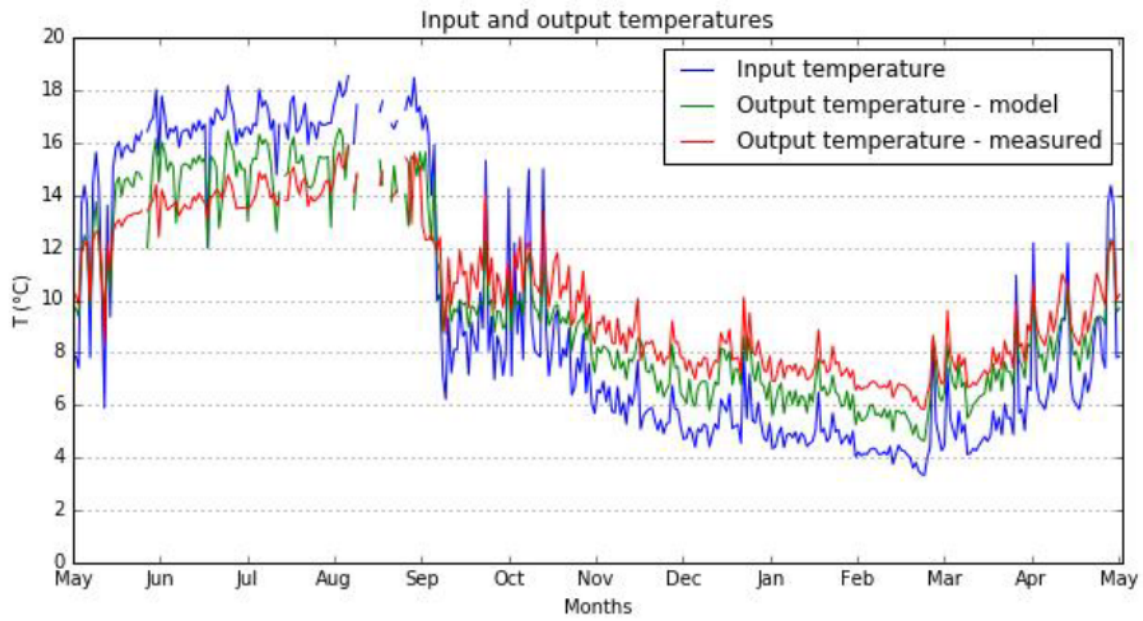
Figure A.2: Simulation results from a BHE case study by Panteli (Panteli et al., 2018)
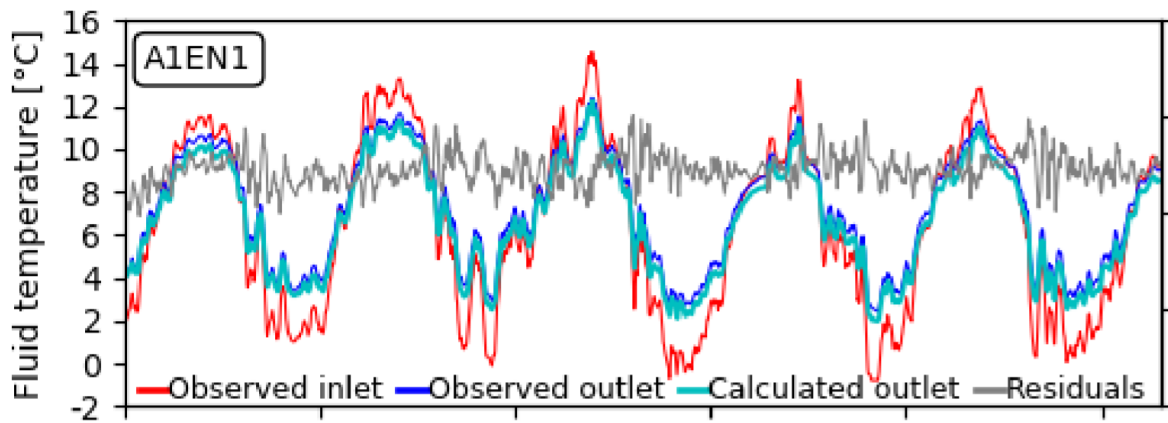

Figure A.3: Simulation results from a BHE case study by Korhonen et al. (Korhonen et al., 2018)
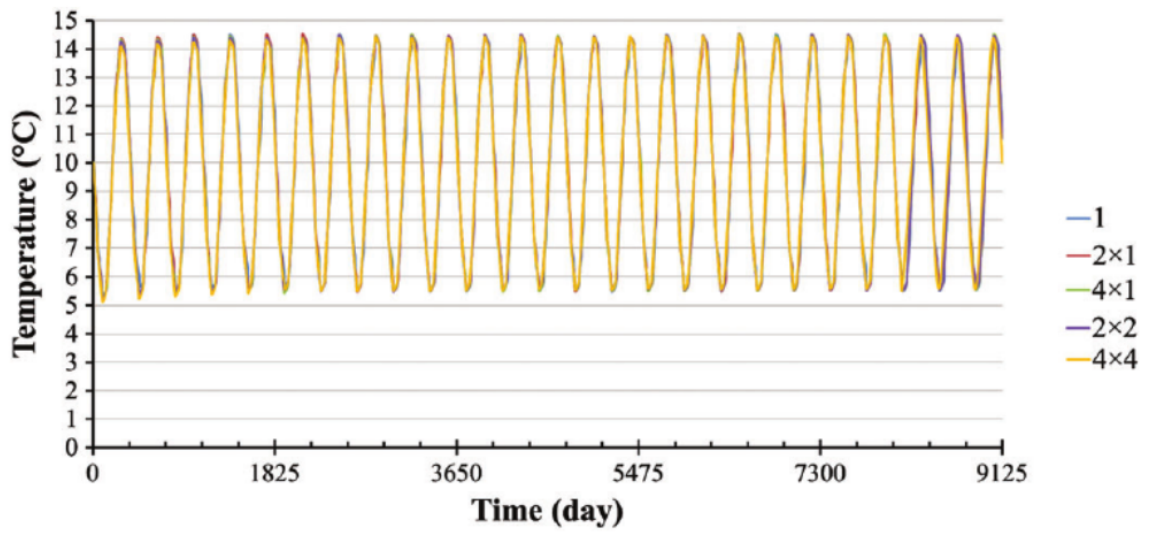
Figure A.4: Average loop fluid temperatures for multiple BHE array types under the influence of groundwater flow (Dehkordi et al., 2015)
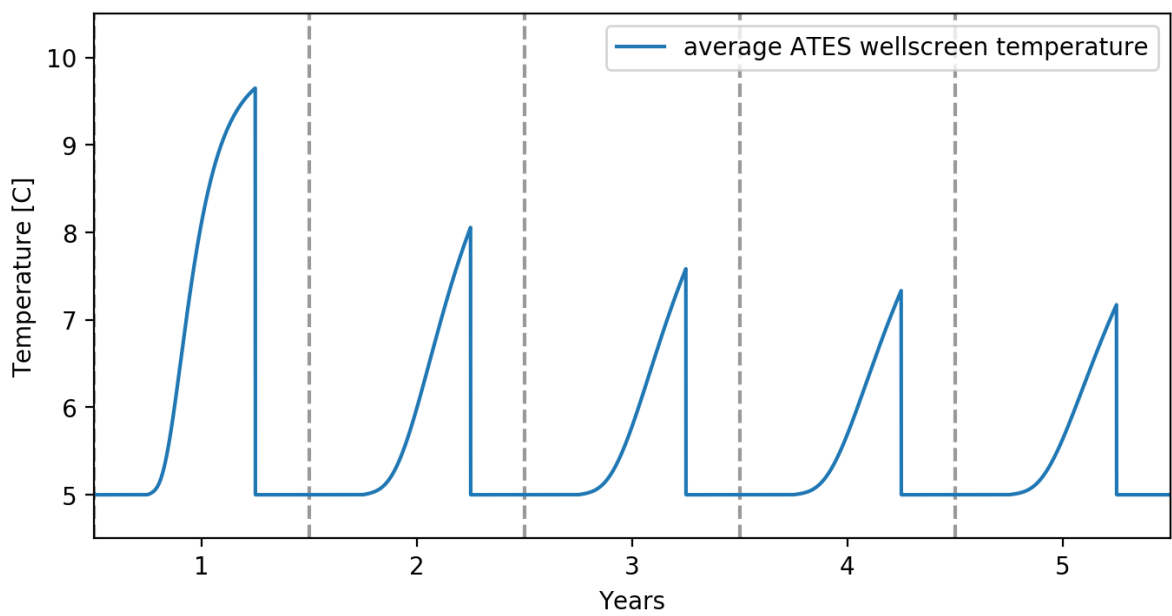

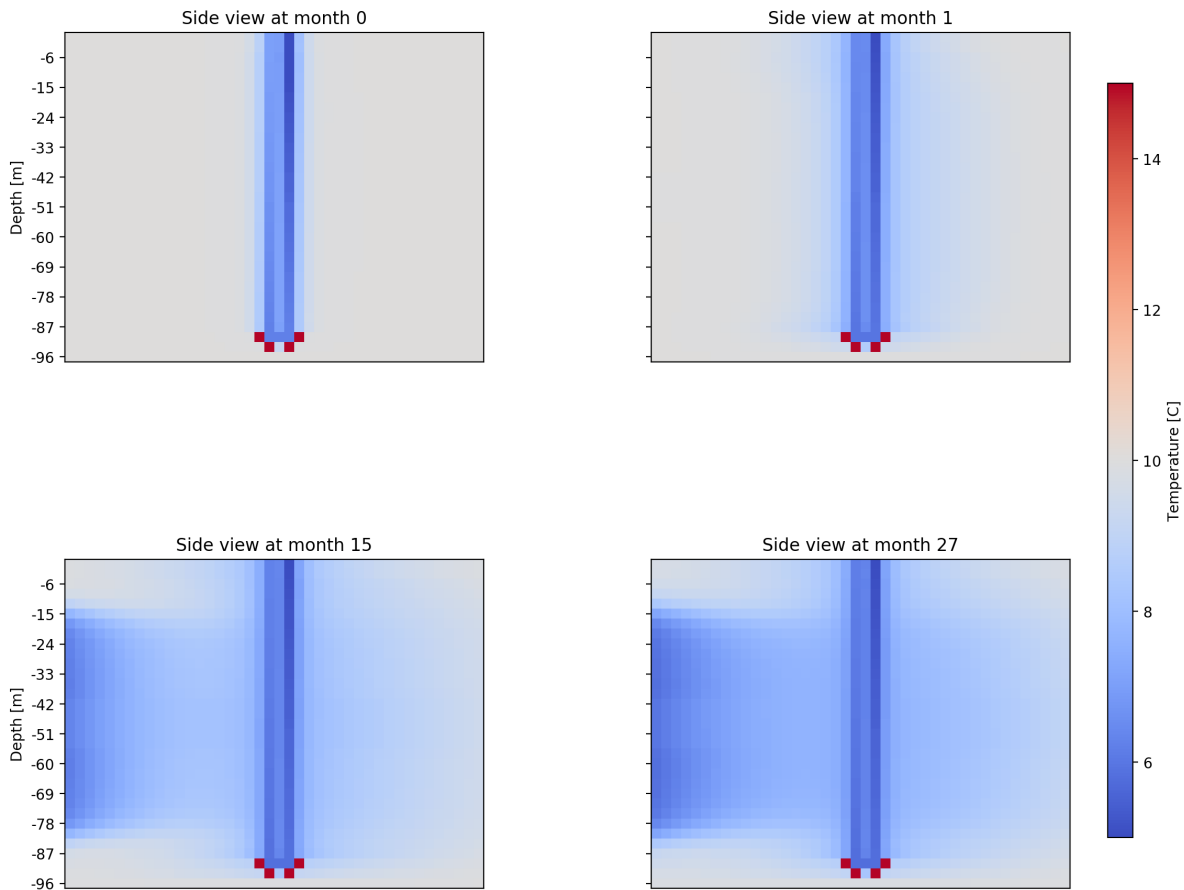Figure A.5: Simulation results for the ATES system over five years.

Figure A.6: Subsurface temperatures around the BHE system at four different moments.

The four red cells near the bottom of the installation are cells where water nor solute can travel through.

Conduction can be observed in the top right figure, which shows the side view after one month of simulations. The ATES system has not yet affected the BHE system at this point. However, it is clear that the subsurface around the BHE pipe is colder compared to the start of the simulation, portrayed in the top left figure. This is due to conduction. Next, in the bottom figures, interference from the cold ATES well is present. This interference occurs dominantly due to convection, as well as partly conduction. Dispersion cannot be located with the results. It occurs dominantly around the ATES well when the thermal radius of the well is small and the well is injecting. Thus, around the start of the model and the start of periods of injection. However, as grid cells near the ATES system are relatively large, dispersion occurs within the area of a single cell and cannot be seen in the results.

A.4. Contour plots

Figures A.7 and A.8 show contour plots of the subsurface around a BHE system from above at six different time steps. In both simulations, the BHE system is balanced and no interference takes place. Figure A.7 comes from a simulation starting with a heating period. In Figure A.8 the simulation starts with a cooling period. The time steps on the left side of the figure are during the middle of a heating or cooling phase. On the right side, the time steps come just after the a switch from heating to cooling or vice versa. This can also be seen in the contour lines. Left hand side temperatures are all on the same side of the subsurface (either below or above). Right hand side figures show the new temperature slowly moving from the BHE system outwards.
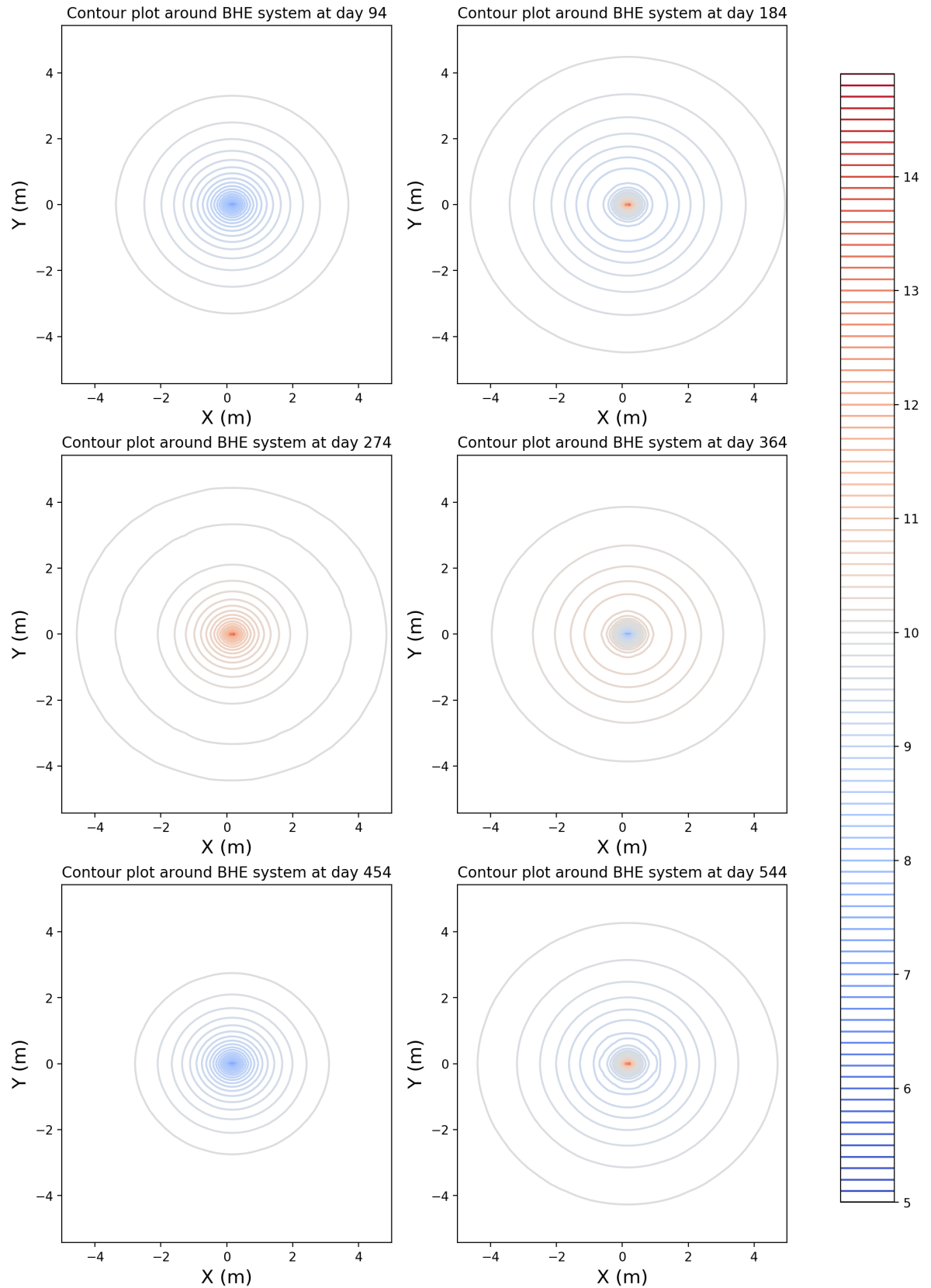
Figure A.7: Subsurface temperatures around the BHE system as seen from above at six different moments for a simulation starting with a heating period with a balanced BHE system without interference.
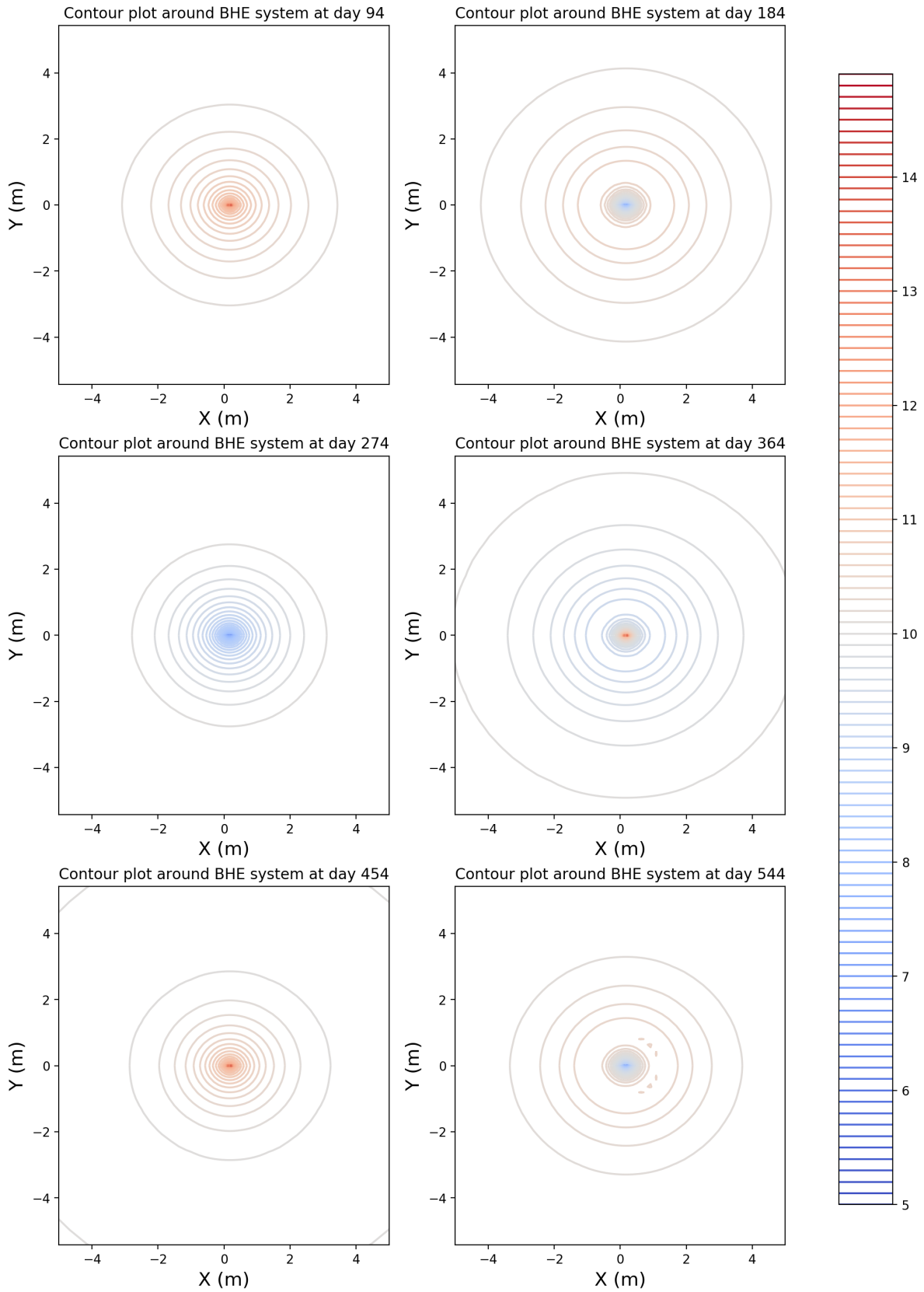
Figure A.8: Subsurface temperatures around the BHE system as seen from above at six different moments for a simulation starting with a cooling period with a balanced BHE system without interference.